



Phanerozoic paleoenvironmental and paleoclimatic evolution in Svalbard

Aleksandra Smyrak-Sikora^{1,2}, Peter Betlem³, Victoria S. Engelschiøn⁴, William J. Foster⁵, Sten-Andreas Grundvåg⁶, Mads E. Jelby⁷, Morgan T. Jones^{8,9}, Grace E. Shephard^{10,11}, Kasia K. Śliwińska¹², Madeleine L. Vickers⁸, Valentin Zuchuat^{13,14}, Lars Eivind Augland⁹, Jan Inge Faleide⁹, Jennifer M. Galloway¹⁵,
5 William Helland-Hansen⁷, Maria A. Jensen², Erik P. Johannessen¹⁶, Maayke Koevoets¹⁷, Denise Kulhanek¹⁸, Gareth S. Lord¹⁹, Tereza Mosociova^{2,9}, Snorre Olaussen², Sverre Planke^{9,20}, Gregory D. Price²¹, Lars Stemmerik¹², Kim Senger²

¹ Department of Geosciences, Norwegian University of Science and Technology (NTNU), Trondheim 7031, Norway.

² Department of Arctic Geology, The University Centre in Svalbard (UNIS), Longyearbyen 9171, Norway.

10 ³ Norwegian Geotechnical Institute (NGI), Oslo NO-0806, Norway.

⁴ Natural History Museum, University of Oslo, Oslo 0562, Norway.

⁵ Institute for Geology, University of Hamburg, Hamburg 20146, Germany.

⁶ Department of Geosciences, The Arctic University of Norway, Tromsø 9019, Norway.

⁷ Department of Earth Science, University of Bergen, Bergen N-5020, Norway.

15 ⁸ Department of Ecology and Environmental Science (EMG), Umeå University, Sweden.

⁹ Department of Geosciences, University of Oslo, Oslo 0315, Norway.

¹⁰ Centre for Planetary Habitability (PHAB), University of Oslo, Oslo 0315, Norway.

¹¹ Research School of Earth Sciences, Australian National University, Acton, Canberra, Australia.

20 ¹² Department of Geo-energy and Storage, The Geological Survey of Denmark and Greenland (GEUS), Copenhagen 1350, Denmark.

¹³ Mineral Resources, CSIRO, Australia.

¹⁴ Geological Institute, RWTH-Aachen University, Aachen 52062, Germany.

¹⁵ Geological Survey of Canada (GSC)/Commission géologique du Canada, Calgary, AB, Canada.

¹⁶ EP Skolithos, Sisikveien 36, 4022 Stavanger, Norway.

25 ¹⁷ Geological Survey of the Netherlands (TNO), Utrecht 3584 CB, the Netherlands.

¹⁸ Institute of Geosciences, Kiel University, Kiel 24118, Germany.

¹⁹ Equinor, Norway

²⁰ Volcanic Basin Petroleum Research AS (VBPR), Oslo

30 ²¹ School of Geography, Earth and Environmental Sciences, University of Plymouth, Devon PL4 8AA United Kingdom

Correspondence to: Aleksandra Smyrak-Sikora (aleksandra.a.smyrak-sikora@ntnu.no)

35

Abstract. Sedimentary rocks can provide information about the Earth paleoenvironment and are studied extensively to
40 understand the causes and consequences of global climate changes in deep time. They facilitate long-time perspectives that



constrain climate models and provide analogues for how Earth systems may respond to, and recover from, intervals of profound environmental change, including projected anthropogenic change. The Norwegian Svalbard archipelago offers an extensive Phanerozoic stratigraphic record that reflects the geological evolution of the northern flanks of continental assemblages that include Laurentia, Eurasia, and Pangea. Svalbard's Phanerozoic sedimentary and paleoclimatic archive is controlled largely by Svalbard's overall northward plate-tectonic motion from equatorial to high latitudes, but also by regional to local formation of topography and basins in response to long-term plate reorganization, as well as the near- and far-field influence of large igneous province activity on the tectono-stratigraphic and paleoclimatic development. Various sedimentary and geochemical proxies, such as bentonite beds and carbon isotope excursions associated with the far-reaching environmental effects of the Siberian Traps, the High Arctic Large Igneous Province, and the North Atlantic Igneous Province are present in Svalbard's near complete geological record. As such, Svalbard is unique in that these and numerous other global environmental perturbations are recorded within a relatively restricted study area, with most of the key events preserved and recorded in easily accessible drill cores and well-exposed outcrop sections. Here we review deep-time paleoenvironmental and paleoclimate research in Svalbard by summarizing 148 peer-reviewed scientific articles. The review builds on the well-established tectono-stratigraphic and lithostratigraphic framework, as well as state-of-the art environmental reconstructions to provide insights into the Earth system during the Phanerozoic northward drift of Svalbard and the many major biotic crises in the geological past. We focus on globally significant events including i) the expansion of Devonian vegetation, ii) the Carboniferous-Permian response to icehouse conditions during the Late Paleozoic Ice Age (LPIA), iii) the End-Permian Mass Extinction (EPME) and the subsequent Triassic recovery, the iv) Carnian Pluvial Episode, v) Jurassic-Early Cretaceous climate perturbations including the Volgian Isotopic Carbon Excursion (VOICE) and the Aptian Ocean Anoxic Event 1a (OAE1a), and vi) the Paleocene-Eocene Thermal Maximum (PETM). We present and synthesize existing core and outcrop data that preserve biological and geochemical proxies and climate sensitive sedimentary facies that reflect environmental change in terrestrial and marine settings. Finally, we discuss the Phanerozoic climate recorded in Svalbard and its role in providing high latitude calibration points for several global paleoclimate events to provide a higher latitude perspective to complement the dominance of mid- and low-latitude locations and datasets in the literature.

1 Introduction

The recent Intergovernmental Panel on Climate Change report (IPCC; Pörtner et al., 2022) and the Intergovernmental Science-Policy Platform on Biodiversity and Ecosystem Services (Watson et al., 2019) highlight the challenges humanity is facing due to ongoing and projected climate change. Human-environment interactions have accelerated dramatically through the industrial revolution, and the human species is now considered to be a dominant geological force on the planet (Stewart, 2016). The rate of change the planet is experiencing is unprecedented for at least the last 66 Ma (Zeebe et al., 2016), which could lead to a biodiversity crisis of similar amplitude to those experienced during previous hyperthermals throughout the Phanerozoic. However, it is still uncertain when ecological tipping points occur, at which an ecosystem can no longer cope with

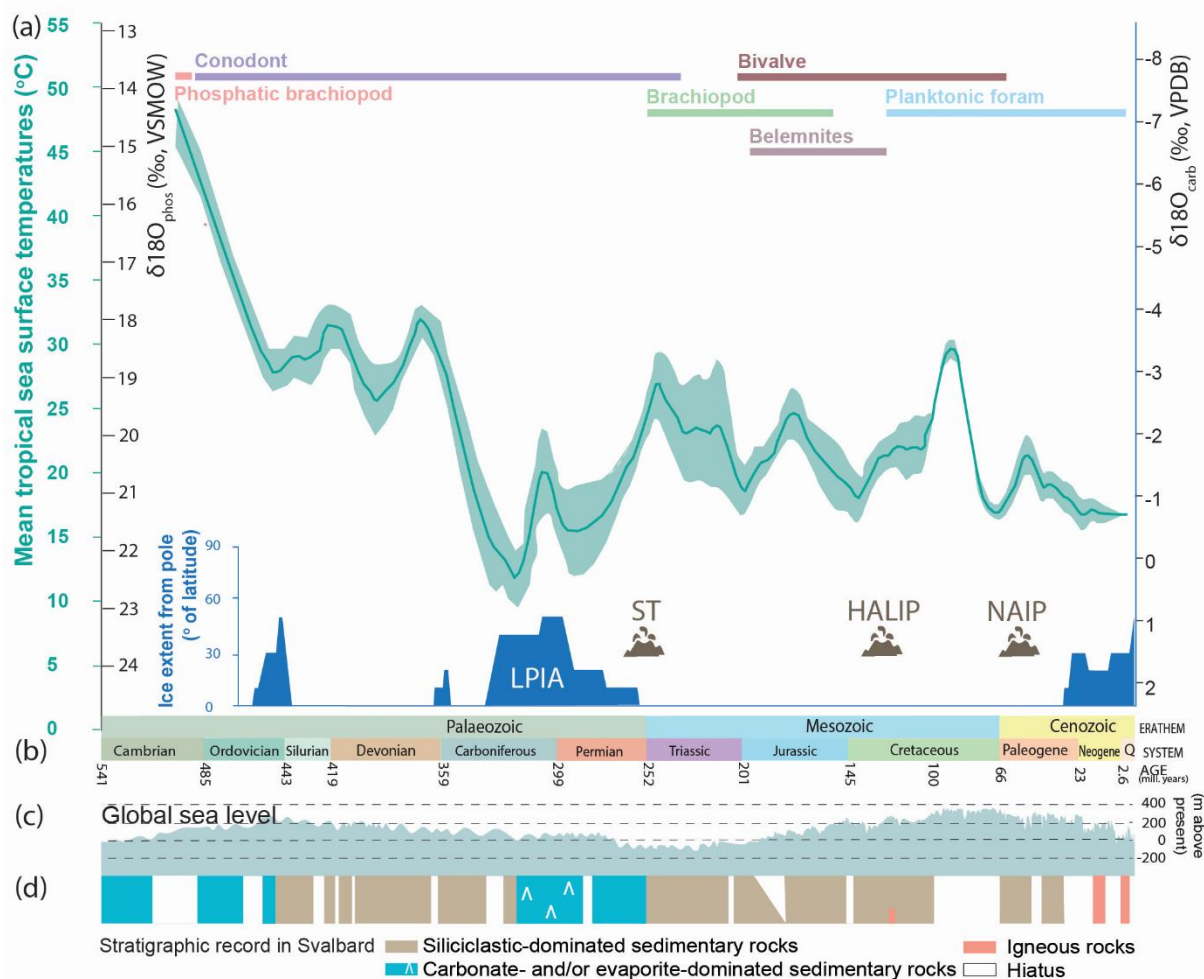


environmental change, will be reached. It is thus critical to understand and define the trajectories and pace of ecological change that is the result of a major climate perturbation.

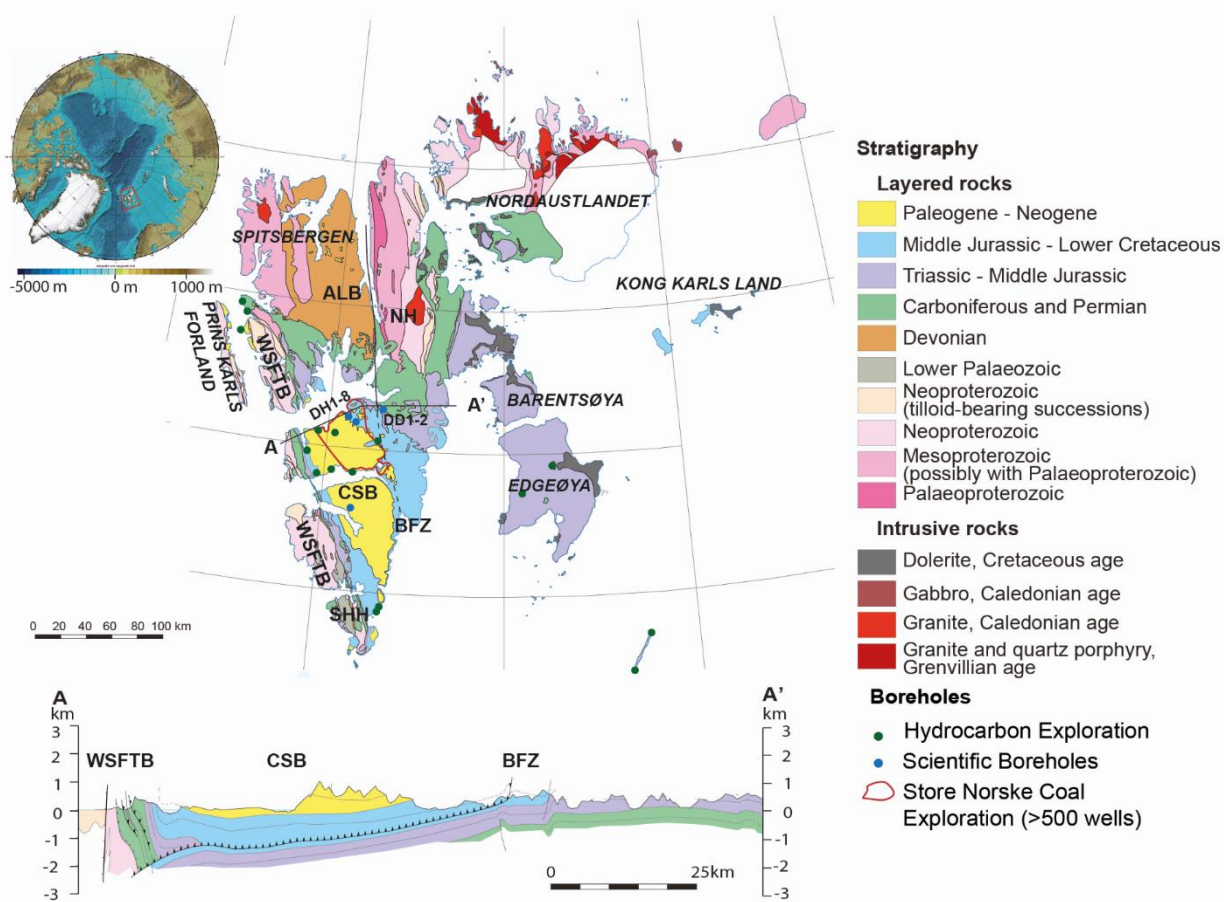
75 Studying episodes of past climate change, as recorded in the geological record, can provide insights into the response of Earth system processes to climate perturbations. Deep-time paleoclimatology, here considered to be pre-Quaternary (i.e., older than 2.58 Ma; all absolute ages refer to the International Stratigraphic Chart 2023/09), in its broadest sense refers to deciphering how and why the climate changed in the past, and the consequences of those changes to life on Earth. Throughout the pre-Quaternary Phanerozoic (ca. 538.8 Ma to 2.58 Ma), mass extinctions or smaller scale biodiversity crises occurred repeatedly, often in response to rapid climate change (Fig.1.; e.g., Bond and Grasby 2017; Kemp et al., 2015). Understanding past climate trends and episodes of major environmental perturbations will better constrain our understanding of the causes and consequences of future change (e.g., Soreghan 2004; Jansen et al., 2007). Many proxies exist to constrain past paleoenvironmental and climatic settings, grouped into biological, chemical and geophysical including climate sensitive sedimentary facies. Different proxies are suitable for quantifying various paleoclimatic signals, including volcanic activity, atmospheric gas concentration, land/sea temperature, seasonality, precipitation, and ocean oxygenation.

85 Significant perturbations to global climate are often related to relatively short-lived catastrophic events (from minutes to 1-2 Myr), including meteorite impacts, volcanic and kimberlite eruptions, the emplacement of large igneous provinces (LIPs; Bryan and Ernst, 2008; Green et al., 2022) and the biogeochemical cascades that these events cause. These events disturb Earth's biosphere by causing extreme changes in temperature, precipitation, wildfire frequency, sea level, oxygen level, and saturation states of biologically important elements (e.g., aragonite saturation state of the oceans; Hönisch et al., 2012), release of deleterious substances such as mercury (e.g., Grasby et al., 2011; Sanei et al., 2012; Galloway and Lindström, 2023), and trophic knock-on effects, affecting both the atmosphere and marine realms (Jenkyns, 2010). LIP volcanism in particular directly perturbs the climate system via release of gasses directly to the atmosphere, including SO₂, CH₄ and CO₂, as well as HCl, halocarbons, and Hg. LIP emplacements are in turn often associated with global environmental changes, including mass extinctions and smaller scale biotic crises such as oceanic anoxic events (OAEs; Grasby et al. 2011; Bond et al, 2014; Ernst and Youbi, 2017; Jones et al., 2016; Svensen et al., 2019). LIPs, by definition (Bryan and Ernst, 2008), involve significant igneous volumes if igneous material (>0.1 million km³) emplaced or erupted over large areas (>0.1 million km²) in an intraplate setting and within a short duration (1-5 Myr pulse for >75% of the volume, 50 Myr maximum lifespan), although some igneous activity broadly accepted as LIPs have protracted histories (e.g., the High Arctic Large Igneous Province; HALIP; Dockman et al., 2018; Heyn et al., 2024).

90
95
100



105 **Figure 1: The stratigraphic record of Svalbard in a global deep-time climate context. (a) global data coverage including mean tropical**
sea surface temperatures per Myr marked as a green curve, with shaded area 95% confidence intervals, based on oxygen isotopes
from phosphatic and carbonate fossils from Scotese et al., (2021), after Song et al., (2019); The scale of $\delta^{18}\text{O}_{\text{Phos}}$, black axis on the left
represents phosphatic fossils (phosphatic brachiopod, conodont, and fish). The scale of $\delta^{18}\text{O}_{\text{Carb}}$ black axis on the right, represents
carbonate fossils, (belemnite, bivalve, brachiopod, planktonic foraminifera). The Ice extent from pole after Macdonald (2020); major
LIPs recorded in Svalbard: ST-Siberian Traps, HALIP- High Arctic Large Igneous Province, NAIP- North Atlantic Igneous
 110 **Province, (b) Phanerozoic time scale, (c) Sea level curve (after Dallmann (ed) (2015), based on work of the International Commission**
on Stratigraphy,) (d) overview of the geological record of Svalbard (modified from Dallmann (ed) (2015)).



115 **Figure 2: Geological map of Svalbard and a regional cross-section illustrating the major structural elements of central Spitsbergen and spatial coverage of industrial and research boreholes of relevance to deep time paleoclimatic studies. Upper left: International Bathymetric Chart of the Arctic Ocean (IBCAO; Jakobsson et al. (2012)). Geological Map of Svalbard and cross-section (A-A'; bottom) from Dallmann (ed) (2015), Norwegian Polar Institute. Location of boreholes from Senger et al., (2019). NH- Nordfjorden High, SHH- Sørkap Hornsund High, ALB- Andrée Land Basin, BFZ- Billefjorden Fault Zone, WSFTB- West Spitsbergen Fold and Thrust Belt.**

120 Svalbard is a Norwegian archipelago comprising all islands between 74°–81°N and 15°–35°E, including the largest island of Spitsbergen (Fig. 2). Extensive amounts of geological data have been acquired from outcrops and drill cores across Svalbard. This data collection was largely triggered by the importance of Svalbard as an equivalent to the sedimentary successions in the offshore areas of the Norwegian Barents Sea (Steel and Worsley 1984; Olaussen et al., 2025 and references therein). The stratigraphic succession in Svalbard is almost complete (Fig. 1) with distinctive shifts in deposition over time, indicating a

125 genetic link between deposition and paleolatitude position (Fig. 3), as initially identified by Steel and Worsley (1984). Svalbard's Phanerozoic paleoenvironmental evolution is largely controlled by two main factors: 1) the northward tectonic



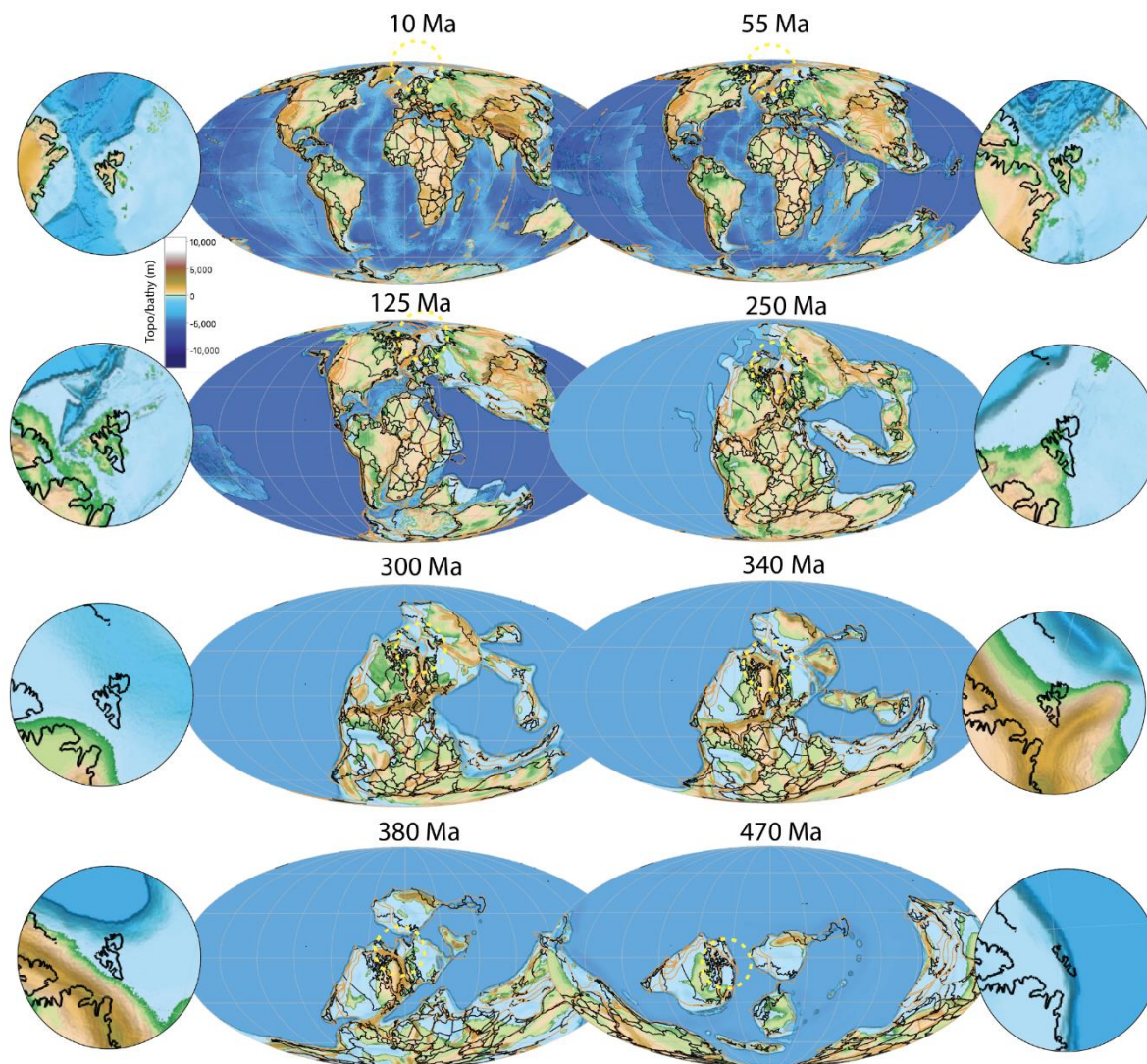
130 motion of Svalbard from equatorial to polar latitudes (Fig. 3), and 2) the influence of proximal and distant LIPs (Fig. 1). Svalbard's lower Paleozoic geological record expresses its affinity to Laurentia. Broadly speaking, Svalbard was part of the Laurasian or Eurasian plates during its post-Devonian history. The overall northward motion from an equatorial position in the Devonian and early Carboniferous to its present polar location during the Late Cretaceous (Fig. 3) was a response to absolute plate movement and relates to the break-up of the supercontinent Pangea near the end of the Jurassic. The LIPs influencing the depositional record in Svalbard (Fig.3) include the Siberian Traps, implicated as the causal factor of the end-Permian mass extinction (EPME; ca. 252 Ma; Reichow et al., 2009; Burgess et al., 2017), the High Arctic Large Igneous Province (HALIP) that influenced paleoenvironments of Svalbard and much of the circum-Arctic area during the Early Cretaceous (Midtkandal et al., 2016; Vickers et al., 2019; Galloway et al., 2022; 2023; Galloway and Lindström, 2023), and the North Atlantic Igneous Province (NAIP), associated with the opening of the North Atlantic and the warming of the Paleocene-Eocene Thermal Maximum (PETM; started ca. 56 Ma; Charles et al., 2011). Many of these regional to global-scale events can be directly studied on the exceptional sedimentary rock exposures of Svalbard, notably the vertically tilted Festningen section in western Spitsbergen (e.g., Grasby et al., 2015; Vickers et al., 2019; 2023; Senger et al., 2022). These and other events have also been recorded in drill cores collected for coal exploration, research purposes, and CO₂ storage in central Spitsbergen (e.g., Dypvik et al., 2011; Midtkandal et al., 2016; Grundvåg et al., 2017; Olaussen et al., 2019; Senger et al., 2019; Zuchuat et al., 2020; Jelby et al., 2025).

145 The Arctic has warmed twice to nearly four times faster than the rest of the globe in recent decades (Rantanen et al., 2022). This phenomenon, known as polar amplification, is largely due to oceanographic and atmospheric feedback processes (e.g., Screen and Simmonds, 2010). Polar amplification is apparent from the geological past as extreme climates that are inexplicable in current model gradients (Evans et al., 2018; Price et al., 2020). Due to the current position of Svalbard and its paleogeographic history, the nearly continuous Phanerozoic record on Svalbard provides an ideal site to study polar amplification; and prior to the Cretaceous, to elucidate the effects of the break-up of supercontinents and subsequent northward plate tectonic movement (Fig.3).

150 Currently, there are no compilations of paleoclimate and paleoenvironmental research from Svalbard addressing the pre-Quaternary Phanerozoic depositional record that is available. As a first, this study synthesizes the stratigraphic record covered by drill core material and high-quality outcrops with reliable geochronological constraints. This contribution also provides an overview of the range of proxies used to reconstruct Svalbard's paleoenvironmental evolution. Owing to its own unique tectonostratigraphic evolution, we do not include the successions exposed on Bjørnøya (the southernmost island of the Svalbard archipelago) in this review (see papers by Worsley et al., 2001; Grundvåg et al., 2023; Janocha et al., 2024, for details on this succession). To provide a framework for the review of Svalbard's deep-time climate history, the five-step paleoclimate classification of Zhang et al., (2016) was used which recognizes five major climates. These are: A- Tropical, B-Dry, C-Temperate, D-Continental and E-Polar. This division enables the deep-time climate classification estimated primarily from climatically sensitive deposits and paleontological evidence supplemented by geochemical proxies including isotope data. We systematically compile published literature (n=148) with relevance for deep-time paleoclimate and paleoenvironments in



Svalbard. The synthesized data proxies (e.g., TOC, $\delta^{18}\text{O}$, and $\delta^{13}\text{C}$) reflect environmental changes in terrestrial and marine ecosystems that are presented in the broader context of pan-hemispherical and global climate events. The overall evolution of the paleoclimate preserved in the geological record of Svalbard is discussed and compared with the paleo-position of Svalbard and global average temperature trends.



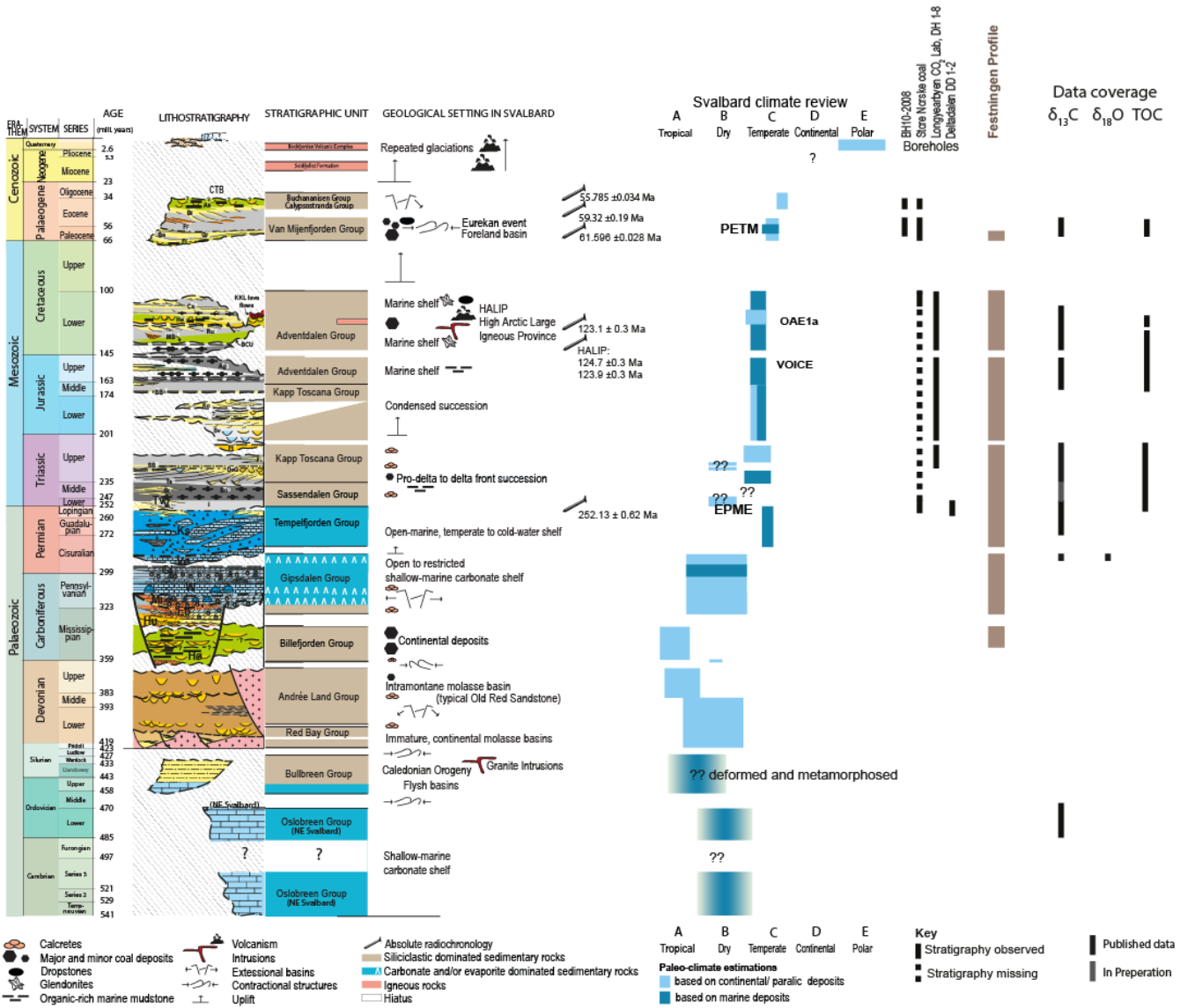
165

Figure 3: Global paleogeography (PaleoDEMs) from Scotese and Wright (2018), redrawn via export from GPlates (v2.5 Müller et al. 2018) for selected timesteps. Terrane boundaries in orange and political boundaries and present-day coastlines in black. Yellow dashed ring in the global Mollweide projections identifies the approximate location of Svalbard at the selected time periods with zoom in shown to the side of global maps. As this is a global model there may be discrepancies from regional Svalbard paleogeography whereby the reader is directed to Dallmann (ed) (2015) for regional resolution.

170

2. Tectonic and stratigraphic development

The sedimentary successions preserved in Svalbard record a changing climate controlled to a large degree by the paleo-latitude of Svalbard along with global climatic transitions (e.g., Steel and Worsley, 1984). Since the start of the Paleozoic, Svalbard gradually drifted from near-equatorial latitudes to its present position at 74–81°N (Fig. 3; Scotese et al., 1979; Torsvik et al., 2002; Torsvik and Cocks, 2019).



180 **Figure 4: Stratigraphic column and climate summary of Svalbard highlighting the nearly continuous sedimentary record from the Devonian to the Neogene. The stratigraphic coverage of research boreholes is indicated. Post-Devonian lithostratigraphic column after Olausen et al. (2025). The Climate zones from Zhang et al., (2016). Illustration of data coverage is based on Gruszczynski et al., (1989); Mii et al., (1997); Wignall et al., (1998; 2016); Galfetti et al., (2007); Cui et al., (2011); Buggisch et al., (2012); Mueller**



185 et al., (2014); Bond et al., (2015); Grasby et al. (2015a); Koevoets et al., (2016); Midtkandal et al., (2016); Vickers et al., (2016; 2019a; 2023), Hammer et al., (2019); Doerner et al., (2020); Jelby et al., (2020); Zuchuat et al. (2020); Wesenlund et al., (2021); Blattmann et al., (2024); Leu et al., (2024).

2.1. Paleozoic (Cambrian to Permian ca. 538-252 Ma)

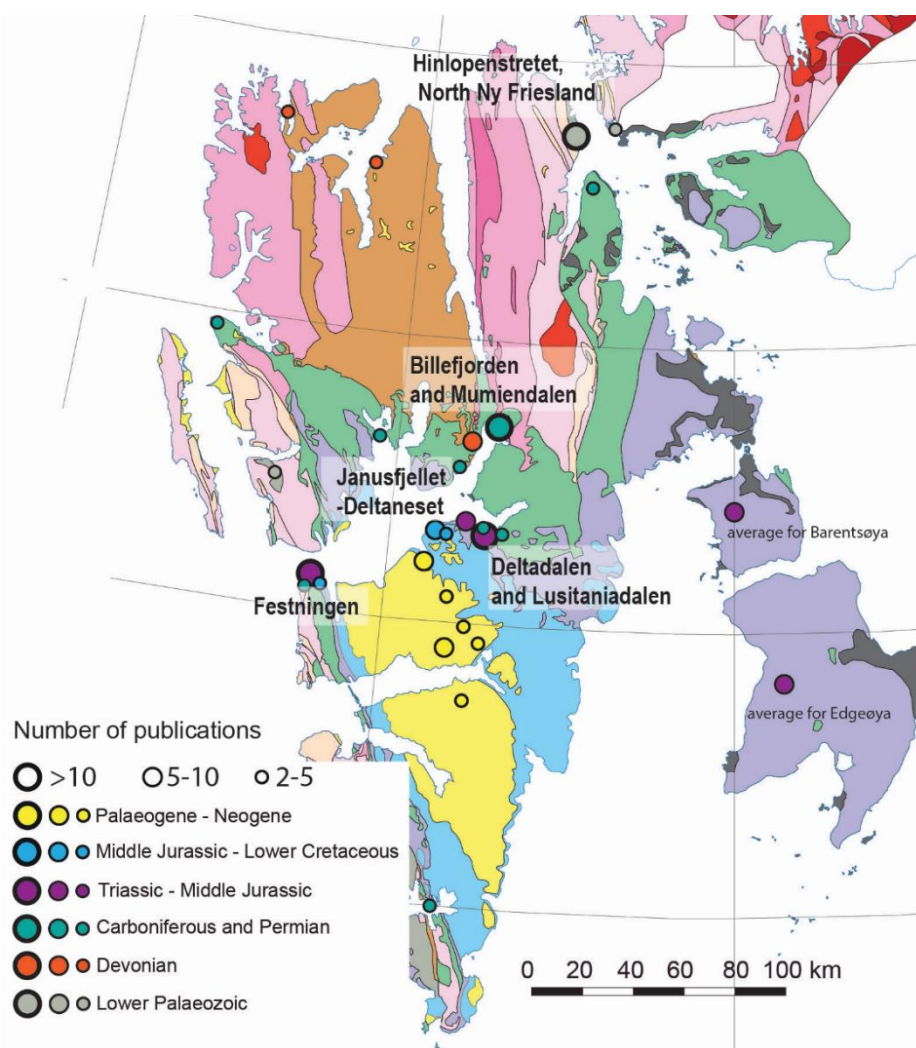
The early Paleozoic succession of the Oslobreen Group (Fig. 4) preserved in northeastern Svalbard (Fig. 2) was deposited on the northern margin of Laurentia in a post-rift to a passive margin setting (Fig. 3; Smelror et al., 2024). Later, the Caledonian Orogeny started with the closure of the Iapetus Ocean and subsequent collision of Laurentia and Baltica in the Early Ordovician-Early Devonian (ca. 485–410 Ma; Barentsian Caledonides in Gee et al., 2006; 2008; Gee and Tebenkov, 2004; Harland et al., 1974). Caledonian deformation, metamorphism, and late crustal magmatism impacted mainly western and central-northern Svalbard, leaving the north-eastern parts of the archipelago practically undeformed (Johansson et al. 2004; 2005; Smelror et al., 2024).

195 The syn- to post-Caledonian, Upper Silurian (Pridoli?) to Upper Devonian (Fransian) Old Red Sandstone (ORS) succession (ca. 423–372 Ma) represented by the Siktefjellet, Red Bay and Andrée Land groups (Fig. 4; Friend et al., 1997; Blomeier et al., 2003a; 2003b) is preserved in post-orogen collapse basins located in the central part of northern Spitsbergen (Fig. 2; Piepjohn et al., 2000; Blomeier et al., 2003; Braathen et al., 2018; Smelror et al., 2024). Significant deformation of the ORS succession subsequently took place during the Late Devonian compressional Svalbardian Event that is correlated with 200 Ellesmerian Orogeny in Arctic Canada (McCann, 2000; Piepjohn, 2000; Bergh et al., 2011; Piepjohn and Dallmann 2014; Piepjohn and von Gosen, 2018; Beranek et al., 2020).

The Tournaisian (?)– Viséan (ca. 359–330 Ma) continental coal-bearing deposits of the Billefjorden Group are widespread across Spitsbergen (Fig. 2) and unconformably overlie the deformed Devonian and pre-Caledonian succession (Piepjohn et al., 2000). The thickness of the Billefjorden Group reaches up to 250 m in central Spitsbergen (Cutbill and Challinor, 1965; 205 Gjelberg and Steel, 1981) and 40–100 m in northeastern Spitsbergen (Lauritzen and Worsley, 1975; Scheibner et al., 2012). The thickness along the west coast of Spitsbergen is uncertain due to younger deformation and repetition of the succession. The Billefjorden Group is unconformably overlain by the Serpukhovian (upper Mississippian) to Artinskian (Cisuralian) mixed siliciclastic-carbonate-evaporite deposits of the Gipsdalen Group (ca. 331–284 Ma). The lower Gipsdalen Group consists of syn-tectonic units filling up rift basins, the Billefjorden, Lomfjorden, St Jonsfjorden, and Inner Hornsund troughs, developed 210 along north-south striking long-lived lineaments formed in response to regional-scale extension (Fig. 4; Holliday and Cutbill, 1972; Gjelberg and Steel, 1981; Johannessen and Steel, 1992; Faleide et al., 2008; Braathen et al., 2012). The thickest (> 1.5 km) and best-preserved basin fill occurs in the Billefjorden Trough while corresponding succession is missing on the structural highs (Fig. 2; Cutbill and Challinor 1965; Johannessen and Steel, 1992; Braathen et al., 2012; Smyrak-Sikora et al., 2018; 2021). The syn-rift units of the lower Gipsdalen Group were subsequently overlain by an up to 500 m thick warm-water 215 carbonate-platform deposits of the upper Gipsdalen Group (Hüneke et al., 2001; Blomeier et al., 2011; Ahlborn and Stemmerik



2015; Sorento et al., 2020). The Gipsdalen Group is overlain by upper Artinskian (Cisuralian) to Changhsingian (Lopingian) cool-water carbonate and spiculitic platform sediments of the Tempelfjorden Group (ca. 284 (?)–252 Ma). The thickness of Tempelfjorden Group varies across Spitsbergen from 6 m to 460 m (Blomeier et al., 2013; Uchman et al., 2016; Matsyik et al., 2018), including complete absence of Permian deposits on the Sørkapp–Hornsund High, where Carboniferous fluvial deposits are unconformably overlain by Lower Triassic continental conglomerates (Zuchuat, 2014). These thickness variations indicate ongoing uplift of the Nordfjorden High and the Sørkapp–Hornsund High that can be linked with the late Permian rift event along the western Barents shelf margin (Faleide et al., 2008; Olausen et al., 2025).



225

Figure 5: Location of data presented in the reviewed articles summed up in Table A1 (Supplementary table) highlighting the most studied sections in Svalbard. The size of a circle corresponds to the number of publications addressing deep-time paleoclimate proxies. For legend to the geological map see Fig. 2.



230 2.2. Mesozoic

In the Early to Middle Triassic (ca. 252–237 Ma), Svalbard was part of a shallow shelf that experienced significant subsidence and which was filled with up to 700 m of sediments sourced from west and east (the Sassendalen Group; Fig. 4; Mørk et al., 1982; 1999; Wesenlund et al., 2022; Bjerger et al., 2023). By the end of the Middle Triassic (ca. 237 Ma), deltaic systems sourced in the Uralides and the Fennoscandian Shield reached and probably traversed Svalbard (Riis et al., 2008; Glørstad-Clark et al., 2010; Høy and Lundschieen, 2011; Anell et al., 2013; Klausen et al., 2017; 2019; Gilmulina et al., 2022). Towards the latest Triassic and Early Jurassic, subsidence rates gradually decreased and sometimes even became negative, as expressed by condensed units with a 20 m-thick, shallow-marine and continental sandstone-shale unit of Rhaethian (latest Triassic; ca. 208–201 Ma) to Bathonian (?) age (Middle Jurassic; ca. 168–165 Ma), truncated by several subaerial unconformities (Drachev, 2016; Faleide et al., 2018; Olaussen et al., 2018; Rismyhr et al., 2018; Müller et al., 2019). This Upper Triassic deltaic and Upper Triassic to Middle Jurassic condensed section belongs to the Kapp Toscana Group. Subsidence rates increased again during the Late Jurassic (ca. 161–145 Ma), which led to the deposition of organic-rich marine strata of the lower Adventdalen Group (e.g., Koevoets et al., 2016; 2019).

The upper Middle and Upper Jurassic/lowermost Cretaceous succession preserved in Svalbard consist of the Agardhfjellet Formation, and the Lower Cretaceous succession is represented by the Rurikfjellet, Helvetiafjellet, and Carolinefjellet formations, all assigned to the Adventdalen Group (Fig. 4). These marine to continental units reflect increased subsidence with uplift in the north and northwest that formed a continental, siliciclastic platform. This uplift is related to emplacement of the HALIP across the Arctic, including Svalbard, Franz Josef Land, the New Siberian Islands, the Barents Shelf, Sverdrup Basin, northern Greenland, and the Alpha-Mendeleev Ridge, via both subaerial eruptive and intrusive magmatism (Maher, 2001; Estrada and Henjes-Kunst, 2013; Senger et al., 2014; Evenchick et al., 2015; Polteau et al., 2016; Davis et al., 2017; Dockman et al., 2018; Naber et al., 2021; Bédard et al., 2021; Galloway et al., 2022). HALIP magmatism is thought to be derived from the arrival of a thermally elevated mantle plume that caused large volumes of mafic rocks including sills, dykes, lavas, and pyroclastic material (Maher, 2001; Senger et al., 2014; Buchan and Ernst, 2018; Bédard et al., 2021; Naber et al., 2021; Heyn et al., 2024). Robust U-Pb dating points to a short magmatic pulse affecting Svalbard at ca. 124.5 Ma (Corfu et al., 2013). However, in the adjacent Sverdrup Basin (Arctic Canada), multiple magma emplacement episodes have been identified, with pulses peaking at 122 ± 2 Ma, at 95 ± 4 Ma and at 81 ± 4 Ma (Jens et al., 2015; Kingsbury et al., 2017; Davis et al., 2017; Dockman et al., 2018; Bédard et al., 2021; Dummann et al., 2024). In Spitsbergen, the HALIP-activity triggered southward tilting of the platform, which resulted in progradation of a sand-rich fluviodeltaic system towards the south (Steel and Worsley, 1984; Gjelberg and Steel, 1995; Worsley, 2008; Midtkandal and Nystuen, 2009; Grundvåg and Olaussen, 2017; Grundvåg et al., 2017). The extent of the uplifted and eroded area increased during the Late Cretaceous (ca. 100–66 Ma) to the whole of Svalbard, which resulted in the upper middle Albian deposits (uppermost Lower Cretaceous; ca. 113–100 Ma; Hurum et al., 2016) being unconformably overlain by Paleocene strata (Jochmann et al., 2019; Helland-Hansen and Grundvåg, 2021).



2.3. Cenozoic

The mid-Paleocene saw the recommencement of sediment deposition in Svalbard after a ~60 Myr hiatus in response to large-scale regional changes in plate tectonic configurations (Fig. 3). The base of the Paleocene strata in Svalbard has been dated to 265 61.8 Ma (Jones et al., 2017), close to the Danian–Selandian boundary (ca. 61.6 Ma). This age is contemporaneous with several changes around the Greenland microplate, including increased rifting between Greenland and Eurasia in the proto-Northeast Atlantic region (Abdelmalak et al., 2023), the first pulse of North Atlantic Igneous Province (NAIP) volcanism (Storey et al., 2007a), a change from carbonate- to siliciclastic-dominated sediments in the North Sea (Clemmensen and Thomas, 2005), widespread shear deformation along eastern Greenland (Guarnieri, 2015), and an increase in the rate of seafloor spreading in 270 the Labrador Sea (Roest and Srivastava, 1989; Oakey and Chalmers, 2012). The combination of seafloor spreading in the Labrador Sea and rifting along the mid-Norwegian margin instigated compression between Greenland and Svalbard, which evolved into a dextral transpressional regime as rifting transitioned to seafloor spreading in the NE Atlantic by 55 Ma (Storey et al., 2007b). This period was also coincident with the rifting and breakup of the Eurasia Basin to the north of Svalbard. The dextral transpression along the Greenland–Svalbard margin caused localized crustal shortening and the formation of the West 275 Spitsbergen Fold and Thrust Belt, WSFTB (Fig. 3; Harland, 1965), linked to the Eurekan deformation (ca. 63–35 Ma) and plate reorganization in the North Atlantic (Dallmann et al., 1993; Braathen et al., 1995; 1999; Maher and Braathen, 1995; Bergh et al., 1997; Gee and Tebenkov 2004; Faleide et al., 2008; Leever et al., 2011; Blinova et al., 2013; Piepjohn et al., 2015; 2016; Gion et al., 2017). A north-south trending foreland basin, known as the Central Spitsbergen Basin (CSB) or the Central Tertiary Basin (CTB) in older literature, formed east of the WSFTB and was filled with over 1.9 km thick Paleocene 280 to Eocene (Oligocene?) deposits of the Van Mijenfjorden Group (Figs 3; Steel et al., 1981; 1985; Helland-Hansen, 1990; Müller and Spielhagen, 1990; Bruhn and Steel, 2003; Jochmann et al., 2020; Helland-Hansen and Grundvåg, 2021). During the Paleocene–Eocene transition (ca. 56 Ma), a passive margin started to develop to the north of Svalbard as a result of the opening of the Eurasia Basin. Finally, an Oligocene (ca. 34–23 Ma) transtensional rift phase eventually gave way to the formation of a passive margin west of Spitsbergen (Faleide et al., 2008; Lasabuda et al., 2018; Haaland et al., 2024).

285 The transpressional deformation related to the WSFTB was followed by NW–SE transtensional rifting that formed a series of grabens along the western Svalbard margin (Steel et al., 1985; Blinova et al., 2009; Kleinspehn and Teyssier, 2016; Kristoffersen et al., 2020; Haaland et al. 2024). The Forlandsundet Graben, one of the grabens cropping out between the islands of Prins Karls Forland and Spitsbergen (Fig. 2) contains between 1000–3000 m of Eocene to potentially Oligocene strata (Gabrielsen et al., 1992; Schaaf et al., 2021). The final separation between Greenland and the Barents Shelf margin eventually 290 led to the opening of the Fram Strait. A shallow and narrow gateway was initially established around 20 Ma (Jokat et al., 2016; Fyhn and Hopper, 2025), and the transition from a restricted to fully ventilated Arctic Ocean took place around 17.5 Ma (Jakobsson et al., 2007). The establishment of a deep-water connection through the Fram Strait is currently debated, with suggested ages of 13.7 Ma (Jakobsson et al., 2007), 10 Ma (e.g., Kristoffersen and Husebye, 1985; Kristoffersen, 1990), and



5 Ma (Lawver et al., 1990). During these times, Svalbard and the rest of the Barents Shelf margin experienced several changes
295 in motion relative to the adjacent Greenland plate.

The present archipelago configuration of Svalbard with respect to the otherwise submerged setting of the Barents Shelf is
thought to be a consequence of a combination of uplift during the Late Cretaceous, Paleocene-Eocene Eureka deformation,
and ongoing Holocene (last 11.7 kyr) isostatic rebound (Dimakis et al., 1998; Worsley, 2008; Henriksen et al., 2011; Dörr et
al., 2013; Lasabuda et al., 2021). This uplift and exposed nature of Svalbard has resulted in the present-day exhumation of the
300 metamorphic succession along the northern and western coasts of Svalbard and the younger sedimentary cover as described
above (Fig. 3).

3. Data

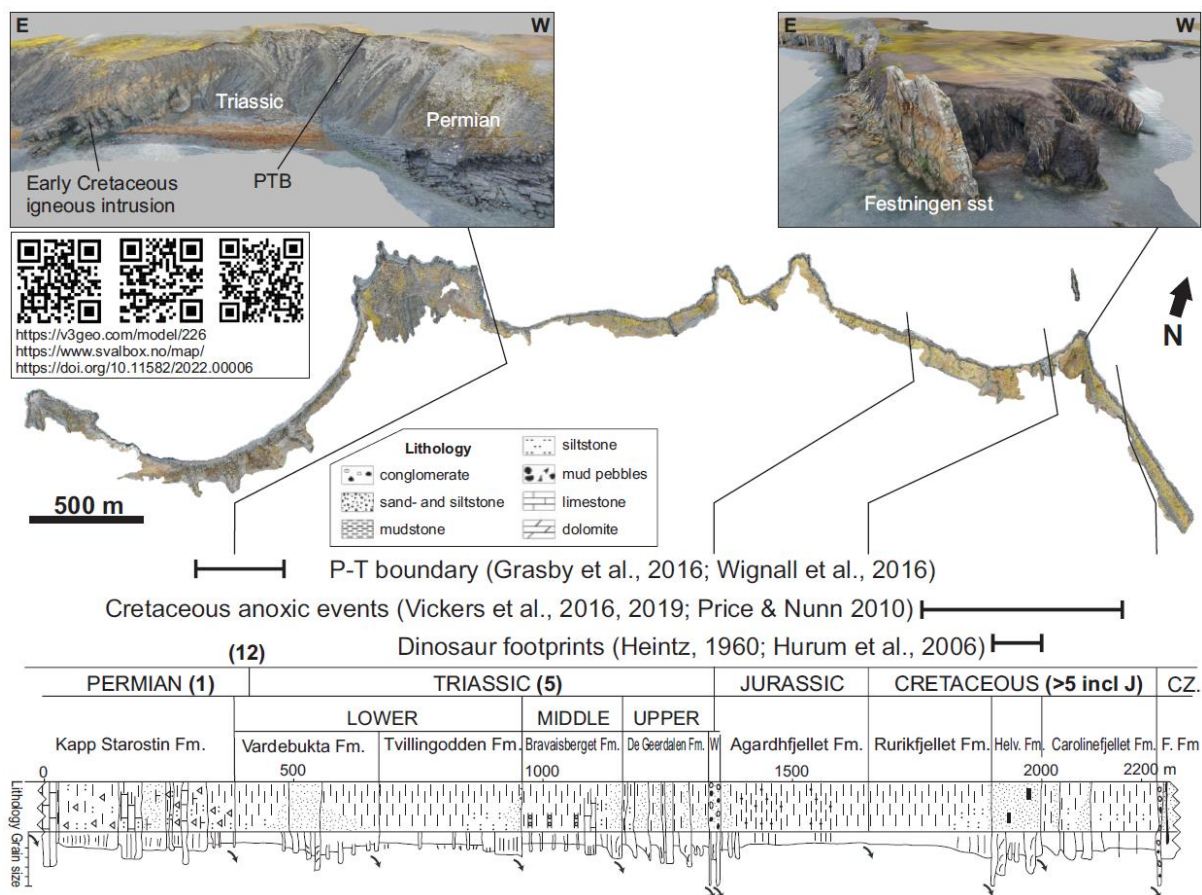
Paleoclimate research in Svalbard has traditionally relied on the exceptionally exposed and vegetation-free outcrops, typical
305 of the present Arctic landscape. For the last two decades, research drilling across Svalbard has increasingly been utilized and
provides unique drill core material suitable for high-resolution paleoenvironmental and paleoclimate research.

3.1 Key stratigraphic sections

Figure 5 shows the geographic distribution of the primary study sites referenced in the 148 key publications summed up in
Table 1 and in Table 2 (listed with more details in Supplementary table). Many of these articles are centered on important sites
310 with good chronological and lithological constraints. Most of the outcrops are also covered by high-resolution digital outcrop
models freely available through the Svalbox database (Betlem et al, 2023), facilitating data integration. Four of the localities
are represented by 10 or more publications and are described below.

3.1.1 Festningen

The Festningen section in western Spitsbergen offers a nearly complete stratigraphic section spanning from the Mississippian
315 (ca. 359 Ma) to the Paleocene (Fig. 6). The ~7 km long section is easily accessible along the shoreline, with nearly-vertical
sedimentary layers due to Eureka deformation. Festningen is an important regional stratigraphic profile and routinely targeted
by geologists (Hoel and Orvin 1937; Steel et al., 1978; Mørk et al., 1982; Nagy and Berge 2008; Midtkandal and Nystuen,
2009; Grundvåg et al., 2019), including those interested in deep-time paleoclimate (e.g., Grasby et al., 2015; Vickers et al.,
2023). Mørk and Grundvåg (2020) offers a geological guidebook for the section, whereas Senger et al., (2022) provided an
320 open-access digital outcrop model (DOM) of the 5 km long part of the protected section. The high-resolution (7 mm pixel
resolution) DOM is suitable for planning additional sampling, quantitative structural and sedimentological analyses, and
integrating existing paleoclimatic research (Fig. 6).



325 **Figure 6: Stratigraphic column of the best-preserved part of the Festningen section, from Mørk and Grundvåg (2020), tied to the**
digital model of the entire Festningen section as presented in Senger et al., (2022). The inset images of the Permian-Triassic boundary
and the Festningen sandstone illustrate screenshots of the digital outcrop model that is accessible online and freely available for
download by following the QR codes and URLs. Paleoclimate-related research conducted on the section is highlighted for key events.
These include amongst others the end-Permian mass extinction and the subsequent recovery phase (e.g. Wignall et al., 1998; Grasby
et al., 2016), as well as several Cretaceous cooling events, anoxic events, and their associated deposits (Price & Nunn, 2010; Vickers
 330 **et al., 2016, 2019; Grundvåg et al., 2019). Abbreviations: CZ = Cenozoic, W = Wilhelmøya Subgroup, Helv. Fm = Helvetiafjellet Fm,**
F. Fm = Firkanten Fm. The QR codes provide direct access to the digital model. Figure modified after Senger et al. (2022).

3.1.2 Janusfjellet-Deltaneset

The Janusfjellet section in central Spitsbergen exposes an Upper Triassic to Paleocene siliciclastic-dominated succession that
 335 has been extensively studied as part of the Longyearbyen CO₂ lab project (Olaussen et al., 2019). The succession includes both
 the Upper Triassic-Middle Jurassic sandstone reservoirs of the Kapp Toscana Group as well as the overlying Upper Jurassic-
 Lower Cretaceous Adventdalen Group. The Agardhfjellet Formation, the lowermost part of the Adventdalen Group, has also
 been extensively studied as one of the richest marine reptile sites in the world, yielding sixty specimens so far (Hurum et al.,
 2012; Delsett et al., 2016; 2019), along with an abundant seep fauna (Hryniewicz et al., 2015). The outcropping section dips



340 gently at about 3° to the south-west and exposes the same stratigraphy as in the fully cored boreholes in Adventdalen (Olaussen
et al., 2019). As an excellent analog to the Longyearbyen CO₂ lab reservoir-caprock system, the outcrops have been
systematically studied with focus on sedimentology (Rismyhr et al., 2018; Jelby et al., 2020a), fault and fracture
characterization (Ogata et al., 2014a; 2014b; Mulrooney et al., 2018; Betlem et al., 2024; Rizzo et al., 2024), sandstone
injectites (Ogata et al., 2023) and paleoclimatic signals (Koevoets et al., 2018; Jelby et al., 2020b).

345 **3.1.3 Sassendalen**

Sassendalen is a key region for understanding the Permian-Triassic transition and evolution of Svalbard, and within
Sassendalen there are many key sections for defining different aspects of the lithostratigraphic framework of central
Spitsbergen (e.g., Mørk et al., 1999). It is also a unique area to study global ecosystem recovery after the end-Permian mass
extinction (see Hurum et al. 2018; Kear et al. 2023). Deltadalen and Lusitaniadalen are two valleys on the western side of
350 Sassendalen that excellently expose the Permian Kapp Starostin to Botneheia formations. In addition is the more eastern
Fulmardalen (Hammer et al., 2019; Hansen et al., 2024). The Deltadalen outcrop is directly next to the Deltadalen research
boreholes, where deposits of the EPME and Permian-Triassic boundary were cored (Zuchuat et al., 2020). As such, it provides
excellent borehole-outcrop correlation with the benefit of facilitating detailed sedimentological studies and high-resolution
sampling away from the boreholes. In addition, a well-exposed section of Permian-Triassic transition crops out along
355 Lusitaniadalen located around 5 km northwest from Deltadalen and has been the focus of multiple studies directly focussed on
the Permian-Triassic boundary (e.g., Mørk et al., 1999a; 1999b; Foster et al., 2017; Rauzi et al., 2024).

3.1.4 Hinlopenstretet, North Ny Friesland

The Ny Friesland section in northeastern Spitsbergen is exposed along the south coast of the Hinlopen Strait (Fig. 2) and
consists of a ~1 km thick Terreneuvian-Middle Ordovician carbonaceous succession of the Oslobreen Group (ca. 539–458
360 Ma; Hansen and Holmer, 2010; Stouge et al., 2012; Lehnert et al., 2013; Abay et al., 2022; Smelror et al., 2024). This
succession, consisting of siliciclastic shoreline facies at the base, passing up to a shallow marine warm water carbonate
platform deposits, belongs to the North Atlantic/Arctic warm water carbonate platform formed on eastern Laurentia
(McKerrow et al., 1991; Stouge et al., 2012).

365

Table 1: Overview of selected drill core material and key sections (including digital sections)

370



Key, selected boreholes with significant core or cuttings material						
Borehole(s)	Penetrated strata (age and formation)		Depth (meters)	Drill core availability	Complementary data sets	Key reference
	Youngest	Oldest				
Gipsdalen (DD1-DD8)	Pennsylvanian Ebbadalen Fm	Precambrian Basement	91,90 - 210.50	Berlin-Spandau and Uni Oslo	Technical reports	Senger et al. (2019).
Deltadalen (DD1 and DD2)	Lower Triassic Vikinghøgda Fm	Lopingian Kapp Starostin Fm	92,9 -99,3	Oslo	Reports	Zuchuat et al. (2020); Schobben et al., (2020); Rodríguez-Tovar et al. (2021)
Tromsøbreen II	Lower Cretaceous Carolinefjellet Fm	Pennsylvanian (?) Minkinfjellet Fm (?)	2337	5 cores, in Lund	Reports	Senger et al. (2019).
Reindalspasset	Lower Cretaceous Carolinefjellet Fm	Mississippian, Billefjorden Gr	2315	Cuttings, in Endalen Svalbard	Reports	Senger et al. (2019).
UNIS CO ₂ lab (DH1-DH8)	Lower Cretaceous Carolinefjellet Fm	Upper triassic De Geerdalen Fm	down to 969,7	Longyearbyen	Reports, wireline logs, publications	Corfu et al., (2013); Midtkandal et al., (2016); Polteau et al., (2016); Olausen et al. (2019); Senger et al. (2024).
SNSK boreholes, including core BH9/05	Eocene Frysjaodden Fm	Metamorphic basement	numerous	Endalen	Reports	Cui et al. (2010); Dypvik et al. (2011); Charles et al. (2011); Nagy et al. (2013); Jones et al. (2019).
Sysselembreen (BH2008-10)	Eocene (?) Oligocene (?) Aspelintoppen Fm	Late Paleocene Basilika Fm	1085	Endalen, Equinor lab (Bergen)	Reports	Johannessen et al. (2011); Doerner et al. (2020).
Key outcrop sections (> 10 publications)						
Outcrop sections	Penetrated strata (age and formation)		Extent	Key reference(s)		
	Youngest	Oldest				
Hinlopenstretet, North Ny Friesland	Ordovician	Cambrian	around 10 km	Hansen and Holmer (2010); Stouge et al. (2012); Lehnert et al. (2013); Abay et al. (2022).		
Billefjorden	Lower Permian	Upper Devonian	over 20 km of composite sections	Cutbill and Challinor (1965); Gjelberg and Steel (1981) Ahlborn and Stemmerik (2015) Berry & Marshall (2015); Davies et al. (2021); Smyrak-Sikora et al., (2021).		



Festningen	Paleogene Firkanten Fm	Carboniferous Billefjorden Gr	5-6 km	Hoel & Orvin (1937); Steel et al. (1978); Mørk et al. (1982); Nagy & Berge (2008); Midtkandal & Nystuen (2009); Grasby et al. (2015); Grundvåg et al. (2019); Mørk & Grundvåg (2020); Senger et al. (2022); Vickers et al. (2023).
Deltadalen and Lusitaniadalen	Lower Triassic Vikingshøgda Fm	Lopingian Kapp Starostin Fm	around 7 km	Dagis & Korcinskaja (1987); Mørk et al. (1999); Foster et al., (2017); Zuchuat et al., (2020);
Deltaniset- Janusfjellet	Lower Cretaceous Carolinefjellet Formation		around 7 km	Hurum et al., (2018); Rismyhr et al., (2018); Olausen et al. (2019); Koevoets et al. (2018); Jelby et al. (2020a; 2020b).

3.1.5 Billefjorden and Mumiendalen

The inner part of Billefjorden exposes the Billefjorden Fault Zone, where the several km-thick Devonian Old Red Sandstone (ORS) deposits on the west are faulted against the several metamorphic and sedimentary successions in the east. These include
375 pre-Devonian metamorphic basement, up to 250 m of Mississippian units and over 2 km of Pennsylvanian to Permian deposits (Braathen et al., 2012; Smyrak-Sikora et al., 2018; 2021). In Mumiendalen, the lowermost Upper Devonian deposits of the André Land Group expose plant fossils that represent terrestrialization and evolution of one of the oldest forests in the world, that likely thrived in a monsoonal climate (Berry and Marshall, 2015; Davies et al., 2021). Above the fossil Devonian forests
380 units, Mississippian siliciclastics with coal seams belonging to the Billefjorden Group were deposited in a humid and tropical climate (Cutbill and Challinor 1965; Gjelberg and Steel, 1981). The transition to the overlying mixed siliciclastic-carbonate-
evaporite units of the Gipsdalen Group illustrates that the climate changed from subtropical semi-arid to an arid climate prevailing in through the Pennsylvanian to Cisuralian (Holliday and Cutbill, 1972; Gjelberg and Steel, 1981; Johannessen and
Steel, 1992; Blomeier et al., 2011; Ahlborn and Stemmerik, 2015; Sorento et al., 2020; Smyrak-Sikora et al., 2021). Up section,
385 the Bashkirian to Sakmarian part of the Gipsdalen Group consisting of interbedded evaporites and carbonates formed in response to glacioeustatic sea level fluctuations (Stemmerik, 2000; 2008; Ahlborn and Stemmerik., 2015; Sorento et al., 2020; Smyrak-Sikora et al., 2021) related to the late Paleozoic Ice Age (LPIA; Gastaldo et al., 1996; Montañez et al., 2007; Isbell et al., 2008).

3.2 Drill cores

Table 1 summarizes the drill cores presently available from Svalbard. They are mostly from coal exploration by Store Norske
390 Spitsbergen Kulkompani (SNSK) and CO₂ storage research drilling in Adventdalen by The University Centre in Svalbard (UNIS); Olausen et al., 2019; Senger et al., 2024). In addition, stratigraphic research boreholes, drilled purely out of scientific interests also exist, including the Sysselembreen (Johannessen et al., 2011) and Deltadalen (Zuchuat et al., 2020) boreholes. Limited core material from past petroleum exploration efforts are known to exist (eighteen boreholes were drilled from 1960



to 1994; see review by Senger et al., 2019), but these have, hitherto, not been used in any paleoclimate investigations.
395 Nonetheless, the associated wireline data from these wells are important calibration points for regional correlation of outcrops
and onshore seismic reflection data.

3.2.1 Coal drilling

Exploration coal drilling focused on Paleocene stratigraphy of the Van Mijenfjorden Group in the Central Spitsbergen Basin
400 (CSB) and Mississippian coal-rich strata of the Billefjorden Group near Pyramididen. Lower Cretaceous and Eocene coal bearing
strata were targeted in minor campaigns. Cores from the Russian/Soviet coal mining company Trust Arktikugol including sites
near Barentsburg, Colesdalen and Pyramididen, are not available and likely lost as evidenced by defunct core sheds scattered
around Svalbard. However, reports from these drill cores (Verba, 2013) have been used locally to constrain surface geological
mapping, such as in Mimerdalen (Piepjohn and Dallmann, 2014) and in the Billefjorden Trough (Smyrak-Sikora et al., 2021).
405 The Norwegian coal mining company SNSK stores most of its cores in Endalen near Longyearbyen with drill dates ranging
from the late 1960s to 2014, the last year of Norwegian coal exploration. These cores were investigated in several paleoclimate-
related studies, particularly across the PETM and North Atlantic Igneous Province (NAIP)-related ash deposits (Table 1;
Dypvik et al 2011; Jones et al, 2019).

3.2.2 Longyearbyen CO₂ lab, DH1 to DH8

410 Eight boreholes were fully cored near Longyearbyen from 2007 to 2013 to characterize a potential CO₂ storage site (Braathen
et al., 2012; Olaussen et al., 2019; Senger et al., 2024). Four of the boreholes reach the planned Upper Triassic units of the
Kapp Toscana Group target storage unit at 670-700 m, while the other boreholes focus on the cap rock and overburden
succession of the Adventdalen Group. The full coring across the shale-dominated cap rocks provides important constraints on
the stratigraphy of the Jurassic-Cretaceous strata (Koevoets et al., 2016; Midtkandal et al., 2016; Jelby et al., 2020a; 2020b;
415 Śliwińska et al., 2020) and also contributed to refining the global geological time scale (Zhang et al., 2021). Senger et al.
(2024) provide a full overview of the data sets generated by the project including a live database of the resulting publications,
including those focusing on deep-time paleoclimate.

3.3.3 Sysselmannbreen, BH10-2008

The BH10-2008 (also known as Sysselmannbreen) research borehole was drilled and fully cored in 2008 to recover a full
420 section of the world-famous Eocene-Oligocene (?) clinoform succession of the Van Mijenfjorden Group in the CSB
(Johannessen et al., 2011). The 1085 m-long core was split with one half stored in a container in Endalen, outside of
Longyearbyen, and the other half stored in Equinor's laboratory in Bergen (Doerner et al., 2020).



3.3.5 Deltadalen, DD-1 and DD-2

425 The most recent research drilling in Svalbard was conducted in 2014 at Deltadalen specifically to target the uppermost Permian part of the Tempelfjorden Group and Lower Triassic succession of the Sassendalen Group with a specific interest in the EPME and its aftermath (Zuchuat et al., 2020). The two ca. 100 m deep boreholes were drilled and fully cored over a 1-week period, with all equipment transported onsite by helicopter. The drill cores are stored at the University of Oslo.

430 **Table 2. Summary of proxies based on Table A1 (Supplementary material), which reviews 148 selected papers. The data set is plotted in Figure 13.**

N of articles	N of papers	10	11	27	22	30	30	18
	-boreholes	0	0	0	3	2	10	9
	-outcrops	10	11	27	21	30	27	11
Proxies and data	Biological indicators	8	8	15	14	22	24	10
	Climate sensitive facies	3	7	18	2	2	3	9
	Carbon isotopes $\delta^{13}\text{C}$	2	2	8	8	6	13	6
	Oxygen isotopes $\delta^{18}\text{O}$	1	1	4	0	0	4	1
	TOC/Rock-Eval	2	2	1	3	6	7	6
	Mercury, Hg	0	0	0	2	1	1	1
Stratigraphic intervals	Cambro-Silurian	Devonian	Carboniferous-Permian	Permian-Triassic boundary	Triassic	Jurassic-Cretaceous	Paleogene	

Deep-time paleoclimate in Svalbard

4.1 Early Paleozoic (Cambrian, Ordovician, Silurian, 538.8-419.2 Ma)

4.1.1. Cambrian to Middle Ordovician- the Great Ordovician Biodiversification Event

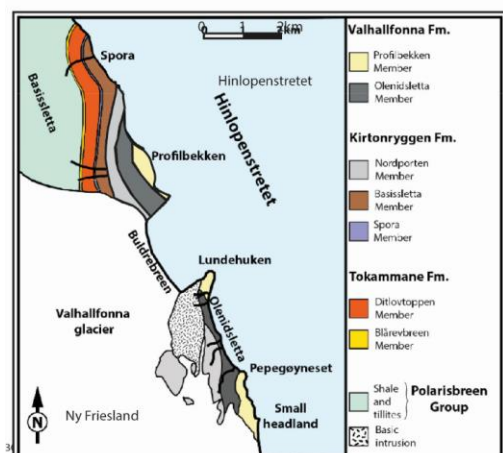
435 The early Paleozoic registered two of the greatest evolutionary events in the history of life: the Cambrian Explosion (ca. 540–510 Ma), and the Great Ordovician Biodiversification Event (GOBE; ca. 497–445 Ma.; Webby et al., 2004; Servais and Harper,



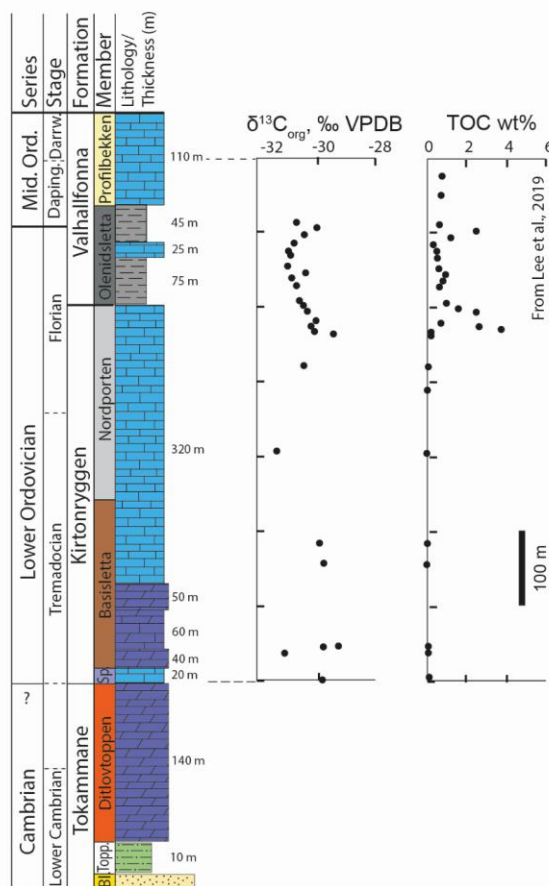
2018). This upper Furongian to Upper Ordovician diversification event is linked to cooling of previously very warm tropical oceans (Webby et al., 2004; Servais and Harper, 2018).

During the Cambrian and Ordovician, Svalbard was in a near-equatorial position (Torsvik et al., 2012; Fig. 2). The Terreneuvian to Middle Ordovician Oslobreen Group (Fig. 4) strata preserved in Svalbard formed on a large carbonate platform along the northern margin of Laurentia, also exposed in the Northeast Greenland Basin and eastern North Greenland Basin (Stouge et al., 2012; Fig. 2). The mildly deformed, 1–1.2 km thick sandstones, fossiliferous limestone and dolomite are preserved in northeastern Spitsbergen (Fig. 7; Harland and Wilson, 1956; Oslobreen Series in Gobbett and Wilson, 1960; Fortey and Bruton, 1973; Stouge et al., 2011; 2012; Dallmann et al., 2015). The succession is potentially interrupted by a ~15 Myr-hiatus spanning over the Series 2, Miaolingian, Furongian, and possibly the earliest Ordovician (Fortey and Bruton, 1973; Smelror et al., 2024), although the lack of dateable fossils might affect this interpretation (Smelror et al., 2024). The Oslobreen Group shows surprisingly low maximum burial temperatures (Bergström, 1980; Abay et al., 2022) and eastward increasing tectonothermal influence linked to the Caledonian Orogeny (Johansson et al., 2004). The trilobites and fauna generally show a Pacific and Laurentian affinity (Fortey and Bruton, 1973; Hansen and Holmer, 2010; Stouge et al., 2012).

In Ny Friesland, the Terreneuvian microbial laminated limestone/dolomite contain cm-scale erratic chert nodules. The Lower to Middle Ordovician (ca. 485–458 Ma) carbonates were deposited in a paleotropical marine shelf setting experiencing episodes of water column redox-stratification (Lee et al., 2019). Stouge (2012) also interprets the Tremadocian (Lower Ordovician; ca. 485–478 Ma) environment in Svalbard and Greenland as a typical tropical shelf. Occurrence of oolite beds interbedded with domed stromatolites throughout the Tremadocian on Ny Friesland and adjacent islands (Kröger et al., 2017) is consistent with a peritidal tropical carbonate factory. Uchman and Hanken, (2024) recognise that carbonates of the uppermost part of Terreneuvian and the Cambrian Series 2 contain pseudomorphs after evaporites. Hansen and Holmer (2010) recognize strong ties of Lower and Middle Ordovician brachiopods to faunas in North America and Greenland at the generic level. Hansen and Holmer (2010) also discuss the transition from low diversity brachiopod fauna in the Tremadocian and early Floian (Early Ordovician; ca. 478–470 Ma), followed by an abrupt diversification event in the late Floian and into the Middle Ordovician. The hypersaline conditions, however, mask the expected record of the Great Ordovician Biodiversification Event (Uchman and Hanken, 2024). The Middle Ordovician part of the succession represents an overall deepening, transgressive sequence (Kröger et al., 2017; Lee et al., 2019). Kröger et al., (2017) suggest that the gradual transition to deeper deposits with more shale and local siltstone and glauconitic horizons accompanied with increased burrowing and fossiliferous, cherty mud-wackestone and skeletal grainstone are evidence of general climate cooling in the transition to the Middle Ordovician (i.e., the incipient phase of Ordovician cooling). Although changing to colder sea floor conditions, tropical carbonate production continued in an inner carbonate ramp while a cold-water carbonate factory prevailed in the outer ramp (Smelror et al., 2024).



From Abay et al., 2022



From Lee et al., 2019

470 **Figure 7** Stratigraphic section of the Cambrian and Ordovician Oslobreen Group succession in Ny Friesland, northern Spitsbergen (see Fig. 5 for location) After Fortey and Bruton (1973); Harland (1997); Stouge et al. (2012); Lehnert et al. (2013); Lee et al., (2019). Bulk organic carbon isotopes ($\delta^{13}C_{org}$, in ‰ VPDB); Total Organic Carbon (TOC, in weight percent); Bl.- Blårevbreen Member; Topp.- Topiggane Member; Sp.- Spora Member.



4.2 Late Paleozoic (Devonian, Carboniferous, Permian, 419.2-251.9 Ma)

475 The Devonian, Carboniferous, and Permian periods record the only complete greenhouse to icehouse to greenhouse cycle (LPIA) on a vegetated Earth (cf. Isbell et al., 2008). In Svalbard, the relatively complete Devonian to Permian sedimentary succession, which encompasses the Old Red Sandstone, Billefjorden, Gipsdalen, and Tempelfjorden groups (Fig. 4), provides a unique opportunity to study responses of the tropical and near-tropical depositional systems with the terrestrial and shallow-marine settings to the LPIA glaciations. Svalbard occupied a near equatorial position for most of the Devonian and Carboniferous and from Permian started northwards drift (Fig. 2; Torsvik and Cocks, 2019).

480 4.2.1. Devonian: Old Red Sandstone, terrestrialization, and first forest

The advent of terrestrial vascular plants in the latest Silurian-earliest Devonian influenced weathering processes, soil formation, and strongly impacted the CO₂ cycle and global climate (Gensel et al., 2008 and references therein; Kenrick et al., 2012). The impact of vascular plants can be observed in Svalbard in the Uppermost Silurian to Upper Devonian Old Red Sandstone succession (Friend et al., 1997; Blomeier et al., 2003a; 2003b). This >8 km thick succession is restricted to 485 extensional collapse basins formed in pure extensional (Piepjohn and Dallmann, 2014), or more likely, transtensional settings (Braathen et al., 2018). The Andrée Land Basin exposed in central-north Spitsbergen was filled mainly by a terrestrial succession, with marginal-marine conditions recorded in the northernmost part (Blomeier et al., 2003a). It notably includes red and gray-green fluvial, alluvial, lacustrine, and coastal sedimentary strata arranged into fining-upward units, with abundant plant material (Friend, 1965; Moody-Stuart, 1966; Blomeier et al., 2003a; 2003b; Piepjohn and Dallmann 2014). The 490 succession recorded indications of long-term climatic variability, such as shifts in paleosols from calcretes and vertisols to coal and preservation of in situ tropical forests (Berry and Marshall, 2015). The biological evidence of environmental conditions recorded in the Old Red Sandstone come from plant fossils (Berry 2005; Berry and Marshall 2015; Davies et al., 2021), palynomorphs (Vigran, 1964; Allen, 1965; 1967; Friend et al., 1997), vegetation-induced sedimentary structures (Davies et al., 2021), and scarce marine-influenced fauna including ostracods and bivalves (e.g., Friend, 1961; Worsley, 1972). Bulk 495 geochemistry along with extraction and biomarker analysis of Middle Devonian coal indicate a terrestrial plant origin with high liptinite content (Vogt, 1941; Blumenberg et al., 2018). The flora evolved over time from diminutive plants in the Middle Devonian to the first in situ forests of lycopsids and archaeopterids in the early Frasnian (Late Devonian; ca. 383–372 Ma; Berry and Marshall 2015; Davies et al., 2021). Based on sedimentological and biological evidence for highly variable seasonal discharge and scarcity of thick calcretes, Davies et al., (2021) suggested that the precipitation regime in the Devonian was 500 tropical and monsoonal, and that the stratigraphic partitioning into red bed and gray-green strata attest to long-term fluctuations in drainage and oxidizing conditions.



4.2.2. Carboniferous to Cisuralian: Late Paleozoic Ice Age (LPIA)

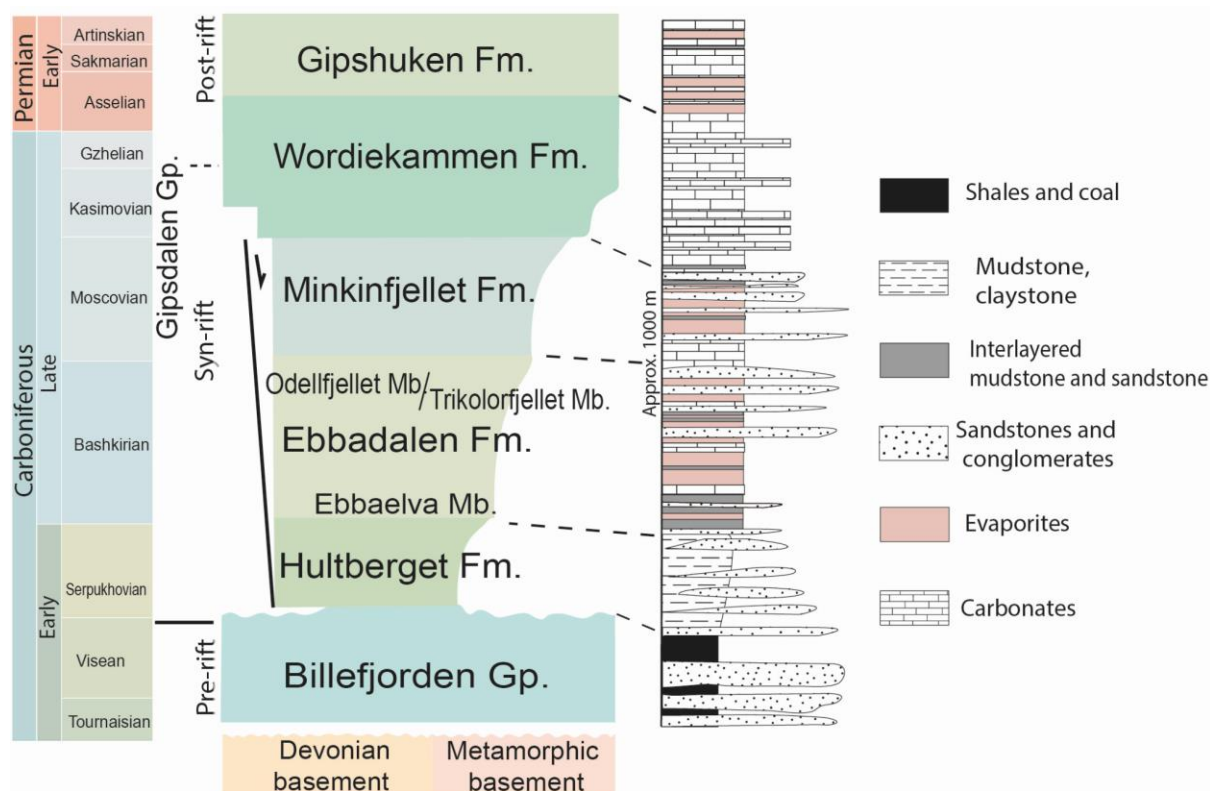
The Late Paleozoic Ice Age (LPIA) is one of the most important climatic events of the Phanerozoic that significantly influenced climate and depositional systems on Earth (Gastaldo et al., 1996; Montañez et al., 2007; Isbell et al., 2008). The LPIA is the closest analog to present climate conditions, characterized by discrete periods of glaciations separated by warm interglacials (Montañez and Poulsen, 2013). The LPIA glaciations started ca. 347 Ma at the onset of the Viséan (Mississippian), and lasted at least until ca. 285 Ma during the middle of the Artinskian (Cisuralian), potentially extending until ca. 260 Ma around the Guadalupian-Lopingian transition in the more Alpine settings in eastern Gondwana (Montañez and Poulsen, 2013). During this time, Svalbard drifted from a tropical position into the northern subtropical warm arid zone (Fig.2; e.g. Torsvik and Cocks, 2019).

The early stage of the LPIA coincided with deposition of the Mississippian Billefjorden Group. This succession unconformably overlies the folded Paleo-Neoproterozoic and Devonian successions. The terrestrial deposition occurred on broad floodplains and included abundant coal seams deposited under the humid tropical climate (Fig. 3; Gjelberg and Steel, 1981; Fairchild et al., 1982; Steel and Worsley, 1984; Lopes et al., 2019). The coal-bearing succession reaches up to 55 m thickness in eastern Spitsbergen (Scheibner et al., 2012), and 350 m in central Spitsbergen (Gjelberg and Steel, 1981; see borehole SLE 116 in Smyrak-Sikora et al., 2021). Over 1200 m of cumulative thickness is reported along the west and south parts of Spitsbergen (Gjelberg and Steel, 1981), where this succession is repeated several times due to the Paleocene and Eocene WSFTB (Maher et al., 1995; Braathen and Bergh 1995; Fig.10 in Horota et al., 2022). The fluvio-lacustrine coal deposits were commercially mined in Pyramiden from 1910 to 1998. The coal is characterized by relatively heavy $\delta^{13}\text{C}$ values, a low gammacerane index and high Pr/Ph ratios, distinctive from the Pennsylvanian coals associated with evaporites (Nicholaisen et al., 2019). Based on spores and plant fossils, Scheibner et al., (2012) suggested that the Billefjorden Group strata were deposited in a humid climate, in accordance with a paleogeographic position 10-15 °N (Fig. 2).

The shift from humid tropical to warm, arid to semi-arid depositional environments occurred during the late Serpukhovian (Mississippian) at the boundary between the Billefjorden and Gipsdalen groups (Fig. 3; Holliday and Cutbill, 1972; Gjelberg and Steel, 1981; Johannessen and Steel, 1992) and coincides with the initiation of regional-scale rifting in Svalbard and the Barents Shelf (Nøttvedt et al., 1993; Faleide et al., 2008; Braathen et al., 2012; Smyrak-Sikora et al., 2018; 2021). The following mixed siliciclastic-evaporite-carbonates succession of the lower Gipsdalen Group was deposited during the Pennsylvanian in an array of north-south striking rift basins (Gjelberg and Steel 1981; Smyrak-Sikora et al., 2021). The shift from the Billefjorden Group to the Gipsdalen Group is abrupt across most of Svalbard, and the boundary likely represents a period of non-deposition or erosion, especially on the structural highs. Contrastingly, in the inner part of one of the Billefjorden Trough, the transition is more gradual and occurs in a fluvial succession where the only changes recorded in the meandering river system is the shift from humid to arid-climate soil profiles (Olaussen et al., 2023). This change in climate setting does not correspond to recognized northward drift of Svalbard (Torsvik and Cocks, 2019) and the reasons for this change are poorly



535 understood. The Billefjorden Trough began as a continental rift basin followed by the opening of a connection to the ocean in the Bashkirian, which made the preposition sensitive to glacio-eustatic sea level variations (Smyrak-Sikora et al., 2019; 2021).



540 **Figure 8. Carboniferous stratigraphy and simplified lithological profile demonstrating a shift from humid-tropical climate during deposition of the coal-bearing Billefjorden Group to the semi-arid to arid climate of the Gipsdalen Group seen as a change of climate sensitive facies from coal-bearing units to red siliciclastics, evaporites and warm water carbonates. Modified from Braathen et al. (2011) and Smyrak-Sikora et al. (2021).**

545 The impact of the LPIA glaciations and deglaciations is most readily recognized in the Bashkirian (Mississippian; onset ca. 323 Ma) to Sakmarian (Cisuralian; ca. 293–290 Ma) part of Gipsdalen Group, namely the paralic to marine syn- to post-rift succession comprising the upper Ebbadalen to Gipshuken formations (Fig. 8). Glacio-eustatic sea-level variations related to LPIA significantly impacted sedimentation in shallow shelf and coastal environments. Episodes of sea-level lowstands are represented by terrestrial siliciclastics, gypsum strata that precipitated in salinas and sabkhas, karst and exposure surfaces which are interbedded with restricted to open-marine carbonate deposits formed during the sea level highstands (Stemmerik, 2000; 2008; Ahlborn and Stemmerik., 2015; Sorento et al., 2020; Smyrak-Sikora et al., 2021). The number of cycles in the 550 Bashkirian to Sakmarian part of the Gipsdalen Group exceeds 130 cycles (Ahlborn and Stemmerik, 2015; Sorento et al., 2020;



Smyrak-Sikora et al., 2021), however, the lack of good stratigraphic control limits cyclostratigraphic constraints. The LPIA in Svalbard is manifested also by Asselian (peak icehouse) atmospheric dust load estimated to be higher than the Moscovian (moderate icehouse; Oordt et al., 2020). This is consistent with the record from the Russian Platform that shows a $\delta^{18}\text{O}$ maximum during the glacial maximum in the Asselian (Grossman et al., 2008). Asselian to Artinskian ca. 2.5‰ decrease in $\delta^{18}\text{O}$ in the Southern Urals is attributed to ca. 4-7 °C increase in temperature and used as evidence for glacial retreat (Korte et al., 2005). This glacial retreat is questioned by Grossman et al., (2008) who show increasing $\delta^{18}\text{O}$ values related to aridification. A major deglaciation event is, however, seen in the Sakmarian as regional deepening of the carbonate platforms and temporary stop of glacio-eustatic cyclic deposition (Ahlborn and Stemmerik, 2015; Sorento et al., 2020).

560 4.2.3. Late Permian: cold-water carbonate platform

A transition from warm-water carbonate-evaporite deposition to the temperate to cool-water mixed siliceous-carbonate ramp occurred in the upper Artinskian (Cisuralian; ca. 285 Ma), and corresponds to the transition from the Gipsdalen Group to the Tempelfjorden Group (Ezaki et al., 1994; Stemmerik, 2000; 2008; Hüneke et al., 2001; Stemmerik and Worsley, 2005; Blomeier et al., 2009; 2013; Buggisch et al., 2012; Dustira et al., 2013; Sorento et al., 2020; Olausson et al., 2025). The transition is attributed to the continued northern drift of Svalbard, closure of the Uralian seaway to the warmer Tethys to the southeast (Stemmerik 2008) and was likely also the result of a deepening of the entire shelf (Blomeier et al., 2013). For the remainder of the Permian, cool- to cold-water conditions prevailed along the northwestern margin of Pangea, leading to the deposition of a ca. 460 m thick succession dominated by spiculitic chert and cool-water carbonates (Cutbill and Challinor 1965; Blomeier et al., 2013; Uchman et al., 2016; Matysik et al., 2018).

570 Extensive oxygen isotopic data has been derived from brachiopods from the Artinskian-Changhingian (middle Cisuralian to Lopingian; ca. 285-252 Ma) Kapp Starostin Formation (e.g., Gruszczynski et al., 1989; Mii et al., 1997; Korte et al., 2005; Nielsen et al., 2013). However, the high variability in the isotopic data from these Permian brachiopods (e.g., Gruszczynski et al., 1989; Korte et al., 2005) is inconsistent with the marine habitat of these taxa (Grossman et al., 2008). Diagenetic alteration accounts for the low $\delta^{18}\text{O}$ values of most samples (Mii et al., 1997). To exclude diagenetically altered brachiopods, many researchers have used geochemistry and petrography (e.g., Mii et al., 1997) and targeted the best-preserved parts of shells. Excluding these potentially altered values, brachiopod $\delta^{18}\text{O}$ values are generally -2 to -7 ‰ for the Kungurian-Wuchiapingian (upper Cisuralian-Lopingian; ca. 283–254 Ma) interval of the Kapp Starostin Formation (Mii et al., 1997). The Guadalupian-Lopingian $\delta^{13}\text{C}$ maximum of 7.5‰ represents the highest spiriferid brachiopod $\delta^{13}\text{C}$ values in the Phanerozoic (Gruszczynski et al., 1989; Mii et al., 1997) and may reflect changes in global storage of organic carbon (Mii et al., 1997). Matysik et al. (2017) investigated the multistage diagenesis of the Kapp Starostin Formation, at medium burial depths with deep-burial overprinting. The cement in Kapp Starostin Formation shows $\delta^{18}\text{O}$ values between +2‰ and 30‰ and demonstrates a peak at temperatures of 23 to 43°C corresponding to burial depths of 0.6 to 1.3 km (Matysik et al., 2018).

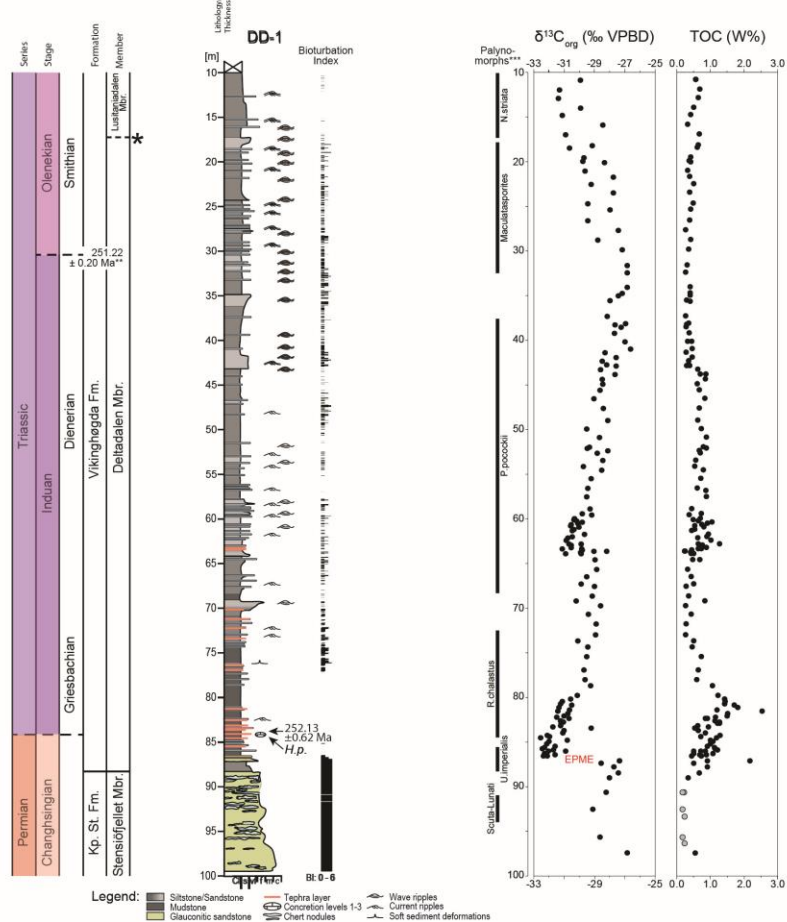
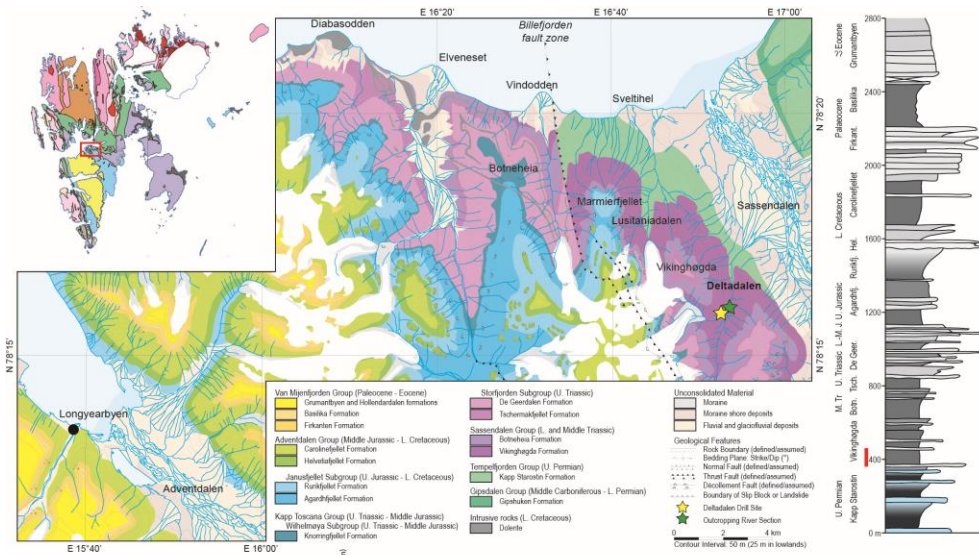


4.2.4. Capitanian Crisis

585 Within the Kapp Starostin Formation, it has also been proposed that a less severe middle Permian (Capitanian) mass extinction
is recorded (Bond et al., 2015). This Capitanian crisis is thought to be indicated by a negative $\delta^{13}\text{C}_{\text{org}}$ isotope excursion, a
lithofacies change (i.e., the loss of carbonate beds), and a drop in species richness (Bond et al., 2015). In addition, these changes
have been correlated to similar changes in the Sverdrup Basin, Arctic Canada (Bond et al., 2020). These changes are also
associated with redox proxies (pyrite framboids, Th/U and V/Al) suggesting the development of anoxic conditions, and the
loss of carbonates from the Kapp Starostin Formation was interpreted to be the consequence of a sustained interval of ocean
590 acidification (Beauchamp and Grasby, 2009; Grasby et al., 2015), making this transition consistent with other hyperthermal
events. The timing of these changes is also consistent with the changes observed at tropical paleolatitudes (Sun et al., 2010;
Wignall et al., 2012), suggesting that the Capitanian crisis was a global event. However, the interpretation that the Capitanian
crisis is recorded in the Kapp Starostin Formation is disputed, owing to the lack of biostratigraphical data confirming the rock
are of Capitanian age (Nakazawa 1999; Shen et al., 2005; Lee et al., 2022). A reanalysis of the same sections using brachiopod
595 data suggested that this event is not the Capitanian crisis, but instead a faunal turnover that occurred during the Kungurian
(Lee et al., 2022). Moreover, the development of ocean acidification is interpreted to have persisted for millions of years
(Grasby and Bauchamp, 2009), although the large carbonate buffering capacity of ocean water suggests that ocean acidification
is unlikely to persist for such long intervals of time (Hönisch et al., 2012). It, therefore, remains equivocal whether the Kapp
Starostin Formation records the Capitanian Crisis.



600 4.3. Mesozoic (Triassic, Jurassic, Cretaceous, 252.2–66 Ma)





605 **Figure 9. Top: Geological map of central Spitsbergen highlighting the drill site (yellow star) and the adjacent Deltadalen river section (green star; geological map adapted from Major et al., 1992). Overview of the sedimentary section illustrating the lithostratigraphic formations in central Spitsbergen (after Dallmann et al. (1999), Mørk et al. (1999b), Midtkandal et al. (2008), Nagy and Berge (2008), Dypvik et al. (2011), Blomeier et al. (2013), Lord et al. (2014), Koevoets et al. (2016), and Smelror and Larssen (2016). Bottom: The Permian/Triassic boundary as it appears in the Deltadalen DD-1 drill core. Modified after Zuchuat et al. (2020). EMPE – End-Permian Mass Extinction Event; Kp. St. Fm. - Kapp Starostin Formation; Mbr. – member; Fm – formation; H.p - *Hindeodus parvus*; * - member boundary after Mørk et al. (1999b); **Induan-Olenekian boundary age after Burgess et al., (2014); ***palynological data from Vigran et al. (2014).**

610

4.3.1 The Permian-Triassic transition

The End-Permian Mass Extinction Event (EPME) at ca. 252 Ma (Burgess et al., 2014) was the most catastrophic extinction event of the Phanerozoic, which decimated 75% of terrestrial species (Hochuli et al., 2010) and 81% of marine species (Stanley, 2016). This extinction is associated with a marked and continuous global negative carbon isotope excursion (CIE; Korte and Kozur, 2010). The cause(s) of the EPME are debated; both a bolide impact, and the emplacement and eruptions of the Siberian Traps LIP are implicated as causal mechanisms (Svensen et al., 2009; 2018; Grasby et al. 2011; Sanei et al. 2012; Ogden and Sleep, 2012; Ivanov et al., 2013; Burgess and Bowring, 2014; Wu et al., 2021). Even though the intrusive and extrusive character of the Siberian Traps LIP is generally accepted as the extinction trigger that led to the cascading environmental changes, it is not fully understood which environmental changes led to the collapse of terrestrial and marine ecosystems (e.g., Hochuli et al., 2010; Korte and Kozur, 2010; Black et al., 2014; Grasby et al., 2015; Joachimski et al., 2020; Scotese et al., 2021; Wu et al., 2021; Galloway and Lindström, 2023a).

In Svalbard, the mass extinction event is expressed differently compared to equatorial Tethyan carbonate successions. In west and central Spitsbergen, the pre-extinction interval belongs to the uppermost part of the Kapp Starostin Formation, which is usually devoid of any skeletal fossil material (Fig. 9; Bond et al., 2015; Grasby et al., 2015; Lee et al., 2022). The only exception is the poorly preserved lingulid brachiopod species documented (e.g., Gobbet 1964) and rare impressions of large brachiopods and bivalves (WJ. Foster, pers. obs.) so far, making it virtually impossible to robustly reconstruct diversity dynamics during this important interval (Uchman et al., 2016; Foster et al., 2022). The Permian Kapp Starostin Formation is, therefore, poorly age-constrained, and no index fossils of Changhsingian (pre-extinction) age have yet been identified. Based on sedimentological evidence as well as on the nature of the sharp negative $\delta^{13}\text{C}_{\text{org}}$ excursion, the upper part of the Kapp Starostin and the overlying Triassic Sassendalen Group (separated in the Vardebukta Formation in the west and Vikinghøgda Formation in the east) have been interpreted to represent continuous deposition across the Permian-Triassic boundary (Wignall et al., 1998; Schobben et al., 2020; Zuchuat et al., 2020). This transition is also associated with the abrupt disappearance of cemented, highly bioturbated, spiculite- and chert-bearing mudstones and sandstones, conformably overlain by easily weathered, usually laminated, scarcely bioturbated, silica-poor mudstones (e.g., Mørk et al., 1993; 1999a; 1999b; Uchman et al., 2016; Rodriguez-Tovar et al., 2021). The EPME has, therefore, been interpreted as a single horizon at the base of the Vardebukta Formation in

635



west Spitsbergen (Wignall et al., 1998) and ~1.6 m into the Vikinghøgda Formation in central Spitsbergen (Mørk et al., 1999; Nabbefeld et al., 2010).

The post-extinction sediments, which in Svalbard are assigned to the Lower Triassic Vardebukta and Vikinghøgda formations, yield a scarce and low-diversity ichno-assemblage (Wignall et al., 1998; Uchman et al., 2016; Rodriguez-Tovar et al., 2021), as well as abundant macrofossils, including key Triassic index fossils (ammonoids and conodonts), which have been useful in inferring the timing of the extinction and the recovery. From the base of both formations, a diverse assemblage of ammonoids have been recorded including *Otoceras boreale*, *Glyptohiceras nielseni*, *Ophiceras spathi*, *O. cf. compressum*, *O. cf. kochi*, *O. cf. poulsenii*, *Paravishnuites paradigma*, and *P. oxynotus* (Mørk et al., 1999), which occur ca. 6 m above the base of the Vikinghøgda Formation (Nakrem et al., 2008) and 2.5 m into the Vardebukta Formation (WJ. Foster, pers. obs.). Mørk et al. (1999), Nakrem et al. (2008), and Zuchuat et al. (2020) also described conodonts from the base of the Vikinghøgda Formation, which suggest that the interpreted extinction horizon in Svalbard is time equivalent with the onset of the mass extinction at the Global Stratotype Section and Point (GSSP) in Meishan, China, and the Permian-Triassic boundary occurs 4.1 m into the Vikinghøgda Formation. This is similar to other high-latitude clastic Permian-Triassic successions in Jameson Land, Greenland (Twitchett et al., 2001), the Sverdrup Basin in Canada (Henderson and Baud, 1997), and South Verkhoyansk region, Russia (Biakov et al., 2016). Furthermore, in South Verkhoyansk, the Changhsingian sandstones record bivalve communities with large *Intomodesma* species that suddenly go extinct at the base of the *Otoceras concavum* ammonoid zone (Biakov et al., 2016), coincident with the change in bioturbation record in Svalbard (Uchman et al., 2016; Rodriguez-Tovar et al., 2021).

Numerous geochemical and sedimentological studies have investigated the environmental changes recorded in Svalbard associated with the EPME. The negative $\delta^{13}\text{C}_{\text{org}}$ and $\delta^{13}\text{C}_{\text{carb}}$ isotope excursions, which occur just prior to the Permian-Triassic boundary, reflects a rapid influx of isotopically light carbon into the atmosphere, while the influx of heavy metals and the presence of abundant tephra layers, including one just above the first appearance datum (FAD) of *Hindeodus parvus* and dated at 252.13 ± 0.62 Ma (Zuchuat et al., 2020), which is in good agreement with the tephra beds from the Induan GSSP section in Meishan (Burgess et al., 2014) that have been inferred to link the Siberian Traps LIP and the mass extinction in Svalbard (Gruszczynski et al., 1989; Grasby et al., 2015; Zuchuat et al., 2020). The reduced Iron (Fe)/Potassium (K) elemental ratio that accompanied the extinction horizon in the Vikinghøgda Formation seems to suggest that the tropical atmospheric circulation (Hadley Cell) could have expanded towards the poles, associated with an increased aridity in the hinterland of the basin (Zuchuat et al., 2020). Redox proxies, including lipid biomarkers (Summons et al., 2022), Fe and P speciation (Schobben et al., 2020), trace-metal data (Grasby et al., 2015; Uchman et al., 2016; Wignall et al., 2016; Zuchuat et al., 2020), and pyrite framboid sizes (Dustira et al., 2013; Wignall et al., 2016) also suggest that the mass extinction is associated with the expansion of oxygen minimum zones in the ocean, bringing anoxic and euxinic conditions into shallow-marine settings, as well as subsequent pulses of redox changes throughout the Early Triassic (Rodriguez-Tovar et al., 2021). Isotopic signatures of lipid biomarkers suggest frequent phytoplankton blooms, and phosphorus speciation data indicate an increase in nutrient supply and the remobilization of biologically available P as a consequence of the mass-extinction event initiating feedback that further developed anoxic conditions (Nabbefeld et al., 2010; Schobben et al., 2020).



670 Thermal stress and ocean acidification are also widely considered as key factors in the EPME, with global average temperature
increases reaching 7°C (Kidder and Worsley, 2004; Svensen et al., 2009; Stordal et al., 2017; Burger et al., 2019), potentially
as much as 9–12°C (Joachimski et al., 2012; 2020; Schobben et al., 2014; Chen et al., 2016). In Svalbard, there are currently
no published geochemical investigations of the environmental changes associated with this hyperthermal event, but the
presence of warm-water taxa such as red algae (Wignall et al., 1998), conodont genus *Clarkina* (Nakrem et al., 2008) and both
675 ostracod and radiolarian species that were equatorial during the Changhsingian (Foster et al., 2023) suggest that higher
paleolatitudinal settings were unusually warm following the mass extinction. The cessation of carbonate rocks at the top of the
Kapp Starostin and across the Boreal Realm have also provided an alternative hypothesis that ocean acidification developed
and persisted for most of the Late Permian (Beauchamp and Grasby, 2009; Grasby et al., 2015). This hypothesis, however,
requires the persistence of undersaturated conditions for millions of years, which is inconsistent with some Earth system
680 models that suggest that ocean acidification events cannot persist for this length of time (e.g., Hönisch et al., 2012). In addition,
the lack of dissolution and repair marks on well-preserved mollusks from the extinction aftermath have also been interpreted
to suggest that ocean acidification was not severe enough to have impacted skeletal calcification in the Boreal realm, at least
at the onset of the Triassic (Foster et al., 2022). More research is, therefore, required to understand the role of thermal stress
and ocean acidification in high-latitude marine extinctions.

685 The impact of EMPE on terrestrial ecosystems can also be investigated from Svalbard's marine successions. The Permian to
Triassic palynological record of Svalbard and the Barents Shelf has been intensely investigated (e.g., Mangerud and
Konieczny, 1993), in-part due to their utility for petroleum exploration (e.g., Vigran et al., 2014). A spore spike demise of
gymnosperms, malformed spores and pollen, a drop in abundance of acritarchs, and compound specific isotopes of algal and
land-plant-derived biomarkers all coincide with the mass extinction event, suggesting near-synchronicity between effects in
690 marine and terrestrial realms (Stemmerik et al., 2001; Nabbfeld et al., 2010; Uchman et al., 2016). The presence of Permian
plant taxa, including major Paleozoic plant groups in the Lower Triassic successions of Svalbard and the Barents Shelf,
however, have led to some authors interpreting that the EMPE only had a minor impact on plant communities (Hochuli et al.,
2010; Vigran et al., 2014). Aberrant pollen and spores reported from the Barents Sea and elsewhere have been suggested to be
a consequence of severe atmospheric pollution and increased UVA-B radiation due to emissions from emplacement of the
695 Siberian Traps (Black et al., 2014; Hochuli et al., 2017; Galloway and Lindström, 2023 and references therein).

4.3.2. Early Triassic ecosystem recovery

The post-EPME survival and recovery of marine organisms recorded from Svalbard and the Boreal realm was unique. Within
the early Griesbachian *H. parvus* conodont zone in central Spitsbergen (Lusitaniadalen and Deltadalen), a diverse assemblage
of macro and microfossils have been recorded, including the only documented fully silicified marine assemblage of the Early
700 Triassic (Foster et al., 2017), the oldest record of post-extinction silica organisms globally (radiolarians and siliceous sponges;
Foster et al., 2023), and the presence of an ecological complex assemblage of trace fossils (Nabbefeld et al., 2010; Rodríguez-
Tovar et al., 2021). In addition, across Svalbard, the Lower Triassic succession preserved many groups, including bryozoans



(Nakrem and Mørk, 1991), algae (Wignall et al., 1998), conodonts (Nakrem et al., 2008), bivalves and gastropods (Buchan, 1965; Tozer and Parker 1968; Foster, 2015; Foster et al., 2017), ammonoids (see Nakrem et al., 2008), ostracods (Olempska and Błaszyk 1996), echinoderms (Salomon et al., 2015), and trace fossils (Wignall et al., 1998). Whilst sedimentation-rate calculations suggest marine ecosystems only required ca. 150 kyr to recover from the mass extinction (Rodríguez-Tovar et al., 2021), based on index conodonts, there is a distinctive pulse of environmental and ecological recovery in the Dienerian (Hatleberg and Clark, 1984; Wignall et al., 1998; Mørk and Worsley, 2006; Salamon et al., 2015).

The Lower Triassic succession of Svalbard is also fundamental for understanding the evolution and radiation of marine vertebrates following the Permian-Triassic transition. The Triassic succession of Svalbard has long been well-known for four described vertebrate fossil horizons (in stratigraphic order): The Fish Niveau, Grippia Niveau, Lower Saurian Niveau, and Upper Saurian Niveau (Wiman, 1910; Wiman, 1928). These bonebeds correspond to the Lusitaniadalen (the Fish Niveau) and Vendomdalen (the Grippia and Lower Saurian Niveau) members of the Vikinghøgda Formation that span the Smithian-Spathian transition (Lower Triassic; ca. 249.2 Ma), and the Ladinian-age (Middle Triassic; ca. 242–237 Ma) Blanknuten Member of the Botneheia Formation (the Upper Saurian Niveau; Maxwell and Kear, 2013; Hurum et al., 2018). Recent work on Early and Middle Triassic ecosystems in Svalbard reveals an exceptionally rapid diversification among marine vertebrates and ichthyosaurs likely evolved prior to the EPME (Kear et al., 2023). The bonebeds reveal a much more complex foodweb than previously thought (Hurum et al., 2014; 2018; Bratvold, 2016; Delsett et al., 2017; Ekeheien, 2018; Engelschiøn et al., 2018; Økland et al., 2018; Roberts et al., 2022; Kear et al., 2023), suggesting that the Boreal Sea served as a climatic refuge after the EPME (Kear et al., 2023; Foster et al., 2023).

It has been hypothesized that the recovery from the EPME was delayed due to subsequent crises throughout the Early Triassic (Payne et al., 2004; Ware et al., 2011; Song et al., 2012; Foster et al., 2017b; Zuchuat et al., 2020; Wu et al., 2021), despite the degree of ichnofacies diversity and intensity reached pre-extinction level in ca. 150 Kyr (Rodríguez-Tovar et al., 2021). The first crisis occurring after the EPME is the “late Dienerian biotic crisis” (late Early Triassic; ca. 251 Ma), which is recognized by a negative CIE in the Vikinghøgda Formation in Deltadalen, central Spitsbergen, where it is sandwiched between two thin tephra layers. This benthic crisis was associated with dysoxic conditions in the water column and the seafloor (Zuchuat et al., 2020) and was first documented from the Tethyan with the Werfen Formation, northern Italy (Hofmann et al., 2015; Foster et al., 2017), as well as from subtropical latitudes along the Panthalassic margin (Ware et al., 2011; Hofmann et al., 2011; 2014). The palynological record from Greenland suggests that this CIE coincides with a more significant turnover in plant communities than at the end-Permian mass extinction (Hochuli et al., 2016). This indicates that the late Dienerian Crisis might have been of global significance. The presence of the two tephra horizons directly above and below the negative CIE of the late Dienerian biotic crisis suggest a volcanic trigger for the event, but the exact nature of this potential biotic crisis in Svalbard and globally requires additional research.

The most prevalent of the biotic crises in the Triassic is the Smithian-Spathian transition, which is associated with a negative CIE greater than at the EPME (Payne et al., 2004; Grasby et al., 2013; 2016b). In Svalbard, the Smithian-Spathian transition is recorded as a regression and subsequent transgression, with numerous fossiliferous horizons (e.g., Hoel and Orvin, 1937;



Buchan, 1965; Tozer, 1967; Weitschat and Lehmann, 1978; Mørk et al., 1999; Foster, 2015; Hammer et al., 2019; Hansen et al., 2024; Leu et al., 2024). While the Smithian-Spathian transition has received considerably less attention than the Permian-Triassic transition, recent research has highlighted the multi-factor nature of this event on the dynamic of the C and P cycles in the Arctic (Hammer et al., 2019; Blattmann et al., 2024). Nevertheless, many outstanding questions remain unanswered both globally and on Svalbard: What was the timing of the event? What caused the CIE? What environmental changes are associated with the CIE? How were terrestrial and marine ecosystems impacted by the event?

At the Festningen section, Hg concentrations and Hg/TOC both show a noticeable spike in the Tvillingodden Formation of the Sassendalen Group, which have been associated with Hg loading associated with increased activity from the Siberian Traps (Grasby et al., 2016). This peak has also been correlated with Hg loading recorded at the Smithian-Spathian boundary at Smith Creek, Arctic Canada, even though the Smithian-Spathian boundary is associated with a carbon isotope peak at most sections globally. In the equivalent Vikinghøgda Formation at the Wallenbergfjellet section, however, the Smithian-Spathian boundary (the top of the *Wasatchites tardus* ammonoid zone) is associated with a positive CIE (Galfetti et al., 2007; Hammer et al., 2019) and the Hg loading occurred prior to the Smithian-Spathian boundary in the middle to late Smithian (Hammer et al., 2019). This is consistent with the Festningen section, which suggests the Hg loading occurred synchronously during the Smithian (Grasby et al., 2016a). At the Kongressfjellet and Vikinghøgda sections, just above the base of the Vendomdalen Member of the Vikinghøgda Formation, a significant shift in the palynological record is recorded (Mørk et al., 1999; Galfetti et al., 2007). This Smithian-Spathian turnover is also recorded in the shallow cores drilled at the Svalis Dome, central Barents Sea (Hochuli and Vigran, 2010). This turnover in the palynological record has been associated with the re-establishment of diverse woody gymnosperm ecosystems, marking a recovery signal from both the Permian-Triassic climate crisis and a “late Smithian Thermal Maximum”. This is supported by the synchronous recovery in the latitudinal diversity gradient of ammonoids (Brayard et al., 2009) and the recovery of equatorial benthic marine communities (Twitchett and Wignall, 1996; Chen et al., 2011; Pietsch and Bottjer, 2014; Hofmann et al., 2014; 2015; Foster et al., 2015; 2017; 2018; 2023a). The Smithian-Spathian transition, therefore, appears to be marked by a late Smithian Thermal Maximum and a subsequent Smithian-Spathian boundary cooling and associated biotic recovery in Svalbard, and pan-Arctic.

4.3.3 Middle to Late Triassic: organic-rich mudstones rich in phosphate

The Middle Triassic succession is dominated by organic-rich mudstone to siltstones of the Anisian-Ladinian (Middle Triassic; ca. 247–237 Ma) Botneheia Formation of the upper Sassendalen Group (Mørk and BJORØY, 1984; Krajewski, 2008, 2013; Wesenlund et al., 2021). The upper Blanknuten Member of the Botneheia Formation (Ladinian) reaches 12 wt.% TOC, and certain stratigraphic intervals, particularly in the underlying Muen Member (Anisian), contain abundant phosphorite nodules (e.g., Krajewski, 2013; Wesenlund et al., 2021; 2022; Engelschiøn et al., 2023a). In the Anisian, nutrient saturated runoff from continental areas, particularly associated with the approaching delta system from the southeast (see next section), coupled with upwelling of nutrient-rich waters from the Panthalassic Ocean, resulted in extensive algal blooms and the formation of oxygen



770 minimum zones, which promoted dysoxia and anoxia and preservation of organic matter and precipitation of phosphate
(Krajewski, 2013; Vigran et al., 2014; Wesenlund et al., 2022; Engelschiøn et al., 2023a). Repeated transgression-regression
events, influenced by the emerging delta system, likely contributed to fossil-preservation potential of the Middle Triassic strata
as the relatively shallow offshore environment was temporarily punctuated by anoxic events (Mørk et al., 1989; Krajewski,
2013; Engelschiøn et al., 2023a). Fossil preservation has also occurred by complete barium sulfate (barite) pseudomorphing,
775 possibly by sulfate remobilization from the organic-rich shales (Engelschiøn et al., 2023b). Moreover, the high TOC values in
the Ladinian Blanknuten Member suggest deposition under euxinic conditions, possibly governed by restricted water
circulation due to shallowing of the basin, as well as water mass stratification caused by the increasing influx of riverine waters
into the marine basin (Wesenlund et al., 2022).

780 **4.3.4. Late Triassic: the Carnian Pluvial Episode and the world's largest delta plain**

The Carnian Pluvial Episode (CPE, ca. 233 Ma) marks a period of climate and biotic changes spanning the Julian 2 and
Tuvalian 1 substages of the Carnian (Simms and Ruffell, 1989; Breda et al., 2009; Dal Corso et al., 2018). The CPE was first
recognized as concomitant to global carbonate platform environments perturbations associated with an increased terrigenous
input into sedimentary basins (Dal Corso et al., 2018) and the rapid diversification of dinosaurs (Benton et al., 2018). The CPE
785 is also associated with several isotope perturbations in terrestrial and marine C and Hg records, which potentially reflects
multiple pulses of volcanic activity of the Wrangellia LIP (Dal Corso et al., 2018; Jin et al., 2023). Analyses of palynological
assemblages, chemical weathering indices, $\delta^{18}\text{O}$ apatite records, and redox-sensitive elements suggest that the CPE was
characterized by an extremely humid climate (e.g., Roghi, 2004; Baranyi et al., 2019), warm temperatures (Rigo and
Joachimski, 2010; Rigo et al., 2012; Sun et al., 2016) and widespread marine dys- and anoxia (Soua, 2014; Sun et al., 2016;
790 Tomimatsu et al., 2021). Shallow-water carbonate production switched as a result of climatic variations and eustatic sea-level
fall (Jin et al., 2020), which impacted both the marine and continental biosphere, with high extinction rates in ammonoids and
conodonts (Rigo et al., 2007; Dal Corso et al., 2022), rapid extinction of terrestrial tetrapods and a subsequent diversification
of dinosaurs (Bernardi et al., 2018), mammals (Benton et al., 2018), scleractinian corals (Stanley, 2003), calcareous
dinoflagellates and plants (e.g., Dal Corso et al., 2022).

795 While the CPE is well-documented in the Tethyan Realm (Dal Corso et al., 2018), evidence from the Boreal Realm remains
limited. In Svalbard, preliminary palynological evidence from the Kapp Toscana Group in central Spitsbergen integrated with
organic carbon isotope and paleomagnetic constraints indicate warming during the late Julian-1 (Mueller et al., 2016; Paterson
et al., 2016) and suggest wetter conditions starting from the Julian-2, which occurs in the lower part of the De Geerdalen
Formation (Mueller et al., 2016). In addition, the detailed study of paleosols in the De Geerdalen Formation above CPE seems
800 to indicate the transition from humid (coal) to warm arid (caliche) climate settings (Lord et al., 2022). Nevertheless, the precise
location of the CPE in Svalbard's stratigraphy remains uncertain, and increased research can help understand the exact
triggering mechanism of these climate perturbations.



4.4.2. Jurassic-Cretaceous: A greenhouse with cold snaps

The Jurassic and Cretaceous saw some of the warmest background global temperatures of the Phanerozoic (Jenkyns et al., 2012). Permanent polar ice caps were not present, although evidence for episodic cooling and the growth and decay of small, ephemeral polar ice caps has been presented (e.g., Price, 1999; Miller et al., 2005; Grasby et al., 2017; Alley et al., 2020). Oxygen isotope records of Jurassic and Early Cretaceous from Svalbard have been derived largely from belemnites (e.g., Ditchfield, 1997; Price and Nunn, 2010; Hammer et al., 2011) and an extensive dataset has been derived from Kong Karls Land (Ditchfield, 1997). The usefulness of these data, however, is hampered by modest biostratigraphic age constraints and pervasive diagenesis. Nonetheless, some well-preserved belemnites were identified, and oxygen isotope data from Hammer et al. (2011) from the upper Agardhfjellet Formation (Volgian–Ryzanian, which approximately correlates with late Tithonian to early Berriasian, Late Jurassic-Early Cretaceous; ca. 149–140 Ma) and Price and Nunn (2010) from the Hauterivian (Early Cretaceous; ca. 133–126 Ma) part of the Rurikfjellet Formation of Festningen (see Jelby et al., 2020b for a discussion of the age constraints) show $\delta^{18}\text{O}$ values ranging from -3.0 to 0.8 ‰ VPDB. The belemnite data from Kong Karls Land (spanning the Aalenian to Valanginian; Middle Jurassic to Early Cretaceous; ca. 175–132 Ma) give $\delta^{18}\text{O}$ values of -0.7 to 1.2 ‰ VPDB. These data argue for cooling and warming episodes at these high paleolatitudes and may indicate high seasonality and/or high frequency climatic variability, although the absolute temperatures they represent are hard to interpret. Common practice would be to assume that the seawater $\delta^{18}\text{O}$ was -1 ‰ SMOW (i.e., that of an ice-free world), and use either the equation for molluscan calcite (Anderson and Arthur, 1983) or experimentally derived synthetic calcite (Kim and O’Neil, 1997) to calculate the precipitation temperature of the calcite. However, Price and Nunn (2010) used the presence of glendonites in certain horizons to independently assess paleotemperature of those intervals, and backcalculated the $\delta^{18}\text{O}_{\text{sw}}$. This suggested that the seawater $\delta^{18}\text{O}$ was much lower than the global average (i.e., heavily meteorically influenced), which is supported by the depositional setting (ranging from marine to terrestrial delta plain). Furthermore, recent work using clumped isotope thermometry on belemnites suggests that the equations of Kim and O’Neil (1997) or Anderson and Arthur (1983) are not suitable for belemnite calcite, and rather, the temperature equations of Kele et al. (2015) or Daëron et al. (2019) should be used (Price and Passey, 2013; Wierzbowski et al., 2018; Bajnai et al., 2020; Price et al., 2020; Vickers et al., 2019b; 2020; 2021). Using the latter results in warmer estimated temperatures than previously thought, even if one assumes a meteorically influenced $\delta^{18}\text{O}_{\text{sw}}$ of -2.5 ‰ SMOW. For example, the belemnite data from Kong Karls Land suggests temperatures closer to 12–20 °C rather than the 8 to 13 °C originally postulated by Ditchfield (1997). The belemnites from Festningen may indicate a temperature range of around 13–30 °C rather than the 9–25 °C originally suggested by Price and Nunn (2010) and Hammer et al. (2011).

4.4.2.1. Jurassic–Cretaceous boundary and the Volgian Isotopic Carbon Excursion (VOICE)

The global carbon-isotope ($\delta^{13}\text{C}$) signal of the Upper Jurassic and Jurassic-Cretaceous (J-K, ca. 145 Ma) boundary as recognized in Tethyan, Atlantic, and Pacific sections is generally characterized by a steady decline. This decline has been attributed to progressive deceleration of the carbon cycle due to the development of more oligotrophic oceanic conditions and



reduced marine primary production (Weissert and Channell, 1989; Weissert et al., 1998; Weissert and Erba, 2004; Tremolada et al., 2006; Price et al., 2016). In Svalbard, however, the upper Kimmeridgian-middle Volgian succession displays a prominent negative CIE termed the “Volgian Isotopic Carbon Excursion” or “VOICE” by Hammer et al. (2012). The VOICE is of much greater magnitude than the entirety of the long-lived decline of the lower-latitude records (Fig. 11; Morgans-Bell et al., 2001; 840 Price and Rogov, 2009; Žák et al., 2011; Hammer et al., 2012; Zakharov et al., 2014; Koevoets et al., 2016; 2018; Galloway et al., 2020; Jelby et al., 2020b). This recently recognized carbon-isotope marker of Boreal sections (observed across Svalbard, northern Siberia, Arctic Canada, the Russian Platform and possibly southern UK; Galloway et al., 2020; Jelby et al., 2020b and references therein) and newly discovered occurrences in the Neuquén Basin of Argentina (Capelli et al., 2022; Weger et al., 2022) and possibly in the eastern Tethys (Fallatah et al., 2024), is characterized by a relatively abrupt negative excursion 845 ($\leq 6.4\%$ in Svalbard) in $\delta^{13}\text{C}_{\text{org}}$ values. This excursion is followed by a positive trend in $\delta^{13}\text{C}_{\text{org}}$ values through the upper Volgian-Ryazanian and across the J-K boundary (Price and Rogov, 2009; Hammer et al., 2012; Dzyuba et al., 2013; Zakharov et al., 2014; Koevoets et al., 2016; Galloway et al., 2020; Jelby et al., 2020b; Vickers et al., 2023).

In Svalbard, the VOICE is documented in both drill core (DH-2, central Spitsbergen) and outcrop sections (e.g., Myklegardfjellet, eastern coast of Spitsbergen; Festningen, western Spitsbergen), and falls within the paper-shale-dominated 850 Oppedalssåta and Slottsmøya members of the Agardhfjellet Formation (Koevoets et al., 2016; 2019; Jelby et al., 2020b; Vickers et al., 2023). The VOICE and positive recovery across the J-K boundary were originally considered unique to the Boreal realm, as a result of decoupling from the global carbon reservoir during the Late Jurassic. Galloway et al. (2020) and Jelby et al. (2020b) attributed this Boreally-limited CIE to restricted oceanographic connectivity between the shallow epeiric seas of the high northern latitudes and open oceans, associated with water-mass stratification and increased continental runoff (Park et al., 855 2024) due to an eustatic sea-level lowstand. As a result, basinal depletion of ^{13}C resulted from oxidation of terrestrial organic matter, or input of isotopically light CO_2 by respiration of marine organisms, and/or riverine dissolved inorganic carbon (DIC) (Patterson and Walter, 1994; Holmden et al., 1998). However, the recent discovery of the VOICE in the southern hemisphere (Rodríguez Blanco et al., 2022; Capelli et al., 2022; Weger et al., 2022), albeit with diachroneity seen also in the Arctic (e.g., Rogov, 2021; Rogov et al., 2023), that may reflect poor age control or a latitudinal climate gradient, indicates that the excursion 860 is not limited to high northern latitudes. Weger et al. (2022) suggested that the VOICE was driven by changes in the input of terrestrially-derived organic matter, controlled by relative sea-level change and climate, although this hypothesis is refuted by Fallatah et al., (2024) and Galloway et al. (2024) because the VOICE may be present in a restricted setting in the Tethys (Fallatah et al., 2024) and because there is a lack of consistent changes in organic matter type (as indicated by OI and HI), indices of weather and grain size across the VOICE in the Canadian and Festningen material (Galloway et al., 2024).

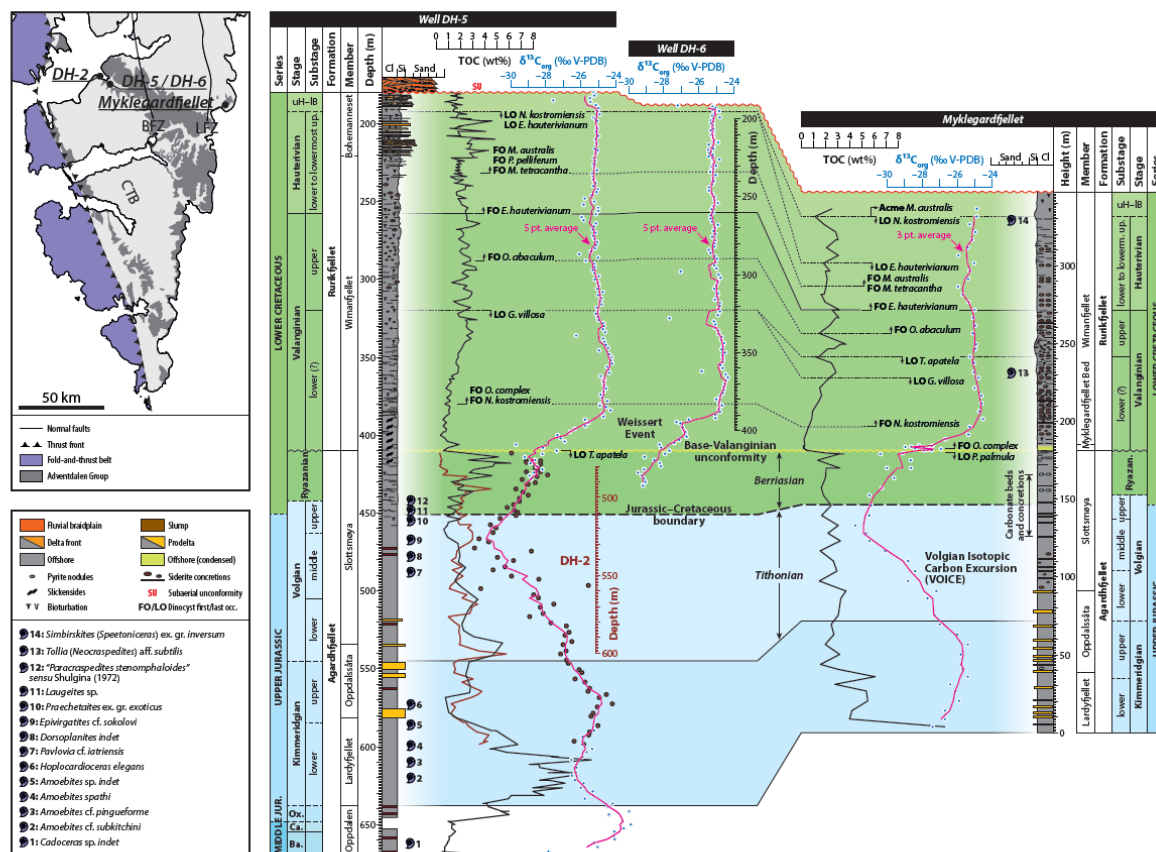
865 Collectively, the VOICE is ascribed variously to restricted circulation (Galloway et al., 2020; Jelby et al., 2020; Śliwińska, et al., 2020, Fallatah et al., 2024), precipitation of authigenic carbonate in reducing conditions (Rodríguez Blanco et al., 2022), or variations in the input of terrestrially derived organic matter that is in turn a manifestation of relative sea level change and climate (Capelli et al., 2021; Weger et al., 2022). However, none of these models alone can explain the contemporaneous



870 enrichment of Ag in Arctic basins (Galloway et al., 2024) and alternatives must be considered. An interval of silver (Ag)
enrichment occurs across the VOICE in the Sverdrup Basin (Canadian Arctic, 3-6x higher than average shale) and at
Festningen (6x higher than average shale). Silver is similarly enriched in black shales of Jurassic and Cretaceous age in the
Barents Sea, Norwegian Shelf, and West Siberia Basin (Lipinski et al., 2003; Zanin et al., 2016). The relationship of Ag to
organic matter, S, Fe, and redox-sensitive trace elements in the strata from Canada and Festningen suggest that an extra-basinal
875 source of Ag to seawater during the Volgian existed and that the source was enhanced hydrothermal flux in the proto-Amerasia
basin during rift climax, with sufficient circulation to transport high Ag-seawater to surrounding shelves (Svalbard) and within
and to extensional basins (Sverdrup Basin). Europium (Eu) values show an anomaly ($Eu/Eu^* > 1$) during the VOICE both in
the Canadian strata and strata at Festningen, suggesting the presence of hydrothermal fluids. It is possible that the negative
carbon isotopic signature of the VOICE is, in part, associated with the putative hydrothermal systems hypothesized to have
880 caused Ag enrichment. Nearly all negative carbon isotope excursions in the geological record, but so far not the VOICE, are
interpreted to reflect episodes of massive carbon release. Its global manifestation could therefore be the result of widespread
rifting and outgassing of large quantities of CO₂ (see Brune et al., 2017) associated with the breakup of Pangea (Galloway et
al., 2024).

885 4.4.2.2. Valanginian Weissert Event

The Weissert Event is a prominent global carbon-cycle perturbation which occurred in the Early Cretaceous (ca. 133 Ma). It
is expressed in carbon isotope records (Lini et al., 1992; Price et al., 2016) and is manifested in Arctic Canada (Galloway et
al., 2020) and Svalbard (Jelby et al., 2020b; Vickers et al., 2023) (Fig. 11). The isotope event consists of a globally recognized
positive CIE of a significant magnitude (2–5 ‰), which is widely documented in marine carbonates, fossil shell material,
890 terrestrial plants, and organic matter (e.g., Lini et al., 1992; Gröcke et al., 2005; Aguirre-Urreta et al., 2008; Price et al., 2016;
Galloway et al., 2020; Jelby et al., 2020b; Vickers et al., 2023; Fallatah et al., 2024). Regional to global climate cooling in the
Valanginian (Early Cretaceous; ca. 140–133 Ma) is well documented (e.g. Pucéat et al., 2003; Weissert and Erba, 2004;
McArthur et al., 2007; Bodin et al., 2015; Meissner et al., 2015; Grasby et al., 2017b), although the timing, magnitude and
extent of this cooling is debated (e.g., van de Schootbrugge et al., 2000; McArthur et al., 2007), as is the mechanism for the
895 CIE. Paleoclimatic reconstructions using biomarkers indicate a ~3°C global surface cooling across the event (Cavalheiro et
al., 2021), and glacial deposits from the Eromanga Basin (Australia) suggest the transient development of a small southern
polar ice-cap (Alley et al., 2020), whereas stable oxygen isotope records show mixed signals, with rising $\delta^{18}O_{\text{belemnite}}$ values
suggesting cooling in the Boreal Realm from the Late Valanginian to Early Hauterivian (Podlaha et al., 1998; McArthur et al.,
2004; Price and Mutterlose, 2004; Bodin et al., 2015; Meissner et al., 2015), with little change in Tethyan records (e.g., van
900 de Schootbrugge et al., 2000; McArthur et al., 2007).



905

910

915

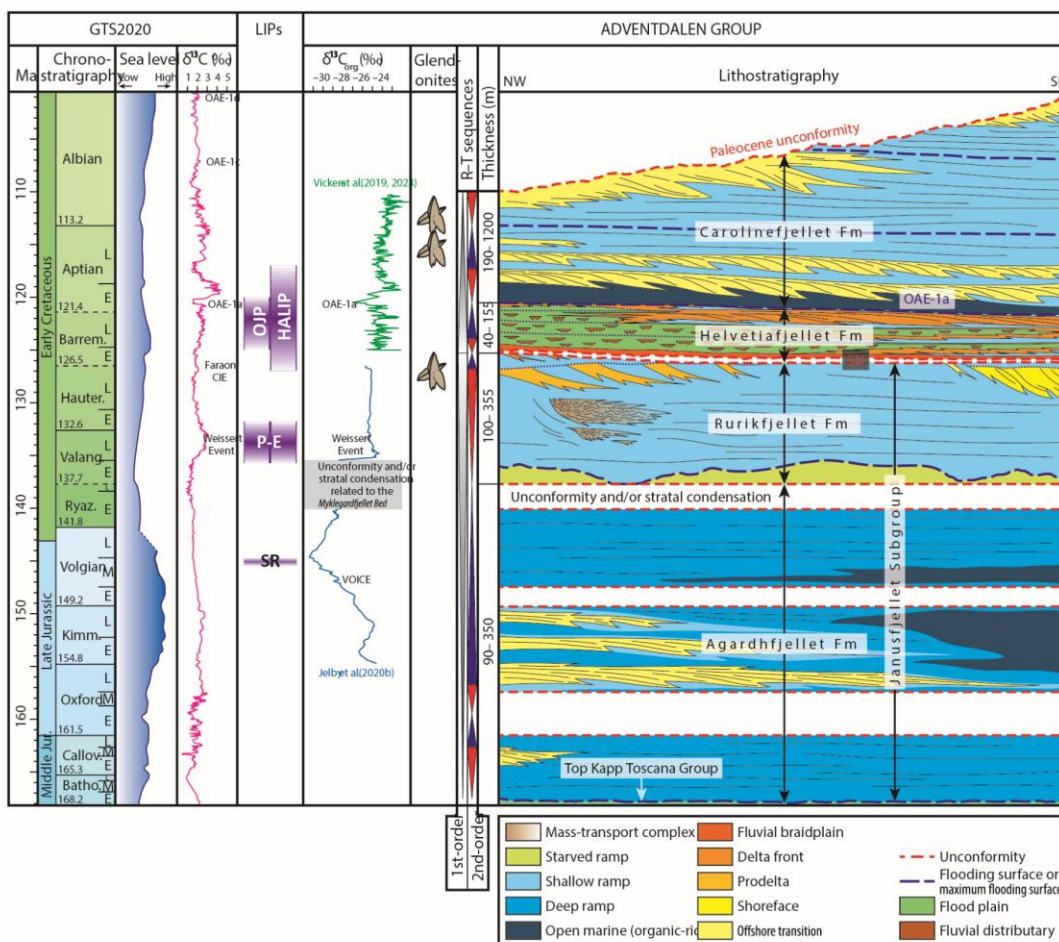
In the Arctic (including Svalbard), the widespread occurrence of glendonites around the Weissert Event interval (from the Berriasian to Hauterivian; Grasby et al., 2017b; Vickers et al., 2019a; Galloway et al., 2020; Jelby et al., 2025) has led to speculation of the cooling being decoupled from the CIE (e.g., Rogov et al., 2017), although this may partially be an artifact of age uncertainties for the Arctic successions (e.g. Vickers et al., 2019a; Jelby et al., 2020b; 2025). It may also suggest that episodic cooling punctuated the background warmth throughout the Early Cretaceous. The emplacement of the Paraná-Etendeka LIP is broadly coincident with the Weissert Event CIE (Fig.11), although uncertainties surrounding the exact relative timings have led to much debate around the causal mechanism for the event (e.g., Weissert and Erba, 2004; Duchamp-Alphonse et al., 2007; Dodd et al., 2015; Rocha et al., 2020; Gomes and Vasconcelos, 2021). Recently, it has been shown that the peak



of Paraná-Etendeka activity coincided with the onset of the Weissert Event (Martinez et al., 2023), supporting a volcanic trigger for this CIE.

In Svalbard, the $\delta^{13}\text{C}_{\text{org}}$ record reveals an abrupt and pronounced positive excursion of up to 5.5‰ in the lower Valanginian, coincident with the base of the Rurikfjellet Formation (Fig. 11; Jelby et al., 2020b; 2025). The excursion is clearly observed in both core (DH-5 and DH-6 in Adventdalen) and outcrop (Myklegardfjellet) sections, where $\delta^{13}\text{C}_{\text{org}}$ reaches the most positive values recorded since the Callovian–Oxfordian (Koevoets et al., 2016). Glendonites are found in numerous horizons in the Festningen locality, although a patchy $\delta^{13}\text{C}_{\text{org}}$ curve and poor stratigraphic dating of this section due to local small-scale tectonism has led to uncertainty as to the relative age of the glendonites with respect to the Weissert Event (Vickers et al., 2019a; 2023; Jelby et al., 2020b; 2025). Glendonites in the Canadian successions occur in Valanginian of the Deer Bay Formation (Grasby et al., 2017b; Galloway et al., 2020).

Examination of the Hg record across this interval at both Festningen and correlative sites in the Sverdrup Basin similarly yielded uncertain results, due to the poor age constraints preventing convincing identification of the Weissert Event CIE (Vickers et al., 2023). Nonetheless, Arctic Hg/TOC ratios are observed to increase across the proposed Weissert Event intervals in both Svalbard and the Sverdrup Basin. This supports recent work indicating that Paraná-Etendeka volcanism was synchronous with the onset of the Weissert Event CIE (Gomes and Vasconcelos, 2021). In other localities on Svalbard (DH-5 borehole in Adventdalen and Myklegardfjellet in eastern Spitsbergen, Fig. 10), the Weissert Event is well dated with age-diagnostic ammonites and palynomorphs (Jelby et al., 2020b; 2025), and with the observed $\delta^{13}\text{C}_{\text{org}}$ trend being consistent with the globally recognized Weissert Event (Fig. 11; Lini et al., 1992; Weissert et al., 1998; Weissert and Erba, 2004). The onset of the Weissert Event in Svalbard appears to have occurred earlier than in other Boreal sites, but this diachroneity may reflect a depositional hiatus and/or stratal condensation in the glauconitic plastic clay of the Myklegardfjellet Bed at the base of the Rurikfjellet Formation, corresponding to the Tethyan *T. pertransiens* – *N. neocomiensiformis* ammonite zones (Jelby et al., 2020b; 2025).



940 **Figure 11. Overview of the Upper Jurassic and Lower Cretaceous stratigraphy of Svalbard plotted against time, from Jelby et al.**
(2024), based on Grundvåg et al. (2017; 2019). To the left of the stratigraphic summary chart, thicknesses of the formations, first-
and second-order regressive-transgressive sequences, occurrence of glendonites (Vickers et al., 2019), LIP volcanic episodes (see
references in Vickers et al., 2023), and organic stable carbon isotopes (see Jelby et al., 2024 and references therein) are shown. These
 945 **are plotted against global $\delta^{13}\text{C}$ trends, sea level, and ages from the Geological Time Scale 2020 (Gale et al., 2020; Hesselbo et al.,**
2020).

In summary, the Weissert Event represents an important recoupling of the carbon cycle between Boreal (including Svalbard) and lower-latitude basins (including Tethyan, Atlantic, and Pacific), probably because of re-established ocean connections in response to a global eustatic sea-level rise and changing oceanic gateway connections (Haq, 2014; Galloway et al., 2020; Jelby et al., 2020b). However, Jelby et al. (2020b) recognized that the decay of the event in Svalbard spanned the late Valanginian to early Barremian (Early Cretaceous; ca. 125.77–121.4 Ma) but is negligible compared to most other Boreal and lower-latitude records, and that the signal remains relatively stable at near-peak values following the positive excursion. This indicates that



the oceanographic reconnection between higher and lower latitudes, and thus ocean ventilation, must have been sufficiently limited to keep some Boreal basins (including Svalbard) relatively deviated from prevailing global carbon-cycle dynamics following the isotopic event due to water exchange only through narrow, shallow straits (Price and Mutterlose, 2004).

4.4.2.3. The Cretaceous HALIP and OAE1a

The largest carbon cycle perturbation of the Early Cretaceous occurred in the early Aptian (a. 121–113 Ma). It is associated with Ocean Anoxic Event 1a (OAE1a, ~120 Ma), when black shale deposition occurred across multiple marine sites, indicative of widespread ocean anoxia (e.g., Jenkyns, 1980). OAE1a is characterized by a globally-recognized sharp negative CIE followed by a twin-peaked positive “recovery” CIE (Fig. 11; Jenkyns, 1995; Menegatti et al., 1998; Ando et al., 2002; Price, 2003; Weissert and Erba, 2004; Herrle et al., 2015; Dummann et al., 2021), which has also been recognized in multiple localities across Svalbard and in the Canadian Arctic (Herrle et al., 2015; Midtkandal et al., 2016; Vickers et al., 2016; 2019a; 2023; Grundvåg et al., 2019; Dummann et al., 2021). Significant perturbations in global climate are believed to have occurred along with the CIE, with global warming followed by cooling being evident from multiple proxies in sites from across the globe (e.g., Bottini et al., 2015; Bodin et al., 2015; Harper et al., 2021; Galloway et al., 2022).

In Svalbard and other Arctic localities, the occurrence of numerous glendonite horizons immediately after the CIE (in Aptian - Albian strata) supports the global extent of the post-OAE1a cooling (Fig. 11; Schröder-Adams et al., 2014; Herrle et al., 2015; Grasby et al., 2017b; Rogov et al., 2017; Vickers et al., 2019a). The OAE1a is believed to be linked to LIP volcanism, as both the Greater Ontong-Java Plateau (OJP) in the Pacific Ocean and the HALIP were being emplaced approximately synchronously with the onset of the event (Fig. 11; Midtkandal et al., 2016; Percival et al., 2021; Galloway et al., 2022). However, uncertainties surrounding the exact relative timings of the volcanism and the OAE1a complicate the interpretation of the cause of the event (Tarduno et al., 1991; Mahoney et al., 1993; Parkinson et al., 2002; Tejada et al., 2002; 2009; Erba et al., 2004; 2015; Chambers et al., 2004; Thordarson, 2004; Dockmann et al., 2018; Kasbohm et al., 2021; Galloway et al., 2022).

Attempts to use Hg as a proxy for volcanism to resolve the question of relative timing of HALIP and OJP with regards to the OAE1a CIE and accompanying climatic/environmental perturbations have yielded ambiguous results (Percival et al., 2021; Vickers et al., 2023), and recent work using palynology suggests HALIP-related landscape disturbances began to occur in the latest Barremian, coincident with the first pulse of the HALIP, but prior to the early Aptian onset of OAE1a (Galloway et al., 2022). The onset of the negative $\delta^{13}\text{C}$ excursion across Svalbard occurs within a sapropel-rich interval which is highly impoverished in marine palynomorphs (dinocysts), but which yield a number of reworked taxa (e.g., in the Ullaberget outcrop section, the DH2, and the DH1 cores near Longyearbyen (Midtkandal et al., 2016; Grundvåg et al., 2019; Śliwińska et al., 2020), narrowing the age to the Barremian-Aptian transitional interval. The regional flooding event that is considered to correlate globally with the OAE1a yields well preserved dinocysts and has been assigned an earliest Aptian age (Midtkandal et al., 2016; Grundvåg et al., 2017; 2019). Younger Cretaceous strata that elsewhere record other OAEs (e.g., OAE1b, OAE 2, OAE3) are absent from Svalbard (Fig. 4).



985 4.5. Cenozoic

The Paleogene succession in Svalbard includes Paleocene to possibly mid-Oligocene age strata (61.8 to ~30 Ma), and thus was deposited during the global climate transition from greenhouse to coolhouse conditions (Zachos et al., 2001; Westerhold et al., 2020). Since the Late Cretaceous, Svalbard was already located north of the Arctic Circle (e.g., Harland, 1997) at paleolatitudes comparable to the present (Fig. 3). Therefore, the Cenozoic geological record in Spitsbergen provides a natural
990 reference interval for future polar amplification to global warming in a warm Arctic. The deposits of the CSB belong to the Van Mijenfjorden Group with thicknesses up to 2200 m. The basin fill begins with the Paleocene coal-bearing successions that demonstrates a transgressive trend from delta plain to prodelta/outer shelf facies, followed by marine mudstones and intensely bioturbated sandstones that mainly were sourced from north and northeast of Svalbard (Petersen et al., 2016; Lüthje et al., 2020; Jochmann et al., 2020). The first evidence of WSFTB-derived sediments occurs in the latest Paleocene with a
995 westerly-derived clastic wedge known as the Hollendardalen Formation. The upper part of the CSB continued to fill into the Eocene and possibly the Oligocene and consists of >800 m thick deposits of shelf and shelf-edge deltas, slope clinotherms, and basin floor fans sourced from the WSFTB to the west (Steel et al., 1981; Johannessen and Steel, 2005; Helland-Hansen and Grundvåg, 2021). Maximum subsidence occurred during the deposition of the Frysjaodden Formation, which contains a significantly expanded (>30 m) Paleocene-Eocene Thermal Maximum (PETM) sequence (Cui, 2010; Charles et al., 2011; Dypvik et al., 2011). The shallowing-upward uppermost CSB fill is seen as a transition from deepwater marine via shallow
1000 marine/delta front to coastal plain and continental strata. The Norwegian-Greenland Seaway became severely restricted at this time, isolating the Arctic from the Atlantic Ocean during the PETM and early Eocene (Blakey, 2021; Hovikoski et al., 2021; Jones et al., 2023). Overall, the Paleogene coal-bearing successions developed in several stratigraphic levels of Svalbard are an excellent archive for reconstruction of the past vegetation and climate. These intervals provide an excellent insight into the
1005 fauna/vegetation of Svalbard at these times (see section c below and 6.3).

4.5.1. Paleocene hothouse from an Arctic Circle perspective

The Paleocene was characterized by hothouse climate (Zachos et al., 2001; Westerholt et al., 2020). In Svalbard, the CSB Paleocene succession consists of the terrestrial to nearshore Firkanten Formation (yielding fossil fauna) and the offshore marine
1010 Basilika, Grumantbyen and lowermost Frysjaodden formations. The Firkanten Formation of early Paleocene age (Selandian) contains fossil plant-bearing units also known as the Barentsburg flora (see Golovneva et al. 2023). These deposits have been extensively investigated due to economic interest and exploitation of coal resources over the last century, yet there are relatively few publications describing the succession in detail (cf. Steel et al., 1981; Nøttvedt, 1985; Nagy, 2005; Jochmann et al., 2020; Lüthje et al., 2020). Coal exploration over the past few decades has provided more than 500 drill cores through the early
1015 Paleogene of Svalbard and focuses in particular on the coal-bearing Todalen Member of the Firkanten Formation. Fission-track ages from the Firkanten Formation dated the unit to 63 ± 2 Ma and 64 ± 2 Ma (Blythe and Kleinspehn, 1998). A more



precise age is derived from an ash layer that cross-cuts the lowermost coal seam in the Firkanten Formation. It has been dated using U-Pb methods to 61.596 ± 0.028 Ma (Jones et al., 2017) at the Danian–Selandian boundary, constraining the main coal deposition to the early Selandian. The Paleocene coals have recently been shown to comprise much higher resolution stratigraphic records than previously anticipated (Large and Marshall, 2015; Large et al., 2021), especially when coals are formed from peat growing in colder climates. The age model developed by Large and Marshall (2015) and an improved understanding of long-term storage of peatland carbon (Large et al., 2021) can be implemented to assess accumulation rates. For example, the 1.5 m-thick Longyear coal seam has a modeled accumulation rate of 59 kyr and 99 kyr for temperate and boreal climates, respectively, which suggests a high-resolution record that can be used to infer variation in atmospheric dust input and the effects of forest fires (Marshall, 2013). Material has been collected from the now closed coal mines in ongoing research projects to expand on these existing datasets. The Selandian coal seams provide details of the vegetation on Svalbard at that time. The paleoflora from Svalbard reveal a temperate (mean annual temperature $10.1 \pm 2^\circ\text{C}$), maritime, humid climate, with warm summers and cool mild winters (e.g., Ulf et al. 2007; Golovneva et al. 2023). Temperate Arctic paleotemperatures are corroborated by Pantodont tracks discovered at the upper boundary of the coal layer of the Firkanten Formation (Lüthje et al. 2010). The climatic conditions were similar in the larger Arctic region (e.g., O'Regan et al., 2011).

4.5.2. The Paleocene-Eocene Thermal Maximum (PETM)

The PETM was a transient period (~150-200 kyr) of rapid global warming that began around 56 Ma, superimposed on already greenhouse conditions of the early Paleogene (Zachos et al., 2001). The event is recognized as a global negative CIE in sections worldwide, attributed to a massive release of ^{13}C -depleted carbon to the ocean-atmosphere system (McInerney and Wing, 2011). Potential sources include surface reservoirs such as dissociation of methane hydrates from marine sediments (e.g., Dickens et al., 1995) and/or volcanic and thermogenic degassing from the emplacement of the NAIP (e.g., Svensen et al., 2004; Gutjahr et al., 2017; Berndt et al., 2023; Jones et al., 2023). Existing High Arctic records for the PETM and following hyperthermal events suggest subtropical temperatures in both marine and terrestrial realms (e.g., Suc et al., 2020; Sluijs et al., 2000). In Svalbard, the PETM and its various environmental effects has been thoroughly documented in several chemostratigraphic to biostratigraphic multi-proxy studies (Charles et al., 2011; Dypvik et al., 2011; Harding et al., 2011; Nagy et al., 2013; Wicczorek et al., 2013; Jones et al., 2019; Cui et al., 2021; Pogge von Strandmann et al., 2021). The bulk of these studies are focused on a SNSK drill core (BH09/05) from a coal-exploration well located on the eastern flank of the CSB (Fig. 2).

The timing and duration of the PETM is well constrained from Svalbard strata with a high-precision U-Pb radiometric age of an ash layer within the CIE outcropping near Longyearbyen, couple with evidence of orbital cycles within the strata of the BH09/05 core (Charles et al., 2011). Other studies explore the myriad consequences of extreme warming in Svalbard strata. The abundance of kaolinite in the PETM interval (Dypvik et al., 2011) and a large negative lithium isotope excursion coincident with the CIE (Pogge von Strandmann et al., 2021) suggests increased weathering rates in response to warmer and wetter



1050 conditions. Increased runoff rates resulted in a stratified water column with a freshwater surface layer and oxygen depleted
bottom waters, which severely reduced the diversity of various fauna elements in the basin (Harding et al., 2011; Dypvik et
al., 2011; Nagy et al., 2013). Osmium isotopes (Wieczorek et al., 2013) and mercury anomalies (Jones et al., 2019) show key
variations in the activity of the NAIP at this time, supporting the hypothesis that NAIP volcanism and magmatism was at least
partially responsible for the extreme carbon emissions at the PETM onset. While studies on the BH09/05 core are now plentiful,
1055 there are numerous other cores and outcrops that contain the PETM strata that have received little to no attention.

4.5.3. The decline of the Eocene greenhouse climate

The hothouse conditions of the early Eocene were followed by a gradual global cooling that culminated in the transition into
the icehouse climate at around 34 Ma (e.g., Westerhold et al., 2020; Hutchinson et al., 2021). Paleobotanical records from the
1060 Arctic suggest that during the middle Eocene, the mean annual precipitation was >120 cm/yr (Greenwood et al., 2010). In
Svalbard, the continental, flora-bearing units are found within the Aspelintoppen Formation (Steel et al. 1978; 1985), probably
spanning from the Middle Eocene and not younger than Late Eocene or Early Oligocene (Matthiessen, 1986; Cepek and
Krutzs, 2001), and the Upper Eocene (Golovneva and Zolina, 2023) or Early Oligocene (Head, 1984) Renardodden
Formation. Abundant paleoflora from the Aspelintoppen Formation and the Renardodden Formation (Manum, 1962, Kvacek
1065 and Manum, 1993; Kvacek et al., 1994 and Cepek and Krutzs, 2001; Uhl et al., 2007) indicates mean annual precipitation
rates of 1423 and 1716 mm/yr, respectively (Golovneva, 2000). Angiosperm morphotypes indicate a strong seasonal
precipitation pattern (from 356 to 656 mm in the three wettest months and 112 -247 mm for the three driest months; Clifton,
2012). The high rates of precipitation and increased weathering rates, in combination with active tectonism, promoted the
transfer of sand into deeper settings via flood-generated hyperpycnal flows at this time (Grundvåg et al., 2023b). In the late
1070 Eocene, Svalbard was only a few degrees south of the present 78°N (Fig. 3), but fossil plant material indicates that the
temperature at that time was much warmer than today, and the estimated mean annual air temperature was around +9 °C
(Golovneva, 2000; Goloneva et al. 2023; Uhl et al., 2007). Several studies have evaluated the abundance and diversity of fossil
plants, the occurrence of coal seams, as well as fossil insects in the terrestrial parts of the Eocene Aspelintoppen Formation
(e.g. Dallmann et al., 1999; Uhl et al., 2007; Marshal et al., 2015). In other areas of the High Arctic, such as Ellesmere Island,
1075 fossil remnants of a varanid lizard, the tortoise *Geochelone*, and the alligator *Allognathosuchus* confirm warm temperatures
that remained above freezing (e.g., Estes and Hutchinson, 1980; Eberle and Greenwood, 2012).

The sporadic occurrence of glendonites and outsized clasts, the latter possibly indicating rafting by temporal sea ice, in the
marine parts of the succession suggests strong seasonal or temporal temperature variations in Svalbard (Kellogg, 1975;
Dalland, 1977; Spielhagen and Tripathi, 2009). This is in accordance with some of the paleo-floristic/insect studies that infer
1080 freezing temperatures during winter months, and an overall cooling trend for the entire interval (Golovneva, 2000; Uhl et al.,
2007; Wappler and Denk, 2011). Some of the signals preserved in the sedimentary rock record may be caused by other
allogenic forcing factors than climate fluctuations, such as tectonics and relative sea-level changes, but similar results from a



1085 range of proxies including plant morphotypes support the validity of paleoclimate reconstructions. As such, deconvolving climatic and tectonic signals in tectonically active basins is of major importance. In the restricted Arctic Ocean during the early middle Eocene (ca. 49 Ma), increased runoff caused stratification of the water column (with a fresh-water lid) and led to the well-known *Azolla* freshwater algal blooms that eventually contributed to the withdrawing of the atmospheric CO₂ and cooling of the global climate from the middle Eocene onwards (Brinkhuis et al., 2006; Speelman et al., 2009).

4.5.4. The Eocene-Oligocene Transition and connection with the Arctic Ocean

1090 A major step in the long-term Cenozoic climate evolution took place at the Eocene Oligocene Transition (EOT, ~34 Ma), when decreasing of atmospheric CO₂, and changes to ocean gateways led to a development of the first permanent ice-cap in Antarctica and initiated the icehouse type of climate which exists until today (Straume et al., 2020; Westerhold et al., 2020; Hutchinson et al., 2021). However, the global scale of the transition is not fully understood, since in contrast to the well-studied deep sea sites from southern and equatorial regions, the signature of the EOT for the northern high latitudes remains poorly
1095 constrained. Climate models suggests that closing and opening the gateways to the Arctic Ocean (such as the Fram Strait) had equally large impact on the temperature development in the high northern latitudes as the CO₂ decrease (e.g., Hutchinson et al., 2019; 2021; Straume et al., 2022; Śliwińska et al., 2023). However, the number of proxy records from the northern polar regions to evaluate the history of the Fram Strait and validate the climate models is limited. The ACEX core (IODP Expedition 302) from the Arctic Ocean contains a hiatus that misses an estimated interval from 44.4 Ma to 18.2 Ma (Backman et al.,
1100 2008). The ODP site 913 from the Greenlandic Sea suffers from a hiatus at the EOT (Eldrett et al., 2004). Furthermore, the existing sea surface temperature proxy data are of extremely low resolution (Liu et al., 2009) in comparison with time-equivalent records from the Labrador Sea and the North Sea (Śliwińska et al., 2019; 2023). Molecular fossil (alkenone) records suggest at least 5°C cooling in the northern high latitudes, associated with the transition towards the coolhouse climate (Liu et al., 2009; Śliwińska et al., 2023). The existing pollen record revealed a significant cooling of ca. 5°C in cold months mean
1105 temperatures on East Greenland across the EOT (Eldrett et al., 2009).

During the EOT, Svalbard was already located at ~80°N and therefore provides unique insights into the climate evolution across the EOT in the northern high latitudes. In the CSB the youngest Paleogene unit is the Aspelintoppen Formation, which is assigned to the Late Eocene (plant fragments) or Oligocene (mollusks) (Manum and Thronsen, 1986). Unfortunately, the age model for this formation remains poorly constrained. With an improved age model, the Eocene–Oligocene succession
1110 could provide a valuable contribution to the atmospheric temperature evolution across the EOT in the northern high latitudes and be further resolved with pollen records, comparable with the Norwegian-Greenland Sea (Eldrett et al., 2009). Marine to terrestrial deposits of possible late Eocene to Oligocene age have also been reported mainly from the exposed parts of the Forlandsundet and Bellsund grabens on the West Spitsbergen margin (Gabrielsen et al., 1992; Weber, 2019; Śliwińska and Head, 2020; Schaaf et al., 2021) . However, these studies are very limited. The foraminifera assemblages collected from the
1115 Sarstangen conglomerate at the Balanuspynten profile on the eastern side of the Forlandsundet Graben reveal the presence of



marine Oligocene strata assigned to the Buchananisen Group (Feyling-Hanssen and Ulleberg, 1984). This age has later been substantiated by palynostratigraphic analyses, which suggests an early to middle Oligocene age, at least for the sediments exposed along the eastern basin margin (Schaaf et al., 2021). The two foraminiferal zones (TA and TB) that were originally assigned to the middle to upper Oligocene, can more accurately can be assigned to the lower Oligocene (lower Rupelian; the TA zone) and the upper Oligocene (lowery Chattian; the TB zone). The early Oligocene age of the marine strata is confirmed by the presence of dinocyst *Svalbardella cooksoniae* (Manum, 1960). The appearance interval of *S. cooksoniae* in the earliest Oligocene seems to be associated with a cooling interval (Śliwińska and Heilmann-Clausen, 2011). A single sample from the Calypsostranda Group at the Renardodden section on the southern shore of Bellsund, a structural outlier interpreted to be an exposed part of the Bellsund Graben, has yielded dinocysts of late Eocene or early Oligocene age (Head, 1984; Śliwińska and Head, 2020). Based on the association of pollen in the Skilvika Formation, an upper Paleocene to Eocene age can be suggested for the lower part of the section (Weber, 2019).

4.5.5 Neogene hiatus

Svalbard experienced two uplift phases in recent times. The first and major uplift phase started in the Eocene (>36 Ma) and persisted to ca. 10 Ma. This was followed by less prominent uplift from ca. 10 Ma onwards that generated the modern topography of the archipelago (Dörr et al., 2013). These uplift events are matched by contemporaneous uplift phases in Greenland, the Barents Shelf, and Baltica (Dörr et al., 2013) and are attributed to crustal thinning and the onset of ocean spreading in the Arctic and North Atlantic driven by mantle processes related to anomalously hot mantle underlying this part of the Arctic (Green and Duddy, 2010). The presence of thick pre-glacial (Miocene and Pliocene? 23 to 2.58 Ma) and glacial (late Pliocene and Pleistocene) offshore clastic wedges along the western and northern margins of Spitsbergen (Hjelstuen et al., 1996; Lasabuda et al., 2018; Alexandropoulou et al., 2021) suggests a net denudation of ca. 3 km (Riis and Fjeldskaar, 1992; Lasabuda et al., 2021). The overall amplitude of Neogene uplift decreases eastwards with the uplift along parts of WSFTB exceeding 2.5 km and over 1.5 km in the CSB (Dörr et al., 2013). Estimates based on organic geochemical proxies suggest total uplift of 2.5 to 3.5 km (Thronsen, 1982; Marshall et al., 2015; Olaussen et al., 2019). As a result, Miocene and Pliocene sedimentary strata are not preserved anywhere on Svalbard, while only intermittent remains of Pleistocene glacial deposits are found (Ingólfsson and Landvik, 2013). Uplift of 9 mm/yr continues in central-western Spitsbergen today, with only 1 mm/yr of that attributed to isostatic rebound due to the recent Weichselian glaciation (Kierulf et al., 2022).

5. Absolute radiochronology of Svalbard stratigraphy

Despite the remarkable continuous stratigraphic successions spanning much of the Phanerozoic in Svalbard, robust absolute radiometric stratigraphic age constraints are scarce. Except for data on Devonian and older magmatic and metamorphic rocks from the pre-Caledonian “basement” (e.g., Myhre et al., 2008; Petterson et al., 2009; Majka and Kosminska, 2017; McClelland



et al., 2019), no robust ages are published from the stratigraphy pre-dating the Permian-Triassic boundary. The first radiometric age comes from an ash layer within the Deltadalen section at the Permian-Triassic boundary (Fig. 10). A zircon U-Pb chemical abrasion isotope dilution thermal ionization mass spectrometry (CA-ID-TIMS) age of 252.13 ± 0.62 Ma from a bentonite bed (volcanic ash) ca. 15 cm above the first appearance datum (FAD) of the age diagnostic *H. parvus* (onset Triassic) in the Vikinghøgda Fm. ties the biostratigraphic record to an absolute age. This age records the onset of the Triassic in Svalbard and the Panthalassic Ocean within error (Zuchuat et al., 2020). Given the sedimentation rate constraints for this section (Zuchuat et al., 2020), and the uncertainty in the age of the bentonite, there is overlap in age between the FAD of *H. parvus* in Svalbard and the FAD of *H. parvus* of 251.902 ± 0.024 Ma at the Induan GSSP (Burgess et al., 2014). This indicates synchronicity of the end-Permian mass extinction in the Panthalassic and Tethyan domains at a 0.2 % (2σ) level of uncertainty.

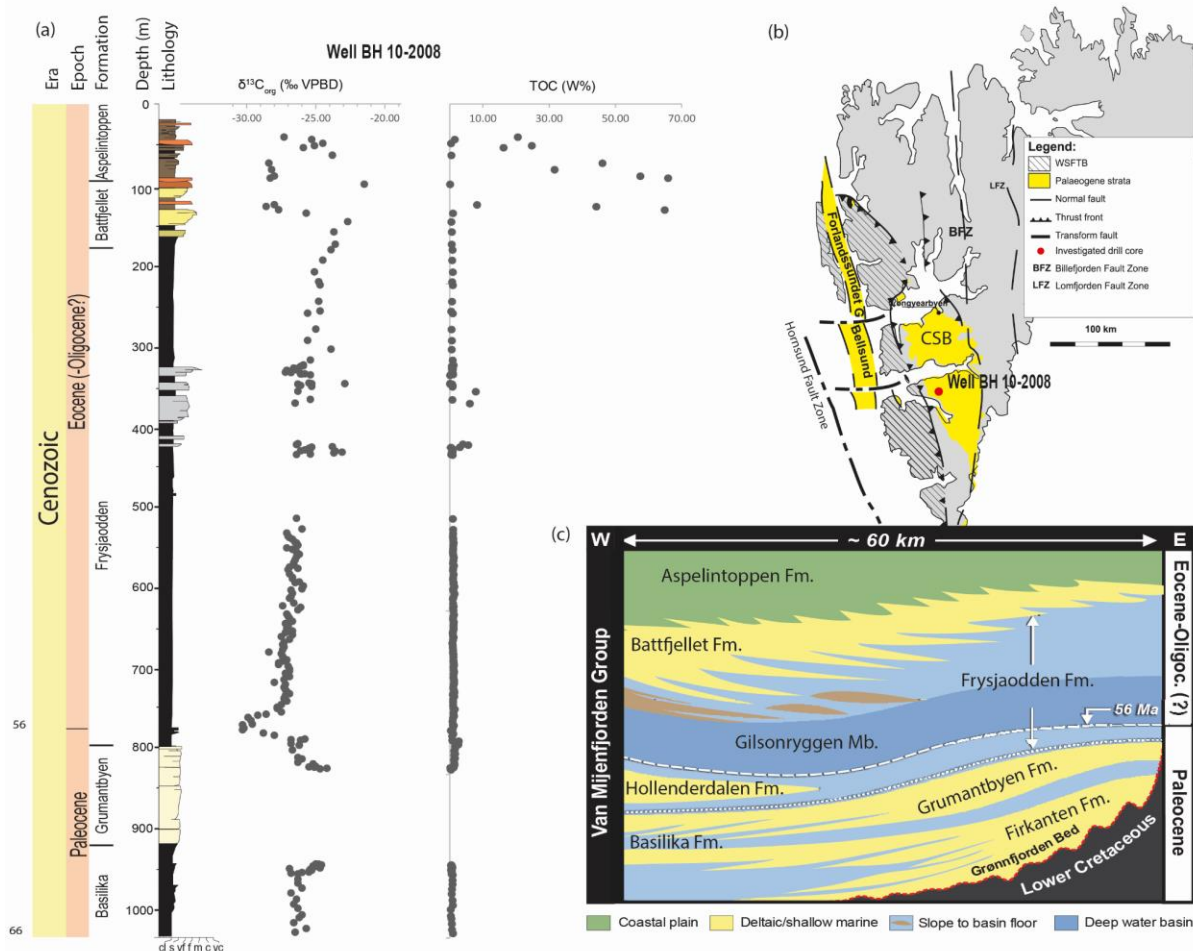
The next absolute stratigraphic tie point occurs in the Barremian to lower Aptian Helvetiafjellet Formation, where a bentonite layer from two cores taken in Longyearbyen (DH-3 and DH-7; Fig. 3) was dated to 123.1 ± 0.3 Ma (zircon U-Pb CA-ID-TIMS; Corfu et al., 2013; Midtkandal et al., 2016). Bio- and chemo-stratigraphical evidence suggests that this bentonite layer is of mid-Barremian age (Midtkandal et al., 2016), and that it occurs ~40 m below the Barremian–Aptian boundary and the onset of the Early Aptian Oceanic Anoxic event 1a (OAE1a). Subsequent magnetostratigraphy tied this bentonite age to the magnetic polarity record and hence Zhang et al. (2021) were able to calculate an age of 121.2 ± 0.4 Ma for the Barremian – Aptian boundary, accepting the M0r magnetochron as a boundary marker. Based on available ages for the HALIP in Svalbard (124.7 ± 0.3 Ma to 123.9 ± 0.3 Ma; Corfu et al., 2013) and Franz Jozef Land (~122–123 Ma; Corfu et al., 2013), there is no overlap in age with a HALIP magmatic pulse of this event with the OAE1a. However, mafic lavas and intrusives from the Sverdrup basin in northern Canada do show overlapping ages (Evenchick et al., 2015; Dockman et al., 2018) with the updated Barremian – Aptian boundary age not precluding a relationship between a pulse of the HALIP with the EAO1a.

To our knowledge, there are no further absolute age constraints published for the Mesozoic stratigraphy of Svalbard. However, the onset of Paleogene sedimentation in the CSB (Fig. 4) and the Paleocene to early Eocene stratigraphy is well constrained through high precision zircon CA-ID-TIMS U-Pb ages (Charles et al., 2011; Jones et al., 2017; Jochmann et al., 2020). A bentonite bed towards the base of the Firkanten Formation (see diagram in Fig. 12), dated from three different parts of the basin, yielded an age of 61.596 ± 0.028 Ma overlapping with the Danian–Selandian boundary, and a bentonite from the lower part of the overlying Basilika Formation has an age of 59.32 ± 0.19 Ma overlapping with the Selandian–Thanetian boundary (Jones et al., 2017). Based on these marker horizons, deposition within the CSB was estimated to start around 61.76 ± 0.09 Ma. A bentonite horizon within the Frysjaodden Formation was dated to 55.785 ± 0.034 Ma by Charles et al. (2011). This ash layer is a key marker bed for constraining the Paleocene–Eocene boundary as it is found within the PETM CIE in Svalbard strata. Charles et al. (2011) used this age and possible precession cycles within borehole BH09/05 to estimate an age of 55.866 ± 0.098 Ma for the Paleocene–Eocene boundary (i.e., the PETM onset).

To date, there are no further robust and precise radiometric ages from Svalbard's Paleozoic strata. However, well-studied outcrop successions and abundant drill core material from much of the Paleozoic offers an excellent possibility to search for



1180 target volcanic rocks in the stratigraphy that may be dated by high precision zircon U-Pb methods, thus improving the
 chronostratigraphy not only of Svalbard but potentially also globally (e.g., Zhang et al., 2021).



1185 **Figure 12.** (a) Geochemical data from well BH 10-2008 is from Doerner et al., (2020), and borehole stratigraphy after Grundvåg et al. (2014). (b) geological map showing the outline of Paleocene deposits and position of BH 10-2008 from Helland-Hansen & Grundvåg (2021). (c) Litostratigraphic summary of the Paleogene deposits of the Central Spitsbergen Basin. Modified from Helland-Hansen & Grundvåg (2021). The age of the Paleocene-Eocene boundary from Charles et al. (2011) and Harding et al. (2011).



6. Evolution of the Phanerozoic climate in Svalbard

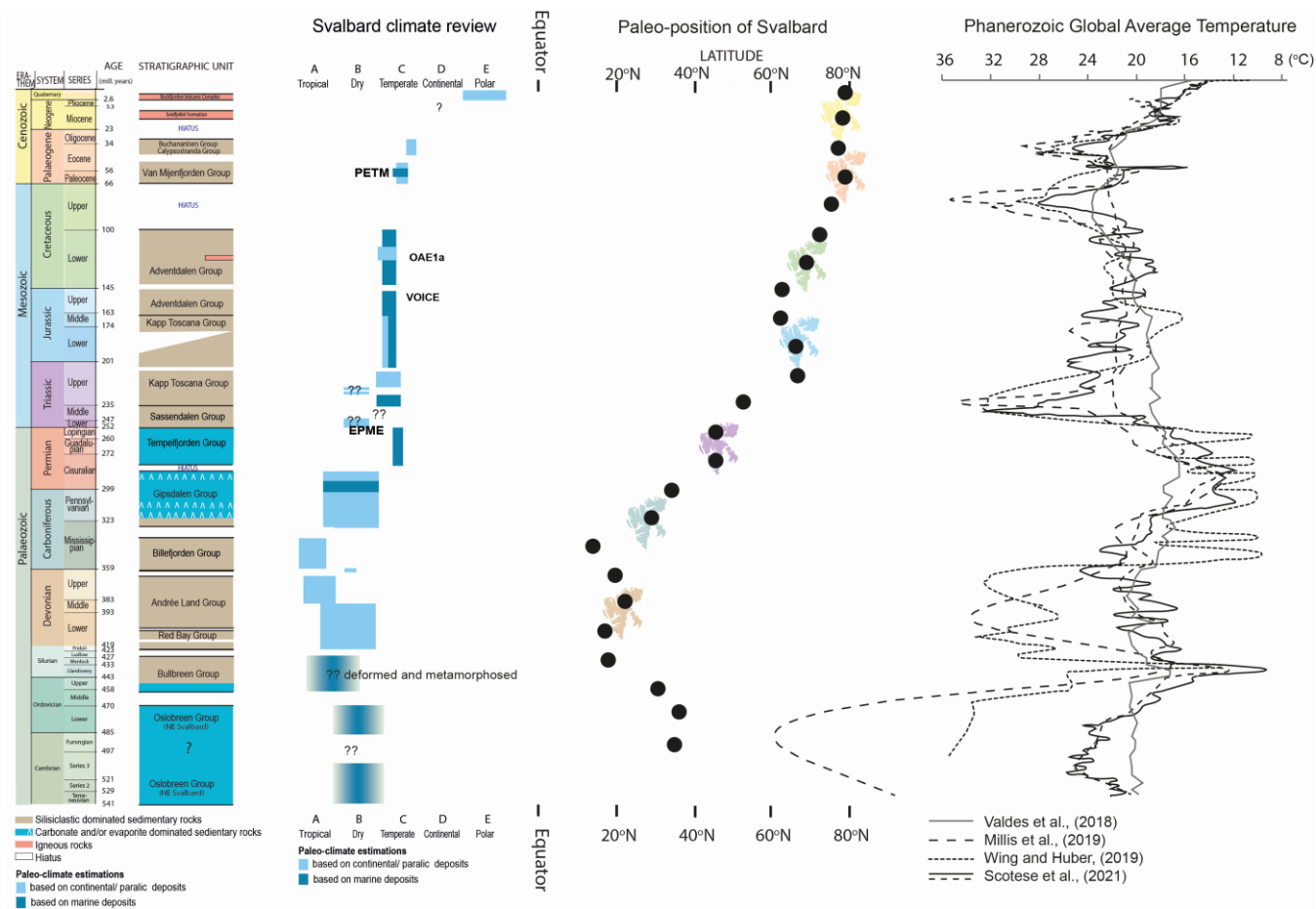
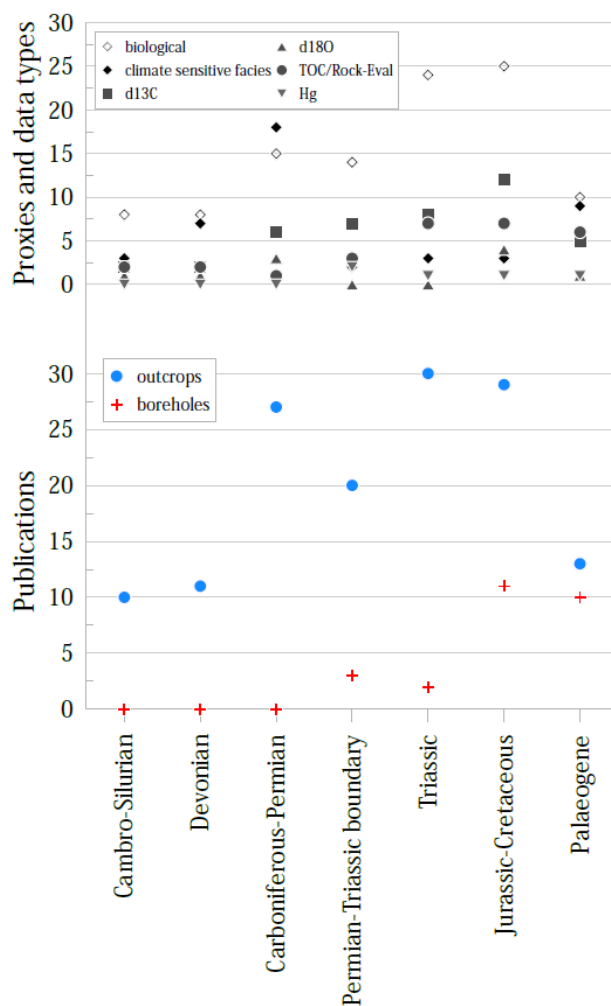


Figure 13. Correlation of the Phanerozoic climate plot based mainly on climate-sensitive facies (See Supplementary material), supplemented by biological and geochemical proxies with the paleogeographic position of Svalbard (Scotese, and Wright, 2018) and compilation of the published global average temperature curves.

1195 The parameters controlling the Phanerozoic climate in Svalbard can be simplified to the two core elements: global distribution of paleo-climatic zones (Köppen belts; e.g., Boucot et al., 2013) and the paleo-latitude of Svalbard (e.g., Steel and Worsley, 1984; Torsvik and Cocks, 2017, Olaussen et al., 2025). The deep-time models of Phanerozoic climate either for low latitude regions between 40°N and 40°S (Fig. 13; based on oxygen isotope record (Song et al., 2019; Verard and Veizer, 2019; Veizer and Prokoph, 2015; Grossman, 2012; Royer et al., 2004) or Global Average Temperature (GAT; Wing and Huber 2019, Valdes et al. 2018, Mills et al. 2019), are characterized by a “Double Hump” pattern (Fig. 13; Fischer, 1981; 1982; 1984; Frakes et al., 1992, Scotese et al., 1999; Summerhayes, 2015). The GAT trends show high temperatures during the early Paleozoic, cooler temperatures during the late Paleozoic, followed by warmer Mesozoic and early Cenozoic temperatures, finally returning to cooler temperatures in the late Cenozoic (Fig. 13). This pattern is formed in response to breakup and accretion of



1205 supercontinents (Nance et al., 2014; van der Meer et al., 2014; 2017). The geochemical proxies, such as oxygen isotopes, have limited application in Svalbard due to burial, diagenetic, and hydrothermal alterations (e.g., Buggies, 2013; Matysik et al., 2017). Therefore, the overall Phanerozoic climate trends illustrated in Figure 14 are based on climate sensitive lithofacies supplemented by biological and geochemical proxies where possible. The data sets used for all deep-time paleo-climatic and paleo-environmental studies in Svalbard are coming mainly for the outcrop’s investigations (See Fig. 14). Only about 18% of the studies mainly of the Mesozoic and Cenozoic strata is addressing borehole data (Fig. 14).



1210

Figure 14. Compilation plot of main proxies as a function of geological time, based on Table 2.



6. 1. Paleozoic

The warm and tropical to subtropical climate recorded in the early Paleozoic sedimentary succession in Svalbard reflects its near equatorial position (Figure 3). The Paleozoic climate slightly oscillates between the tropical and subtropical, dry climate. While the Late Ordovician cooling (ca. 460–440 Ma) is not recorded in Svalbard, likely due to a stratigraphic gap, the highest temperatures were reached in the Mississippian (Fig. 13). The northward drift of the continental plate on which Svalbard is located accelerated in the Mississippian to the late Triassic (Fig. 13; Torsvik and Cocks, 2019), while its impact on the climate can be recognized in the Carboniferous-Permian succession. The Mississippian to Pennsylvanian shift in climate seen as a transition of climate sensitive facies from the Mississippian coal-bearing deposits indicating tropical humid climate, through the Pennsylvanian semi-arid subtropical evaporites and siliciclastic red beds, and warm-water carbonate facies (chapter 4) is potentially accommodated by the changes in paleolatitude (Steel and Worsley, 1984; Torsvik and Cocks, 2019), however, the impact of global cooling related to the LPIA (e.g. Isbell et al., 2008) should be also considered. The following cooling trend expressed by the shift from cool-water to cold-water carbonate platform deposits (chapter 4) takes place despite the overall increased trend of global temperature in the Permian (Fig. 13).

6. 2. Mesozoic

Despite the general northward migration through different climate zones, Svalbard's sedimentary Mesozoic strata recorded a more complex story reflecting both global and regional climatic and environmental trends and the control from the paleolatitude position of Svalbard, which is evident in the Paleozoic, is not clearly seen. Indeed, the Mesozoic is characterized at the global scale by overall warm conditions, punctuated by several established hyperthermal events and potential ones, such as, the EPME, the late Dienerian biotic crisis, the Smithian-Spathian transition, and the Carnian Pluvial Episode. Most of these hyperthermals are associated with the emplacement of LIPs or smaller-scale volcanic activities (see chapter 4 for details). The emplacement of one LIP, however, might have triggered a global cooling rather than a global warming episode (the Weissert Event; Martinez et al., 2023). In addition to these individual events, longer-lived climate perturbations and oscillations are recorded in the Mesozoic strata of Svalbard, including periodic cooling-warming episodes during the Middle Jurassic to Early Cretaceous, as testified by the presence of cool-climate-indicators such as glendonite crystals in certain stratigraphic intervals. These climatic cycles generated (glacio-?) eustatic sea-level variations, leading to changes in global oceanic circulation as shallow seaways were periodically exposed during sea-level lowstands. These climatic and (glacio-?) eustatic sea-level variations impacted the amount and the redistribution of precipitation, runoff, temperature, salinity, water-mass stratification, nutrients and productivity between basins, as well as notably impacting the global carbon- and phosphorus cycles. One of these periodic perturbations recorded in Svalbard was the VOICE event.



6.3. Cenozoic

The Late Cretaceous climate maximum along with the Neogene cooling (Fig. 13) are not recorded in Svalbard due to stratigraphic gaps. During the Cenozoic, Svalbard was positioned at the high northern latitudes (the Arctic Circle). Under the greenhouse conditions of the Paleocene and Eocene, paleoflora of Svalbard suggest a humid and temperate climate at that time, punctuated by hyperthermal conditions during the PETM (Chapter 4). Therefore, palynoflora from Svalbard provides a unique insight into the high latitude end member for estimating the latitudinal gradient under the greenhouse conditions of the early Cenozoic. Notably, the paleoflora suggest slightly warmer temperatures and higher mean annual precipitation during the Paleocene, than in the Eocene-earliest Oligocene. This may be an effect of the decline of the greenhouse climate. During the early Oligocene, Svalbard (located at approximately 80°N) experienced significant cooling: the presence of specific dinocysts suggests a notable cooling interval during this period. The cooling trend is a direct response to the global cooling and the transition to the modern icehouse climate state with a bipolar glaciation (Fig. 13).

Conclusions

In this contribution we synthesized the review of the Pre-Quaternary Phanerozoic (ca. 541 Ma to 2.588 Ma) deep-time paleoclimatic research conducted on Svalbard's sedimentary succession and conclude that:

- Svalbard represents an excellent location for studying multiple globally relevant paleoclimatic events within a spatially constrained area.
- Svalbard's geological record is influenced both by its northward drift and the recurring influence of large igneous provinces that affected its climate. These include, at least, the end-Permian Siberian Traps LIP, the Early Cretaceous High Arctic LIP and the Paleogene North Atlantic Igneous Province.
- Specific events that record environmental perturbations at the global scale imprinted on Svalbard's geological record include the LPIA, the End-Permian Mass Extinction, Early Cretaceous anoxic events and cold snaps, and the Paleocene-Eocene Thermal Maximum.
- These are recorded as changes in biological, lithological, and chemical proxies of past climates preserved in both outcrops and drill cores.
- Absolute radiometric ages constrain the continuous stratigraphic successions but are unevenly distributed throughout the stratigraphy.
- Of the 148 key publications, the most used proxies to quantify past environments and climate are sedimentological studies of biological indicators (104), climate sensitive facies (45), carbon isotopes $\delta^{13}\text{C}$ (42), oxygen isotopes $\delta^{18}\text{O}$ (10), and mercury (5).

This contribution serves as an important foundation for future deep-time paleoclimate studies utilizing outcrops, opportunistic drill cores or dedicated deep-time paleoclimate scientific drilling planned in the near future.



Supplementary material

1275 The supplementary material presents a comprehensive table summarizing 148 scientific articles. The table outlines the diverse proxies utilized in deep-time climate studies conducted in Svalbard, highlighting their respective methodologies, findings, stratigraphic succession and implications for paleoenvironmental reconstructions. It can be accessed here: <https://doi.org/10.5281/zenodo.14334261>.

1280 Data availability

All data sets are coming from published scientific contributions or are part of the manuscript, including The supplement presents a comprehensive table summarizing 148 scientific articles

Authors contributions

AASS- Data Curation, Conceptualization, writing – Original Draft and Editing, visualization, Project administration
1285 PB - Writing-Review and Editing, Visualization
VSE - Writing-Original Draft, Writing-Review and Editing
WJF - Writing-Original Draft, Writing-Review and Editing
SAG - Writing-Original Draft, Writing-Review and Editing
MEJ - Writing-Original Draft, Writing-Review and Editing, Visualization
1290 MTJ - Writing-Original Draft, Writing-Review and Editing
GES - Writing-Original Draft, Writing-Review and Editing, Visualization
KKS - Writing-Original Draft, Writing-Review and Editing
MLV - Writing-Original Draft, Writing-Review and Editing, Visualization
VZ - Writing-Original Draft, Writing-Review and Editing, Visualization
1295 LEA - Writing-Original Draft
JIF - Conceptualization,
JMG - Writing-Original Draft
WHH - Editing
MAJ- Writing- Review and Editing
1300 MMJ-
EJ -Writing- Review and Editing
MK, Visualization and editing,
DK - Writing-Review and Editing
GL -Writing-Original Draft
1305 TM -Data Curation



- AM - Writing-Original Draft
SO - Writing-Original Draft
SP - Conceptualization,
GDP - Writing-Original Draft
1310 LS - Writing-Original Draft
KiS- Conceptualization, Writing - Original Draft, Writing-Review and Editing, visualization, Supervision, Funding acquisition

Competing interests

The authors declare that they have no conflict of interest.

Acknowledgements

- 1315 Lilith Kuckero and Moritz Boehme kindly contributed with reference formatting. Atle Mørk is acknowledged for comments on the manuscript. Copilot was used to help organizing the references.

Funding

- This study was jointly financed by the Research Council of Norway (through Svalbard Strategic Grants (283488, 295781, 352811), research projects (326238, 336293), Centres for Environment-friendly Energy Research (257579), and Centres of
1320 Excellence (223272, 332523), industry funding (Locra, ARCEX), international funding agencies (MagellanPlus) and University of Arctic (UArctic) collaboration projects. Funding was also provided from the European Commission, Horizon 2020 (101024218, and grant no. 754513), the Danish Council for Independent Research/Natural Sciences (DFR/FNU) grant (no. 11-107497), the Geo-Mapping for Energy and Minerals Program and GEM GeoNorth (Geological Survey of Canada, Government of Canada) and a postdoctoral Internationalisation Fellowship from Carlsberg Foundation.

1325 References

A

- Abay, T.B., Karlsen, D.A., Olausen, S., Pedersen, J.H., and Hanken, N.-M.: Organic geochemistry of Cambro-Ordovician succession of Ny Friesland, Svalbard, High Arctic Norway: Petroleum generation potential and bulk geochemical properties, *Journal of Petroleum Science and Engineering*, 218, 111033, 2022.
1330 Abdelmalak, M.M., Gac, S., Faleide, J.I., Shephard, G., Tsikalas, F., Polteau, S., Zastrozhnov, D., and Torsvik, T.H.: Quantification and restoration of the pre-drift extension across the NE Atlantic conjugate margins



during the mid-Permian-early Cenozoic multi-rifting phases, *Tectonics*, 42 (1), e2022TC007386, <https://doi.org/10.1029/2022TC007386>, 2023.

1335 Abdullah, W.H., Murchison, D., Jones, J.M., Telnaes, N. and Gjølberg, J.: Lower carboniferous coal deposition environments on Spitsbergen, Svalbard, *Organic Geochemistry*, 13 (4), 953-964, [https://doi.org/10.1016/0146-6380\(88\)90277-X](https://doi.org/10.1016/0146-6380(88)90277-X), 1988.

Ahlborn, M., and Stemmerik, L.: Depositional evolution of the Upper Carboniferous–Lower Permian Wordiekammen carbonate platform, Nordfjorden High, central Spitsbergen, Arctic Norway, *Norwegian Journal of Geology*, 95 (1), 91-126, <http://dx.doi.org/10.17850/njg95-1-03>, 2015.

1340 Aguirre-Urreta, M.B., Price, G.D., Ruffell, A.H., Lazo, D.G., Kalin, R.M., Ogle, N., and Rawson, P.F.: Southern hemisphere Early Cretaceous (Valanginian-Early Barremian) carbon and oxygen isotope curves from the Neuquén basin, Argentina, *Cretaceous Research*, 29 (1), 87-99, 2008.

Alexandropoulou, N., Winsborrow, M., Andreassen, K., Plaza-Faverola, A., Dessandier, P. A., Mattingsdal, R., Baeten, N., and Knies, J.: A continuous seismostratigraphic framework for the Western Svalbard-Barents
1345 Sea Margin over the last 2.7 Ma: Implications for the late Cenozoic Glacial history of the Svalbard-Barents Sea Ice Sheet, *Frontiers in Earth Science*, 9, 656732, 2021.

Allen, K. C.: Lower and Middle Devonian spores of North and Central Vestspitsbergen, *Palaeontology* 8, 687–748, p1. 94–108, 1965.

1350 Allen, K. C.: Spore assemblages and their stratigraphical application in the Lower and Middle Devonian of North and Central Vestspitsbergen, *Palaeontology* 10, 280–97, 1967.

Alley, N.F., Hore, S.B., and Frakes, L.A.: Glaciations at high-latitude Southern Australia during the Early Cretaceous, *Australian Journal of Earth Sciences*, 67(8): 1045-1095, 2020.

Anderson, T. F. and Arthur, M. A.: Stable isotopes in sedimentary geology and their application to sedimentologic and paleoenvironmental problems. In: society of Economic Paleontologists and Mineralogists Short Course
1355 Notes, Arthur, M.A. et al. (Eds), SEPM 10, 1–151, 1983.

Ando, A., Kakegawa, T., Takashima, R., and Saito, T.: New perspective on Aptian carbon isotope stratigraphy: data from $\delta^{13}\text{C}$ records of terrestrial organic matter, *Geology*, 30 (3), 227-230, 2002.

Anell, I., Braathen, A., Olaussen, S., and Osmundsen, P.: Evidence of faulting contradicts a quiescent northern Barents Shelf during the Triassic, *First Break*, 31 (6), <https://doi.org/10.3997/1365-2397.2013017>, 2013.

1360 Aretz, M., Herbig, H.-G., Wang, X., Gradstein, F., Agterberg, F., and Ogg, J.: The carboniferous period, Geologic time scale 2020. Elsevier, pp. 811-874 <https://doi.org/10.1016/B978-0-12-824360-2.00023-1>, 2020.

Armstroff, A., Wilkes, H., Schwarzbauer, J., Littke, R. and Horsfield, B.: Aromatic hydrocarbon biomarkers in terrestrial organic matter of Devonian to Permian age, *Palaeogeography, Palaeoclimatology, Palaeoecology*, 240 (1), 253-274, <https://doi.org/10.1016/j.palaeo.2006.03.052>, 2006.



- 1365 Armstrong, H.A., Nakrem, H.A., and Ohta, Y.: Ordovician conodonts from the Bulltinden Formation, Motalafjella, central-western Spitsbergen, *Polar Research*, 4 (1): 17-23, 1986.
- B**
- Backman, J., Jakobsson, M., Frank, M., Sangiorgi, F., Brinkhuis, H., Stickley, C., O'Regan, M., Løvlie, R., Pälike, H., Spofforth, D., Gattacecca, J., Moran, K., King, J., and Heil, C.: Age model and core-seismic integration
1370 for the Cenozoic Arctic Coring Expedition sediments from the Lomonosov Ridge, *Paleoceanography*, 23 (1), PA1S03, <https://doi.org/10.1029/2007PA001476>, 2008.
- Backman, J., Jakobsson, M., Løvlie, R., Polyak, L., and Febo, L.A.: Is the central Arctic Ocean a sediment starved basin? *Quaternary Science Reviews*, 23 (11-13), 1435-1454, <https://doi.org/10.1029/2007PA001476>, 2004a.
- 1375 Backman, J., Moran, K., McInroy, D., and Mayer, L.: the Expedition 302 Scientists: Proc. IODP, 302, Edinburgh (Integrated Ocean Drilling Program Management International, Inc.), 2004b.
- Bajnai, D., Guo, W., Spötl, C., Coplen, T.B., Methner, K., Löffler, N., Krsnik, E., Gischler, E., Hansen, M., Henkel, D., and Price, G.D.: Dual clumped isotope thermometry resolves kinetic biases in carbonate formation temperatures, *Nat. Commun.*, 11 (1), 4005, 2020.
- 1380 Bambach, R.K.: Phanerozoic biodiversity mass extinctions, *Annu. Rev. Earth Planet. Sci.*, 34, 127-155, <https://doi.org/10.1146/annurev.earth.33.092203.122654>, 2006.
- Baranyi, V., Miller, C.S., Ruffell, A., Hounslow, M.W., and Kürschner, W.M.: A continental record of the Carnian Pluvial Episode (CPE) from the Mercia Mudstone Group (UK): palynology and climatic implications, *Journal of the Geological Society*, 176 (1), 149-166, 2019.
- 1385 Beauchamp, B. and Baud, A.: Growth and demise of Permian biogenic chert along northwest Pangea: evidence for end-Permian collapse of thermohaline circulation, *Palaeogeography, Palaeoclimatology, Palaeoecology*, 184 (1), 37-63, [https://doi.org/10.1016/S0031-0182\(02\)00245-6](https://doi.org/10.1016/S0031-0182(02)00245-6), 2002.
- Beauchamp, B., Henderson, C.M., Grasby, S.E., Gates, L.T., Beatty, T.W., Utting, J., and James, N.P.: Late Permian Sedimentation in the Sverdrup Basin, Canadian Arctic: The Lindström and Black Stripe
1390 Formations, *Bulletin of Canadian Petroleum Geology*, 57 (2), 167-191, <https://doi.org/10.2113/gscpgbull.57.2.167>, 2009.
- Bédard, J.H., Saumur, B.M., Tegner, C., Troll, V.R., Deegan, F.M., Evenchick, C.A., Grasby, S.E., and Dewing, K.: Geochemical systematics of High Arctic Large Igneous Province continental tholeiites from Canada—evidence for progressive crustal contamination in the plumbing system, *Journal of Petrology*, 62 (9), egab041, 2021.
- 1395 Benn, D.I., Le Hir, G., Bao, H., Donnadieu, Y., Dumas, C., Fleming, E.J., Hambrey, M.J., McMillan, E.A., Petronis, M.S., and Ramstein, G.: Orbitally forced ice sheet fluctuations during the Marinoan Snowball Earth glaciation, *Nature Geoscience*, 8 (9), 704-707, <http://dx.doi.org/10.1038/ngeo2502>, 2015.



- 1400 Benton, M. J., Bernardi, M., and Kinsella, C.: The Carnian Pluvial Episode and the origin of dinosaurs, *Journal of the Geological Society*, 175 (6), 1019-1026, 2018.
- Beranek, L.P., Gee, D.G., and Fisher, C.M.: Detrital zircon U-Pb-Hf isotope signatures of Old Red Sandstone strata constrain the Silurian to Devonian paleogeography, tectonics, and crustal evolution of the Svalbard Caledonides, *GSA Bulletin*, 132 (9-10), 1987-2003, <http://dx.doi.org/10.1130/b35318.1>, 2020.
- 1405 Bergh, S.G., Braathen, A., and Andresen, A.: Interaction of Basement-Involved and Thin-Skinned Tectonism in the Tertiary Fold-Thrust Belt of Central Spitsbergen, Svalbard, *AAPG Bulletin*, 81 (4), 637-661, <http://dx.doi.org/10.1306/522b43f7-1727-11d7-8645000102c1865d>, 1997.
- Bergh, S., Maher Jr, H. and Braathen, A.: Late Devonian transpressional tectonics in Spitsbergen, Svalbard, and implications for basement uplift of the Sørkapp–Hornsund High, *Journal of the Geological Society*, 168 (2), 441-456, 2011.
- 1410 Bergström, S.M.: Conodonts as paleotemperature tools in Ordovician rocks of the Caledonides and adjacent areas in Scandinavia and the British Isles, *Geologiska Föreningen i Stockholm Förhandlingar*, 102 (4), 377-392, 1980.
- Bernardi, M., Petti, F.M., and Benton, M.J.: Tetrapod distribution and temperature rise during the Permian–Triassic mass extinction, *Proceedings of the Royal Society B: Biological Sciences*, 285 (1870), 20172331, 2018.
- 1415 Berndt, C., Planke, S., Alvarez Zariqian, C.A., Frieling, J., Jones, M.T., Millett, J.M., Brinkhuis, H., Bünz, S., Svensen, H.H., Longman, J., Scherer, R.P., Karstens, J., Manton, B., Nelissen, M., Reed, B., Faleide, J.I., Huismans, R.S., Agarwal, A., Andrews, G.D.M., Betlem, P., Bhattacharya, J., Chatterjee, S., Christopoulou, M., Clementi, V.J., Ferré, E.C., Filina, I.Y., Guo, P., Harper, D.T., Lambart, S., Mohn, G., Nakaoka R., Tegner, C., Varela, N., Wang, M., Xu, W., and Yager, S.L.: Shallow-water hydrothermal venting linked to the Palaeocene–Eocene Thermal Maximum, *Nature Geoscience*, 16 (9), 803-809, 2023.
- 1420 Berry, C.M.: 'Hyenia'vogtii Høeg from the Middle Devonian of Spitsbergen—Its morphology and systematic position, *Review of Palaeobotany and Palynology*, 135 (1-2), 109-116, 2005.
- Berry, C.M., and Marshall, J.E.A.: Lycopoid forests in the early Late Devonian paleoequatorial zone of Svalbard, *Geology*, 43 (12), 1043-1046, <http://dx.doi.org/10.1130/g37000.1>, 2015.
- 1425 Betlem, P., Rodés, N., Birchall, T., Dahlin, A., Smyrak-Sikora, A., and Senger, K.: Svalbox Digital Model Database: A geoscientific window into the High Arctic, *Geosphere*, 19 (6), 1640-1666, 2023.
- Betlem, P., Birchall, T., Lord, G., Oldfield, S., Nakken, L., Ogata, K., and Senger, K.: High-resolution digital outcrop model of the faults, fractures, and stratigraphy of the Agardhfjellet Formation cap rock shales at Konusdalen West, central Spitsbergen, *Earth System Science Data*, 16 (2), 985-1006, 2024.
- 1430 Biakov, A.S., Zakharov, Y.D., Horacek, M., Richoz, S., Kutugin, R.V., Ivanov, Y.Y., Kolesov, E.V., Konstantinov, A.G., Tuchkova, M.I., and Mikhailitsyna, T.I.: New data on the structure and age of the terminal Permian



strata in the South Verkhojansk region (*northeastern Asia*), *Russian Geology and Geophysics*, 57 (2), 282-293, 2016.

1435 Birkenmajer, K. and Narebski, W.: Dolerite drift blocks in marine Tertiary of Sørkapp Land and some remarks on the geology of the eastern part of this area, *Norsk Polarinstitut Årbok*, 1962, 68-79, 1963.

Bjerager, M., Alsen, P., Bojesen-Koefoed, J.A., Fyhn, M.B.W., Hovikoski, J., Keulen, N., Lindström, S., Therkelsen, J., and Thomsen, T.B.: Triassic in the northernmost Atlantic—Linking North Greenland and the southwestern Barents Sea, *Terra Nova*, 35, 250–259, <https://doi.org/ep.fjernadgang.kb.dk/10.1111/ter.12649>, 2023.

1440 Bjørnerud, M.G.: Stratigraphic record of Neoproterozoic ice sheet collapse: the Kapp Lyell diamictite sequence, SW Spitsbergen, Svalbard. *Geological Magazine*, 147 (3), 380-390, <http://dx.doi.org/10.1017/s0016756809990690>, 2009.

Black, B.A., Lamarque, J.-F., Shields, C.A., Elkins-Tanton, L.T., and Kiehl, J.T.: Acid rain and ozone depletion from pulsed Siberian Traps magmatism, *Geology*, 42 (1), 67-70, <http://dx.doi.org/10.1130/g34875.1>, 2014.

1445 Blakey, R.: Paleotectonic and paleogeographic history of the Arctic region, *Atl. Geol.*, 57, 007-039, 2021.

Blattmann, F.R., Schneebeli-Hermann, E., Adatte, T., Bucher, H.F., Vérard, C., Hammer, Ø., Luz, Z.A.S. and Vennemann, T.W.: Palaeoenvironmental variability and carbon cycle perturbations during the Smithian-Spathian (Early Triassic) in Central Spitsbergen, *Lethaia*, 57 (2), 1-14, 2024.

1450 Blinova, M., Faleide, J.I., Gabrielsen, R.H., and Mjelde, R.: Analysis of structural trends of sub-sea-floor strata in the Isfjorden area of the West Spitsbergen Fold-and-Thrust Belt based on multichannel seismic data, *Journal of the Geological Society*, 170 (4), 657-668, <http://dx.doi.org/10.1144/jgs2012-109>, 2013.

Blinova, M., Thorsen, R., Mjelde, R., and Faleide, J.I.: Structure and evolution of the Bellsund Graben between Forlandsundet and Bellsund (Spitsbergen) based on marine seismic data, *Norwegian Journal of Geology*, 89, 215–228, 2009.

1455 Blomeier, D., Wisshak, M., Dallmann, W., Volohonsky, E., and Freiwald, A.: Facies analysis of the old Red Sandstone of Spitsbergen (Wood Bay Formation): Reconstruction of the depositional environments and implications of basin development, *Facies*, 49 (1), 151-174, <http://dx.doi.org/10.1007/s10347-003-0030-1>, 2003a.

1460 Blomeier, D., Wisshak, M., Joachimski, M., Freiwald, A., and Volohonsky, E.: Calcareous, alluvial and lacustrine deposits in the Old Red Sandstone of central north Spitsbergen (Wood Bay Formation, Early Devonian), *Norwegian Journal of Geology/Norsk Geologisk Forening*, 83 (4), 281-298, 2003b.

1465 Blomeier, D., Scheibner, C., and Forke, H.: Facies arrangement and cyclostratigraphic architecture of a shallow-marine, warm-water carbonate platform: the Late Carboniferous Ny Friesland Platform in eastern Spitsbergen (Pyefjellet Beds, Wordiekammen Formation, Gipsdalen Group), *Facies*, 55 (2): 291-324, <http://dx.doi.org/10.1007/s10347-008-0163-3>, 2009.



- Blomeier, D., Dustira, A., Forke, H., and Scheibner, C.: Environmental change in the Early Permian of NE Svalbard: from a warm-water carbonate platform (Gipshuken Formation) to a temperate, mixed siliciclastic-carbonate ramp (Kapp Starostin Formation), *Facies*, 57 (3), 493-523, <http://dx.doi.org/10.1007/s10347-010-0243-z>, 2011.
- 1470 Blomeier, D., Dustira, A.M., Forke, H., and Scheibner, C.: Facies analysis and depositional environments of a storm-dominated, temperate to cold, mixed siliceous-carbonate ramp: the Permian Kapp Starostin Formation in NE Svalbard, *Norwegian Journal of Geology*, 93 (2), 75-93, 2013.
- Blumenberg, M., Weniger, P., Kus, J., Scheeder, G., Piepjohn, K., Zindler, M., and Reinhardt, L.: Geochemistry of a middle Devonian cannel coal (Munindalen) in comparison with Carboniferous coals from Svalbard, *Arktos*, 4, 1-8, 2018.
- 1475 Blythe, A.E., and Kleinspehn, K.L.: Tectonically versus climatically driven Cenozoic exhumation of the Eurasian plate margin, Svalbard: Fission track analyses, *Tectonics*, 17(4), 621-639, 1998.
- Bodin, S., Meissner, P., Janssen, N.M., Steuber, T., and Mutterlose, J.: Large igneous provinces and organic carbon burial: Controls on global temperature and continental weathering during the Early Cretaceous, *Global and Planetary Change*, 133, 238-253, 2015.
- 1480 Bond, D.P., and Wignall, P.B.: Pyrite framboid study of marine Permian–Triassic boundary sections: a complex anoxic event and its relationship to contemporaneous mass extinction, *GSA Bulletin*, 122 (7-8), 1265-1279, 2010.
- Bond, D.P., Wignall, P.B., Keller, G., and Kerr, A.C.: Large igneous provinces and mass extinctions: an update. *In: Volcanism, impacts, and mass extinctions: causes and effects* (eds. G. Keller & A.C. Kerr), 505, 29-55, 2014.
- 1485 Bond, D.P.G., Wignall, P.B., Joachimski, M.M., Sun, Y., Savov, I., Grasby, S.E., Beauchamp, B., and Blomeier, D.P.G.: An abrupt extinction in the Middle Permian (Capitanian) of the Boreal Realm (Spitsbergen) and its link to anoxia and acidification, *GSA Bulletin*, 127 (9-10), 1411-1421, <http://dx.doi.org/10.1130/b31216.1>, 2015.
- 1490 Bond, D.P.G., and Grasby, S.E.: On the causes of mass extinctions, *Palaeogeography, Palaeoclimatology, Palaeoecology*, 478, 3-29, <https://doi.org/10.1016/j.palaeo.2016.11.005>, 2017.
- Bond, D.P., Blomeier, D.P., Dustira, A.M., Wignall, P.B., Collins, D., Goode, T., Groen, R.D., Buggisch, W., and Grasby, S.E.: Sequence stratigraphy, basin morphology and sea-level history for the Permian Kapp Starostin Formation of Svalbard, Norway, *Geological Magazine*, 155 (5), 1023-1039, <https://doi.org/10.1017/S0016756816001126>, 2018.
- 1495 Bond, D.P., Wignall, P.B., and Grasby, S.E.: The Capitanian (Guadalupian, Middle Permian) mass extinction in NW Pangea (Borup Fiord, Arctic Canada): A global crisis driven by volcanism and anoxia, *GSA Bulletin*, 132 (5-6), 931-942, <http://dx.doi.org/10.1130/B35281.1>, 2020.



- 1500 Boscaini, A., Callegaro, S., Sun, Y. and Marzoli, A.: Late Permian to late Triassic large igneous provinces: timing, eruptive style and paleoenvironmental perturbations, *Frontiers in Earth Science*, 10, 887632, <https://doi.org/10.3389/feart.2022.887632>, 2022.
- Bottini, C., Erba, E., Tiraboschi, D., Jenkyns, H., Schouten, S. and Sinninghe Damsté, J.: Climate variability and ocean fertility during the Aptian Stage, *Climate of the Past*, 11 (3), 383-402, 2015
- 1505 Boucot, A.J., Xu, C., and Scotese, C.R.: Phanerozoic Paleoclimate: An Atlas of Lithologic Indicators of Climate, *SEPM Concepts in Sedimentology and Paleontology*, (Print-on-Demand Version), No. 11, 478 pp., ISBN 978-1-56576-289-3, 2013.
- Braathen, A., Bergh, S., and Maher Jr, H.: Structural outline of a Tertiary Basement-cored uplift/inversion structure in western Spitsbergen, Svalbard: Kinematics and controlling factors, *Tectonics*, 14 (1), 95-119, 1995.
- 1510 Braathen, A., and Bergh, S.G.: Kinematics of Tertiary deformation in the basement-involved fold-thrust complex, western Nordenskiöld Land, Svalbard: tectonic implications based on fault-slip data analysis, *Tectonophysics*, 249 (1-2), 1-29, 1995.
- Braathen, A., Bergh, S.G., and Maher, H.D., Jr.: Application of a critical wedge taper model to the Tertiary transpressional fold-thrust belt on Spitsbergen, Svalbard, *GSA Bulletin*, 111 (10), 1468-1485, [https://doi.org/10.1130/0016-7606\(1999\)111<1468:AOacwt>2.3.Co;2](https://doi.org/10.1130/0016-7606(1999)111<1468:AOacwt>2.3.Co;2) 1999.
- 1515 Braathen, A., Bælum, K., Maher Jr, H., and Buckley, S.J.: Growth of extensional faults and folds during deposition of an evaporite-dominated half-graben basin; the Carboniferous Billefjorden Trough, Svalbard, *Norwegian Journal of Geology*, 91 (3), 137, 2012.
- Braathen, A., Osmundsen, P.T., Maher, H., and Ganerød, M.: The Keisarhjelmen detachment records Silurian–Devonian extensional collapse in northern Svalbard, *Terra Nova*, 30 (1), 34-39, 2018.
- 1520 Bratvold, J.: *Chondrichthyans from the Grippia bonebed (Early Triassic) of Marmierfjellet, Spitsbergen* (Master's thesis, University of Oslo), 2016.
- Breda, A., Preto, N., Roghi, G., Furin, S., Meneguolo, R., Ragazzi, E., Fedele, P., and Gianolla, P.: The Carnian Pluvial Event in the Tofane area (Cortina d'Ampezzo, Dolomites, Italy), *Geo. Alp*, 6, 80-115, 2009.
- 1525 Brinkhuis, H., Schouten, S., Collinson, M.E., Sluijs, A., Damsté, J.S.S., Dickens, G.R., Huber, M., Cronin, T.M., Onodera, J., and Takahashi, K.: Episodic fresh surface waters in the Eocene Arctic Ocean, *Nature*, 441 (7093), 606-609, 2006.
- Brocks, J.J., Jarrett, A.J., Sirantoine, E., Hallmann, C., Hoshino, Y., and Liyanage, T.: The rise of algae in Cryogenian oceans and the emergence of animals, *Nature*, 548 (7669), 578-581, <http://www.nature.com/doi/10.1038/nature23457>, 2017.
- 1530



- Brozena, J., Childers, V., Lawver, L., Gahagan, L., Forsberg, R., Faleide, J., and Eldholm, O.: New aerogeophysical study of the Eurasia Basin and Lomonosov Ridge: Implications for basin development, *Geology*, 31 (9), 825-828, 2003.
- 1535 Burgess, S. D., Bowring, S., and Shen, S. Z.: High-precision timeline for Earth's most severe extinction, *Proceedings of the National Academy of Sciences*, 111 (9), 3316-3321, 2014.
- Bruhn, R., and Steel, R.: High-resolution sequence stratigraphy of a clastic foredeep succession (Paleocene, Spitsbergen): An example of peripheral-bulge-controlled depositional architecture, *Journal of Sedimentary Research*, 73 (5), 745-755, 2003.
- 1540 Brune, S., Williams, S. E., & Müller, R. D. Potential links between continental rifting, CO₂ degassing and climate change through time. *Nature Geoscience*, 10(12), 941–946. <https://doi.org/10.1038/s41561-017-0003-6>, 2017.
- Bryan, S.E., and Ernst, R.E.: Revised definition of large igneous provinces (LIPs), *Earth-Science Reviews*, 86 (1-4), 175-202, 2008.
- 1545 Buchan, S., Challinor, A., Harland, W., and Parker, J.: The Triassic stratigraphy of Svalbard, Norsk Polarinstitut Skriffter, 135, 1965.
- Buchan, K. L. and Ernst, R.E.: Giant dyke swarms and the reconstruction of the Canadian Arctic Islands, Greenland, Svalbard, and Franz Josef Land, in: E. Hanski, S. Mertanen, T. Rämö, J. Vuollo (Eds.), *Dyke Swarms: Time Markers of Crustal Evolution*, Taylor & Francis Balkema, London (2006), pp. 27-48
- 1550 Buchan, K.L., and Ernst, R.E.: A giant circumferential dyke swarm associated with the High Arctic Large Igneous Province (HALIP), *Gondwana Research*, 58, 39-57, 2018.
- Buggisch, W., Blomeier, D. and Joachimski, M.M.: Facies, diagenesis and carbon isotopes of the Early Permian Gipshuken Formation (Svalbard). *Zeitschrift der Deutschen Gesellschaft für Geowissenschaften*, 163(3): 309, 2012.
- 1555 Burger, B.J., Vargas Estrada, M., and Gustin, M.S.: What caused Earth's largest mass extinction event? New evidence from the Permian-Triassic boundary in northeastern Utah, *Global and Planetary Change*, 177, 81-100, <https://doi.org/10.1016/j.gloplacha.2019.03.013>, 2019.
- Burgess, S.D., Bowring, S. and Shen, S.-z.: High-precision timeline for Earth's most severe extinction, *Proceedings of the National Academy of Sciences*, 111 (9), 3316-3321, doi:10.1073/pnas.1317692111, 2014.
- 1560 Burgess, S.D., and Bowring, S.A.: High-precision geochronology confirms voluminous magmatism before, during, and after Earth's most severe extinction, *Science Advances*, 1 (7), e1500470, <https://doi.org/10.1126/sciadv.1500470>, 2015.
- Burgess, S.D., Muirhead, J.D., and Bowring, S.A.: Initial pulse of Siberian Traps sills as the trigger of the end-Permian mass extinction, *Nature Communications*, 8 (1), 164, <https://doi.org/10.1038/s41467-017-00083-9>, 2017.
- 1565



Burov, J.P., Krasilscikov, A., Firsov, L., and Klubov, B.: The age of Spitsbergen dolerites. *Norsk Polarinstitutt Årbok*, 101-108, 1975.

C

- 1570 Canadell, J. G., Monteiro, P. M., Costa, M. H., Cotrim da Cunha, L., Cox, P. M., Eliseev, A. V., ... & Zickfeld, K.:
Intergovernmental Panel on Climate Change (IPCC). Global carbon and other biogeochemical cycles and
feedbacks. In: *Climate change 2021: The physical science basis. Contribution of working group I to the
sixth assessment report of the intergovernmental panel on climate change* (pp. 673-816). Cambridge
University Press, 2023.
- 1575 Capelli, I.A., Scasso, R.A., Spangenberg, J.E., Kietzmann, D.A., Cravero, F., Duperron, M., and Adatte, T.:
Mineralogy and geochemistry of deeply-buried marine sediments of the Vaca Muerta-Quintuco system in
the Neuquén Basin (Chacay Melehue section), Argentina: Paleoclimatic and paleoenvironmental
implications for the global Tithonian-Valanginian reconstructions, *Journal of South American Earth
Sciences*, 107, 103103, 2021.
- 1580 Cavalheiro, L., Wagner, T., Steinig, S., Bottini, C., Dummann, W., Esegbue, O., Gambacorta, G., Giraldo-Gómez,
V., Farnsworth, A., and Flögel, S.: Impact of global cooling on Early Cretaceous high pCO₂ world during
the Weissert Event, *Nature Communications*, 12 (1), 5411, 2021.
- Cepek, P., and Krutzsch, W.: Conflicting interpretations of the Tertiary Biostratigraphy of Spitsbergen and New
Palynological Results. In: Tessensohn F (Ed), *Intra-continental fold belts, CASE 1: West Spitsbergen.*
Geologisches Jahrbuch Reihe B, Polar Issue 7. Federal Institute for Geosciences and Natural Resources,
1585 Hannover, pp. 551–602, 2001.
- Charles, A.J., Condon, D.J., Harding, I.C., Pälike, H., Marshall, J.E., Cui, Y., Kump, L., and Croudace, I.W.:
Constraints on the numerical age of the Paleocene-Eocene boundary, *Geochemistry, Geophysics,
Geosystems*, 12 (6), <https://doi.org/10.1029/2010GC003426>, 2011.
- 1590 Chambers, L.M., Pringle, M.S., and Fitton, J.G.: Phreatomagmatic eruptions on the Ontong Java Plateau: an Aptian
⁴⁰Ar/³⁹Ar age for volcanoclastic rocks at ODP Site 1184, *Geology Society of London, Special Publications*,
229 (1), 325–331, 2004.
- Chen, Z.Q., Tong, J., and Fraiser, M.L.: Trace fossil evidence for restoration of marine ecosystems following the
end-Permian mass extinction in the Lower Yangtze region, South China, *Palaeogeography,
Palaeoclimatology, Palaeoecology*, 299 (3-4), 449-474, 2011.
- 1595 Chen, J., Shen, S., Li, X., Xu, Y., Joachimski, M.M., Bowring, S.A., Erwin, D.H., Yuan, D., Chen, B., Zhang, H.,
Wang, Y., Cao, C., Zheng, Q., and Mu, L.: High-resolution SIMS oxygen isotope analysis on conodont
apatite from South China and implications for the end-Permian mass extinction, *Palaeogeography,
Palaeoclimatology, Palaeoecology*, 448, 26-38, 2016.



- Clemmensen, A., and Thomsen, E.: Palaeoenvironmental changes across the Danian–Selandian boundary in the North Sea Basin, *Palaeogeography, Palaeoclimatology, Palaeoecology*, 219 (3), 351-394, <https://doi.org/10.1016/j.palaeo.2005.01.005>, 2005.
- Clifton, A.: The Eocene flora of Svalbard and its climatic significance, *Unpublished PhD Thesis, The University of Leeds*, Leeds, 401 pp., 2012.
- Coldwell, B.C., and Pankhurst, M.: Evaluating the influence of meteorite impact events on global potassium feldspar availability to the atmosphere since 600 Ma, *Journal of the Geological Society*, 176 (2), 209-224, 2019.
- Coldwell, B.C., and Pankhurst, M.J.: Evaluating the influence of meteorite impact events on global potassium feldspar availability to the atmosphere since 600 Ma, *Journal of the Geological Society*, 176 (2), 209-224, <https://doi.org/10.1144/jgs2018-084>, 2018.
- Corfu, F., Polteau, S., Planke, S., Faleide, J.I., Svensen, H., Zayoncheck, A., and Stolbov, N.: U–Pb geochronology of Cretaceous magmatism on Svalbard and Franz Josef Land, Barents Sea large igneous province. *Geological Magazine*, 150 (6), 1127-1135, <https://doi.org/10.1017/S0016756813000162>, 2013.
- Cramer, B.S., Wright, J.D., Kent, D.V., and Aubry, M.P., 2003. Orbital climate forcing of $\delta^{13}\text{C}$ excursions in the late Paleocene–early Eocene (chrons C24n–C25n), *Paleoceanography*, 18 (4), <https://doi.org/10.1029/2003PA000909>, 2003.
- Cui, Y.: Carbon addition during the Paleocene-Eocene Thermal Maximum: model inversion of a new, high-resolution carbon isotope record from Svalbard, (Master Thesis, The Pennsylvania State University) 2010.
- Cui, Y., Kump, L. R., Ridgwell, A. J., Charles, A. J., Junium, C. K., Diefendorf, A. F., Freeman, K. H., Urban, N. M., and Harding, I. C.: Slow release of fossil carbon during the Palaeocene–Eocene Thermal Maximum. *Nature Geoscience*, 4(7), 481-485, 2011.
- Cui, Y., Diefendorf, A.F., Kump, L.R., Jiang, S., and Freeman, K.H.: Synchronous marine and terrestrial carbon cycle perturbation in the high arctic during the PETM, *Paleoceanography and Paleoclimatology*, 36 (4), e2020PA003942, <https://doi.org/10.1029/2020PA003942>, 2021.
- Cutbill, J., and Challinor, A.: Revision of the stratigraphical scheme for the Carboniferous and Permian rocks of Spitsbergen and Bjørnøya, *Geological Magazine*, 102 (5), 418-439, 1965.

D

- Daëron, M., Drysdale, R.N., Peral, M., Huyghe, D., Blamart, D., Coplen, T.B., Lartaud, F., and Zanchetta, G.: Most Earth-surface calcites precipitate out of isotopic equilibrium. *Nat. Commun.*, 10 (1), 429, 2019.
- Dal Corso, J., Ruffell, A., and Preto, N.: The Carnian Pluvial Episode (Late Triassic): New insights into this important time of global environmental and biological change. *Journal of the Geological Society*, 175 (6), 986-988, 2018.



- 1635 Dal Corso, J., Mills, B.J., Chu, D., Newton, R.J., and Song, H.: Background Earth system state amplified Carnian (Late Triassic) environmental changes. *Earth and Planetary Science Letters*, 578, 117321, <https://doi.org/10.1016/j.epsl.2021.117321>, 2022.
- Dalland, A.: Erratic clasts in the Lower Tertiary deposits of Svalbard--evidence of transport by winter ice, Norsk Polarinstitut Arbok, 1976.
- Dalland, A.: Mesozoic sedimentary succession at Andoy, northern Norway, and relation to structural development of the North Atlantic area, *Geology of the North Atlantic Borderlands — Memoir 7, CSPG Special Publications* 563-584, 1981.
- 1640 Dallmann, W.K., Andresen, A., Bergh, S.G., Maher jr, H.D., and Ohta, Y.: Tertiary fold-and-thrust belt of Spitsbergen, Svalbard, Norsk Polarinstitut, *Meddelelser* Nr 128, Oslo, 1993.
- Dallmann, W.K., Gjelberg, J.G., Harland, W.B., Johannessen, E.P., Keilen, H.B., Lønøy, A., Nilson, I., Worsley, D.: Upper palaeozoic lithostratigraphy. In: Dallmann, W.K. (Ed.), *Lithostratigraphic Lexicon of Svalbard*. Norsk Polarinstitut, Tromsø, pp. 25–126, 1999.
- 1645 Dallmann, W., (Ed): *Lithostratigraphic lexicon of Svalbard*. Norwegian Polar Institute, 1999.
- Dallmann, W.K.E. (Ed): *Geoscience Atlas of Svalbard, Norsk Polarinstitut Rapportserie*, 148 [.http://hdl.handle.net/11250/2580810](http://hdl.handle.net/11250/2580810), 2015.
- Dalseg, T.S., Nakrem, H.A., and Smelror, M.: Dinoflagellate cyst biostratigraphy, palynofacies, depositional environment and sequence stratigraphy of the Agardhfjellet Formation (Upper Jurassic-Lower Cretaceous) in central Spitsbergen (Arctic Norway), *Norwegian Journal of Geology*, 96 (2), 1-14, 2016.
- 1650 David, G.G., Haakon, F., Niels, H., and Anthony, K.H.: From the Early Paleozoic Platforms of Baltica and Laurentia to the Caledonide Orogen of Scandinavia and Greenland, *International Union of Geological Sciences*, 31 (1), 44-51, <https://doi.org/10.18814/epiugs/2008/v31i1/007>, 2008.
- 1655 Davies, N.S., Berry, C.M., Marshall, J.E., Wellman, C.H., and Lindemann, F.-J.: The Devonian landscape factory: plant–sediment interactions in the Old Red Sandstone of Svalbard and the rise of vegetation as a biogeomorphic agent. *Journal of the Geological Society*, 178 (5), <https://doi.org/10.1144/jgs2020-225>, 2021.
- Davis, W.J., Schroeder-Adams, C.J., Galloway, J.M., Herrle, J.O., and Pugh, A.T.: U-Pb geochronology of bentonites from the Upper cretaceous Kanguk Formation, Sverdrup Basin, Arctic Canada: constraints on sedimentation rates, biostratigraphic correlations and the late magmatic history of the High Arctic large Igneous Province. *Geological Magazine*, 154 (4), 757-776, <https://doi.org/10.1017/S0016756816000376>, 2017.
- 1660 Delsett, L.L., Novis, L.K., Roberts, A.J., Koevoets, M.J., Hammer, Ø., Druckenmiller, P.S., and Hurum, J.H.: The Slotsmøya marine reptile Lagerstätte: depositional environments, taphonomy and diagenesis, *Geological Society, London, Special Publications*, 434 (1), 165-188, 2016.
- 1665



- Delsett, L.L., Roberts, A.J., Druckenmiller, P.S., and Hurum, J.H.: A new ophthalmosaurid (Ichthyosauria) from Svalbard, Norway, and evolution of the ichthyopterygian pelvic girdle. *PLoS One*, 12. (1), e0169971, 2017.
- 1670 Derby, J., Fritz, R., Longacre, S., Morgan, W., and Sternbach, C.: The Great American Carbonate Bank: The Geology and Economic Resources of the Cambrian-Ordovician Sauk Megasequence of Laurentia, AAPG Memoir, 98, 2013.
- Dickens, G.R., O'Neil, J.R., Rea, D.K., and Owen, R.M.: Dissociation of oceanic methane hydrate as a cause of the carbon isotope excursion at the end of the Paleocene, *Paleoceanography*, 10 (6), 965-971, 1995.
- 1675 Dickson, A.J., Cohen, A.S., and Davies, M.: The Osmium Isotope Signature of Phanerozoic Large Igneous Provinces, *Large Igneous Provinces: A Driver of Global Environmental and Biotic Changes*, 229-246, <https://doi.org/10.1002/9781119507444.ch10>, 2021.
- Dietmar Müller, R., and Spielhagen, R.F.: Evolution of the Central Tertiary Basin of Spitsbergen: towards a synthesis of sediment and plate tectonic history, *Palaeogeography, Palaeoclimatology, Palaeoecology*, 80 (2), 153-172, [https://doi.org/10.1016/0031-0182\(90\)90127-S](https://doi.org/10.1016/0031-0182(90)90127-S), 1990.
- 1680 Dimakis, P., Braathen, B.I., Faleide, J.I., Elverhøi, A., and Gudlaugsson, S.T.: Cenozoic erosion and the preglacial uplift of the Svalbard–Barents Sea region, *Tectonophysics*, 300 (1), 311-327, [https://doi.org/10.1016/S0040-1951\(98\)00245-5](https://doi.org/10.1016/S0040-1951(98)00245-5), 1998a.
- Dimakis, P., Braathen, B.I., Faleide, J.I., Elverhøi, A., and Gudlaugsson, S.T.: Cenozoic erosion and the preglacial uplift of the Svalbard–Barents Sea region, *Tectonophysics*, 300 (1-4), 311-327, 1998b.
- 1685 Ditchfield, P.W.: High northern palaeolatitude Jurassic-Cretaceous palaeotemperature variation: new data from Kong Karls Land, Svalbard. *Palaeogeography, Palaeoclimatology, Palaeoecology*, 130 (1-4), 163-175, 1997.
- Dockman, D., Pearson, D., Heaman, L., Gibson, S., and Sarkar, C.: Timing and origin of magmatism in the Sverdrup Basin, Northern Canada—Implications for lithospheric evolution in the High Arctic Large Igneous Province (HALIP), *Tectonophysics*, 742, 50-65, 2018.
- 1690 Dodd, S.C., Mac Niocaill, C., and Muxworthy, A.R.: Long duration (> 4 Ma) and steady-state volcanic activity in the early Cretaceous Paraná-Etendeka Large Igneous Province: new palaeomagnetic data from Namibia, *Earth Planet. Sci. Lett.*, 414, 16-29, 2015.
- Doerner, M., Berner, U., Erdmann, M., and Barth, T.: Geochemical characterization of the depositional environment of Paleocene and Eocene sediments of the Tertiary Central Basin of Svalbard, *Chemical Geology*, 542, 119587, <https://doi.org/10.1016/j.chemgeo.2020.119587>, 2020.
- 1695 Drachev, S.: Fold belts and sedimentary basins of the Eurasian Arctic, *Arktos*, 2, 21, 2016.
- Duchamp-Alphonse, S., Gardin, S., Fiet, N., Bartolini, A., Blamart, D., and Pagel, M.: Fertilization of the northwestern Tethys (Vocontian basin, SE France) during the Valanginian carbon isotope perturbation:



- 1700 evidence from calcareous nannofossils and trace element data, *Palaeogeography, Palaeoclimatology, Palaeoecology*, 243 (1-2), 132-151, 2007.
- Dummann, W., Schröder-Adams, C., Hofmann, P., Rethemeyer, J., and Herrle, J.O.: Carbon isotope and sequence stratigraphy of the upper Isachsen Formation on Axel Heiberg Island (Nunavut, Canada): High Arctic expression of oceanic anoxic event 1a in a deltaic environment, *Geosphere*, 17 (2), 501-519, 2021.
- 1705 Dummann, W., Wennrich, V., Schröder-Adams, C. J., Leicher, N., & Herrle, J. O.: Ash deposits link Oceanic Anoxic Event 2 to High Arctic volcanism. *Geology*, 52 (12): 927–932. doi: <https://doi.org/10.1130/G52368.1>, 2024.
- Dustira, A.M., Wignall, P.B., Joachimski, M., Blomeier, D., Hartkopf-Fröder, C., and Bond, D.P.G.: Gradual onset of anoxia across the Permian–Triassic Boundary in Svalbard, Norway, *Palaeogeography, Palaeoclimatology, Palaeoecology*, 374, 303-313, <https://doi.org/10.1016/j.palaeo.2013.02.004>, 2013.
- 1710 Dypvik, H., Håkansson, E., and Heinberg, C.: Jurassic and Cretaceous palaeogeography and stratigraphic comparisons in the North Greenland-Svalbard region, *Polar Research*, 21 (1), 91-108, 2002.
- Dypvik, H., Riber, L., Burca, F., Rütther, D., Jargvoll, D., Nagy, J., and Jochmann, M.: The Paleocene–Eocene thermal maximum (PETM) in Svalbard—clay mineral and geochemical signals, *Palaeogeography, Palaeoclimatology, Palaeoecology*, 302 (3-4), 156-169, 2011.
- 1715 Dzyuba, O.S., Izokh, O.P., and Shurygin, B.N.: Carbon isotope excursions in Boreal Jurassic–Cretaceous boundary sections and their correlation potential, *Palaeogeography, Palaeoclimatology, Palaeoecology*, 381-382, 33-46, <https://doi.org/10.1016/j.palaeo.2013.04.013>, 2013.
- Dörr, N., Lisker, F., Clift, P., Carter, A., Gee, D.G., Tebenkov, A., and Spiegel, C.: Late Mesozoic–Cenozoic exhumation history of northern Svalbard and its regional significance: Constraints from apatite fission track analysis, *Tectonophysics*, 514, 81-92, 2012.
- 1720 Dörr, N., Clift, P., Lisker, F., and Spiegel, C.: Why is Svalbard an island? Evidence for two-stage uplift, magmatic underplating, and mantle thermal anomalies, *Tectonics*, 32 (3), 473-486, 2013.

E

- 1725 Eberle, J., and Greenwood, D.: Life at the top of the greenhouse Eocene world--A review of the Eocene flora and vertebrate fauna from Canada's High Arctic, *Geological Society of America Bulletin*, 124, 3-23, <https://doi.org/10.1130/B30571.1>, 2012.
- Ekeheien, C., Delsett, L.L., Roberts, A.J., and Hurum, J.H.: Preliminary report on ichthyopterygian elements from the Early Triassic (Spathian) of Spitsbergen, *Norwegian Journal of Geology*, 98 (2), 219-238, 2018.
- 1730 Eldrett, J., Greenwood, D., Harding, I., and Huber, M.: Increased seasonality in the latest Eocene to earliest Oligocene in northern high latitudes, *Nature*, 459, 969-973, 2009.



- Eldrett, J.S., Harding, I.C., Firth, J.V., and Roberts, A.P.: Magnetostratigraphic calibration of Eocene–Oligocene dinoflagellate cyst biostratigraphy from the Norwegian–Greenland Sea, *Marine Geology*, 204 (1-2), 91-127, 2004.
- 1735 Engelschiøn, V.S., Bernhardsen, S., Wesenlund, F., Hammer, Ø., Hurum, J.H., and Mørk, A.: Bivalve beds reveal rapid changes in ocean oxygenation in the Boreal Middle Triassic—a case study from Svalbard, Norway, *Norwegian Journal of Geology*, 1-25, <https://dx.doi.org/10.17850/njg103-2-1>, 2023.
- Engelschiøn, V.S., Delsett, L.L., Roberts, A.J., and Hurum, J.H.: Large-sized ichthyosaurs from the Lower Saurian niveau of the Vikinghøgda formation (Early Triassic), Marmierfjellet, Spitsbergen, *Norwegian Journal of*
1740 *Geology*, 98 (2), 239-266, 2018.
- Engen, Ø., Faleide, J.I., and Dyreng, T.K.: Opening of the Fram Strait gateway: A review of plate tectonic constraints, *Tectonophysics*, 450 (1-4), 51-69, 2008.
- Erba, E., Bartolini, A., and Larson, R.L.: Valanginian Weissert oceanic anoxic event, *Geology*, 32 (2), 149-152, 2004.
- 1745 Erba, E., Duncan, R.A., Bottini, C., Tiraboschi, D., Weissert, H., Jenkyns, H.C., and Malinverno, A.: Environmental consequences of Ontong Java Plateau and Kerguelen plateau volcanism. The origin, evolution, and environmental impact of oceanic large igneous provinces, *Geological Society of America Special Paper*, 511, 271-303, [https://doi.org/10.1130/2015.2511\(15\)](https://doi.org/10.1130/2015.2511(15)), 2015.
- Erickson, T.M., Timms, N.E., Kirkland, C.L., Tohver, E., Cavosie, A.J., Pearce, M.A., and Reddy, S.M.: Shocked monazite chronometry: integrating microstructural and in situ isotopic age data for determining precise impact ages, *Contributions to Mineralogy and Petrology*, 172 (2), 11, <https://doi.org/10.1007/s00410-017-1328-2>, 2017.
- 1750 Ernst, R.E., and Youbi, N.: How Large Igneous Provinces affect global climate, sometimes cause mass extinctions, and represent natural markers in the geological record, *Palaeogeography, palaeoclimatology, palaeoecology*, 478, 30-52, 2017
- 1755 Estes, R., and Hutchinson, J.H.: Eocene Lower Vertebrates from Ellesmere Island, Canadian Arctic Archipelago, *Palaeogeogr. Palaeocl.*, 30, 325-347, 1980.
- Estrada, S., and Henjes-Kunst, F.: ^{40}Ar - ^{39}Ar and U-Pb dating of Cretaceous continental rift-related magmatism on the northeast Canadian Arctic margin, *Zeitschrift der Deutschen Gesellschaft für Geowissenschaften*, 164
1760 (1), 107-130, 2013.
- Evans, D., Sagoo, N., Renema, W., Cotton, L.J., Müller, W., Todd, J.A., Saraswati, P.K., Stassen, P., Ziegler, M., and Pearson, P.N.: Eocene greenhouse climate revealed by coupled clumped isotope-Mg/Ca thermometry, *Proceedings of the National Academy of Sciences*, 115 (6), 1174-1179, <http://www.pnas.org/cgi/doi/10.1073/pnas.1714744115>, 2018.



- 1765 Evenchick, C.A., Davis, W.J., Bédard, J.H., Hayward, N., and Friedman, R.M.: Evidence for protracted High Arctic large igneous province magmatism in the central Sverdrup Basin from stratigraphy, geochronology, and paleodepths of saucer-shaped sills, *GSA Bulletin*, 127 (9-10), 1366-1390, <https://doi.org/10.1130/b31190.1>, 2015.
- Ezaki, Y., Kawamura, T., and Nakamura, K.: Kapp Starostin Formation in Spitsbergen: a sedimentary and faunal record of Late Permian palaeoenvironments in an Arctic region, In: *Pangea: Global Environments and Resources — Memoir 17*, 647-655, 1994.
- 1770

F

- Fairchild, I.J.: The Orustdalen Formation of Brøggerhalvøya, Svalbard: A fan delta complex of Dinantian/Namurian age, *Polar Research*, 1982 (1), 17-34, <https://doi.org/10.1111/j.1751-8369.1982.tb00470.x>, 1982.
- 1775 Fairchild, I.J., Fleming, E.J., Bao, H., Benn, D.I., Boomer, I., Dublyansky, Y.V., Halverson, G.P., Hambrey, M.J., Hendy, C., McMillan, E.A., Spötl, C., Stevenson, C.T.E., and Wynn, P.M.: Continental carbonate facies of a Neoproterozoic panglaciacion, north-east Svalbard, *Sedimentology*, 63 (2), 443-497, <https://doi.org/10.1111/sed.12252>, 2016.
- Faleide, J.I., Tsikalas, F., Breivik, A.J., Mjelde, R., Ritzmann, O., Engen, Ø., Wilson, J., and Eldholm, O.: Structure and evolution of the continental margin off Norway and the Barents Sea, *Episodes Journal of International Geoscience*, 31 (1), 82-91, 2008.
- 1780 Faleide Jan, I., Pease, V., Curtis, M., Klitzke, P., Minakov, A., Scheck-Wenderoth, M., Kostyuchenko, S., and Zayonchek, A.: Tectonic implications of the lithospheric structure across the Barents and Kara shelves, *Geological Society, London, Special Publications*, 460 (1), 285-314, <https://doi.org/10.1144/SP460.18>, 2018.
- 1785 Fallatah, M. I., Alnazghah, M., Kerans, C., & Al-Hussaini, A.: Sedimentology and carbon isotope stratigraphy from the Late Jurassic – Early Cretaceous of the Arabian plate: The Weissert event and the VOICE in the Tethys Realm? *Marine and Petroleum Geology*, 161, 106670. <https://doi.org/10.1016/j.marpetgeo.2023.106670>, 2024.
- 1790 Farabegoli, E., Perri, M.C., and Posenato, R.: Environmental and biotic changes across the Permian–Triassic boundary in western Tethys: the Bulla parastratotype, Italy, *Global and Planetary Change*, 55 (1-3), 109-135, <http://dx.doi.org/10.1016/j.gloplacha.2006.06.009>, 2007.
- Franeck, F: Perspectives on the Great Ordovician Biodiversification Event-local to global patterns, (PhD Thesis, University of Oslo), 2020.
- 1795



- Fischer, A.G.: Climatic oscillations in the biosphere. Biotic crises in ecological and evolutionary time, *Academic Press*, 103-131, 1981.
- Fischer, A.G.: Long-term climate oscillations recorded in stratigraphy. *Climate in Earth history*, *Academy Press*, Washington, D.C, 97-104, 1982.
- 1800 Fischer, A.G.: The two Phanerozoic supercycles, *In: Catastrophes and Earth history* (eds. W.A. Berggren & J.A. Van Couvering), Princetown Univeristy Press, 129-150, <https://doi.org/10.1515/9781400853281.129>, 1984.
- Fortey, R., and Bruton, D.: Cambrian-Ordovician rocks adjacent to Hinlopenstretet, North Ny Friesland, Spitsbergen, *Geological Society of America Bulletin*, 84 (7), 2227-2242, 1973.
- 1805 Foster, W.J: Palaeoecology of the late Permian mass extinction and subsequent recovery, Unpublished PhD thesis, Plymouth University, 2015.
- Foster, W.J., Danise, S., Price, G.D., and Twitchett, R.J.: Subsequent biotic crises delayed marine recovery following the late Permian mass extinction event in northern Italy, *PLoS One*, 12 (3), e0172321, <https://doi.org/10.1371/journal.pone.0172321>, 2017a.
- 1810 Foster, W.J., Danise, S., and Twitchett, R.J.: A silicified Early Triassic marine assemblage from Svalbard, *Journal of Systematic Palaeontology*, 15 (10), 851-877, <https://doi.org/10.1080/14772019.2016.1245680>, 2017b.
- Foster, W.J., Lehrmann, D.J., Yu, M., Ji, L., and Martindale, R.C.: Persistent environmental stress delayed the recovery of marine communities in the aftermath of the latest Permian mass extinction. *Paleoceanography and Paleoclimatology*, 33 (4), 338-353, 2018.
- 1815 Foster, W.J., Hirtz, J.A., Farrell, C., Reistroffer, M., Twitchett, R.J., and Martindale, R.C.: Bioindicators of severe ocean acidification are absent from the end-Permian mass extinction, *Scientific Reports*, 12 (1), 1202, <https://doi.org/10.1038/s41598-022-04991-9>, 2022.
- Foster, W.J., Asatryan, G., Rauzi, S., Botting, J., Buchwald, S., Lazarus, D., Isson, T., Renaudie, J., and Kiessling, W.: Response of Siliceous Marine Organisms to the Permian-Triassic Climate Crisis Based on New Findings From Central Spitsbergen, Svalbard, *Paleoceanography and Paleoclimatology*, 38 (12), e2023PA004766, 2023.
- 1820 Frakes, L.A., Francis, J.E., and Syktus, J.I.: Climate modes of the Phanerozoic, *Cambridge University Press*, Cambridge, 274 pp, 1992.
- Franks, P.J., Berry, J.A., Lombardozzi, D.L., and Bonan, G.B.: Stomatal Function across Temporal and Spatial Scales: Deep-Time Trends, Land-Atmosphere Coupling and Global Models, *Plant Physiology*, 174 (2), 583-602, <https://doi.org/10.1104/pp.17.00287>, 2017.
- 1825 Friend, P.: Fluvial sedimentary structures in the Wood Bay series (Devonian) of Spitsbergen, *Sedimentology*, 5 (1), 39-68, 1965.



- 1830 Friend, P., Harland, W., Rogers, D., Snape, I., and Thornley, R.: Late Silurian and Early Devonian stratigraphy and probable strike-slip tectonics in northwestern Spitsbergen, *Geological Magazine*, 134 (4), 459-479, 1997.
- Friend, P.F.: The Devonian stratigraphy of north and central Spitsbergen. *Proceedings of the Yorkshire Geological Society*, 33 (1), 77-118, <https://doi.org/10.1144/pygs.33.1.77>, 1961.
- Friend, P.F., and Moody-Stuart, M.: Carbonate deposition on the river floodplains of the Wood Bay Formation (Devonian) of Spitsbergen, *Geological Magazine*, 107 (3), 181-195, 1835 <https://doi.org/10.1017/S0016756800055655>, 1970.
- Feyling-Hanssen, R.W., and Ulleberg, K.: A Tertiary-Quaternary section at Sarsbukta, Spitsbergen, Svalbard, and its foraminifera, *Polar Research*, 2, 77-106, <https://doi.org/10.3402/polar.v2i1.6963>, 1984.
- Fyhn, M.B.W., and Hopper, J.R.: NE Greenland Composite Tectono-Sedimentary Element, northern Greenland Sea and Fram Strait. *Geological Society, London, Memoirs*, 57, <https://doi.org/10.1144/M57-2017-12>, 1840 [2025](https://doi.org/10.1144/M57-2017-12).
- ## G
- Gabrielsen, R.H., Kløvjan, O.S., Haugsbø, H., Midbøe, P.S., Nøttvedt, A., Rasmussen, E., and Skott, P.H.: A structural outline of Forlandsundet Graben, Prins Karls Forland, Svalbard, *Norsk Geologisk Tidsskrift*, 72, 1845 105-120, 1992.
- Galfetti, T., Hochuli, P.A., Brayard, A., Bucher, H., Weissert, H., and Vigran, J.O.: Smithian-Spathian boundary event: Evidence for global climatic change in the wake of the end-Permian biotic crisis, *Geology*, 35 (4), 291-294, <https://doi.org/10.1130/g23117a.1>, 2007.
- Galloway, J.M., Vickers, M.L., Price, G.D., Poulton, T., Grasby, S.E., Hadlari, T., Beauchamp, B., and Sulphur, K.: 1850 Finding the VOICE: organic carbon isotope chemostratigraphy of Late Jurassic – Early Cretaceous Arctic Canada, *Geological Magazine*, 157 (10), 1643-1657, <https://doi.org/10.1017/s0016756819001316>, 2020.
- Galloway, J.M., Fensome, R.A., Swindles, G.T., Hadlari, T., Fath, J., Schröder-Adams, C., Herrle, J.O., and Pugh, A.: Exploring the role of High Arctic Large Igneous Province volcanism on Early Cretaceous Arctic forests, *Cretaceous Research*, 129, 105022, 2022.
- 1855 Galloway, J.M., Grasby, S.E., Wang, F., Hadlari, T., Dewing, K., Bodin, S., and Sanei, H.: A mercury and trace element geochemical record across Oceanic Anoxic Event 1b in Arctic Canada, *Palaeogeography, Palaeoclimatology, Palaeoecology*, 617, 111490, <https://doi.org/10.1016/j.palaeo.2023.111490>, 2023.
- Galloway, J.M., and Lindström, S.: Impacts of Large-scale Magmatism on Land Plant Ecosystems, *Elements*, 19, 289-295, 2023a.
- 1860 Galloway, J.M., and Lindström, S.: Wildfire in the geological record: Application of Quaternary methods to deep time studies, *Evolving Earth*, 1, 100025, 2023b.



- Galloway, J. M., Hadlari, T., Dewing, K., Poulton, T., Grasby, S. E., Reinhardt, L., Rogov, M., Longman, J., and Vickers, M.: The silent VOICE—Searching for geochemical markers to track the impact of Late Jurassic rift tectonics. *Geochemistry, Geophysics, Geosystems*, 25(10), e2024GC011490, 2024.
- 1865 Gastaldo, R.A., DiMichele, W.A., and Pfefferkorn, H.W.: Out of the icehouse into the greenhouse: a late Paleozoic analogue for modern global vegetational change, *GSA Today*, 6 (10), 1-7, 1996.
- Gee, D.G., Bogolepova, O.K., and Lorenz, H.: The Timanide, Caledonide and Uralide orogens in the Eurasian high Arctic, and relationships to the palaeo-continent Laurentia, Baltica and Siberia, *Geological Society, London, Memoirs*, 32 (1), 507-520, <https://doi.org/10.1144/GSL.MEM.2006.032.01.31>, 2006.
- 1870 Gee, D.G., and Teben'kov, A.: Svalbard: a fragment of the Laurentian margin, *Geological Society, London, Memoirs*, 30 (1), 191-206, 2004.
- Gensel, P.G.: The earliest land plants. *Annual Review of Ecology, Evolution, and Systematics*, 39: 459-477, 2008.
- Gilmullina, A., Klausen, T.G., Doré, A.G., Rossi, V.M., Suslova, A., Eide, C.H.: Linking sediment supply variations and tectonic evolution in deep time, source-to-sink systems - The Triassic Greater Barents Sea Basin. *GSA Bulletin* 134(7-8), 1760-1780. 2022.
- 1875 Gion, A. M., Williams, S. E., and Müller, R. D.: A reconstruction of the Eureka Orogeny incorporating deformation constraints. *Tectonics*, 36(2), 304-320, 2017.
- Gjelberg, J. and Steel, R.: An outline of Lower-Middle Carboniferous sedimentation on Svalbard: Effects of tectonic, climatic and sea level changes in rift basin sequences, *Geology of the North Atlantic Borderlands — Memoir 7*, 543-561, 1981.
- 1880 Gjelberg, J. and Steel, R.J.: Helvetiafjellet Formation (Barremian-Aptian), Spitsbergen: characteristics of a transgressive succession, *Norwegian Petroleum Society Special Publications. Elsevier*, 571-593 [https://doi.org/10.1016/S0928-8937\(06\)80087-1](https://doi.org/10.1016/S0928-8937(06)80087-1), 1995.
- Glørstad-Clark, E., Faleide, J.I., Lundschie, B.A. and Nystuen, J.P.: Triassic seismic sequence stratigraphy and paleogeography of the western Barents Sea area. *Marine and Petroleum geology*, 27(7): 1448-1475, <https://doi.org/10.1016/j.marpetgeo.2010.02.008>, 2010
- 1885 Gobbett, D.J. and Wilson, C.: The Oslobreen Series, Upper Hecla Hoek of Ny Friesland, Spitsbergen. *Geological Magazine*, 97(6): 441-457, 1960.
- Golovneva, L. B.: Palaeogene climates of Spitsbergen. *GFF (Geological Society of Sweden)*, 122(1), 62–63. <https://doi.org/10.1080/11035890001221062>, 2000.
- 1890 Golovneva, L.B., Zolina, A.A. and Spicer, R.A.: The early Paleocene (Danian) climate of Svalbard based on palaeobotanical data. *Papers in Palaeontology*, 9(6): e1533, 2023.
- Golovneva, L., and Zolina, A.: The Renardodden flora of Spitsbergen. *Biological Communications*, 68(4), 307–319. <https://doi.org/10.21638/spbu03.2023.410>, 2023.



- 1895 Gomes, A.S., Vasconcelos, P.M.: Geochronology of the Parana-Etendeka large igneous province. *Earth Sci. Rev.* 220, 103716. 2021.
- Grasby, S.E. and Beauchamp, B.: Intrabasin variability of the carbon-isotope record across the Permian–Triassic transition, Sverdrup Basin, Arctic Canada. *Chemical Geology*, 253(3): 141-150, <https://doi.org/10.1016/j.chemgeo.2008.05.005>, 2008.
- 1900 Grasby, S., Sanei, H. & Beauchamp, B.: Catastrophic dispersion of coal fly ash into oceans during the latest Permian extinction. *Nature Geosci* 4, 104–107. <https://doi.org/10.1038/ngeo1069>, 2011.
- Grasby, S.E., Beauchamp, B., Embry, A. and Sanei, H.: Recurrent Early Triassic Ocean anoxia. *Geology*, 41(2): 175-178, 10.1130/g33599.1, 2013.
- Grasby, S.E., Beauchamp, B., Bond, D.P.G., Wignall, P., Talavera, C., Galloway, J.M., Piepjohn, K., Reinhardt, L. and Blomeier, D.: Progressive environmental deterioration in northwestern Pangea leading to the latest Permian extinction. *GSA Bulletin*, 127(9-10): 1331-1347, 10.1130/b31197.1, 2015a.
- Grasby, S.E., Beauchamp, B., Bond, D.P.G., Wignall, P.B. and Sanei, H.: Mercury anomalies associated with three extinction events (Capitanian Crisis, Latest Permian Extinction and the Smithian/Spathian Extinction) in NW Pangea. *Geological Magazine*, 153(2): 285-297, 10.1017/s0016756815000436, 2015b.
- 1910 Grasby, S.E., Beauchamp, B., Bond, D.P., Wignall, P.B. and Sanei, H.: Mercury anomalies associated with three extinction events (Capitanian crisis, latest Permian extinction and the Smithian/Spathian extinction) in NW Pangea. *Geological magazine*, 153(2): 285-297, 2016a.
- Grasby, S.E., Beauchamp, B. and Knies, J.: Early Triassic productivity crises delayed recovery from world's worst mass extinction. *Geology*, 44(9): 779-782, 2016b.
- 1915 Grasby, S.E., Shen, W., Yin, R., Gleason, J.D., Blum, J.D., Lepak, R.F., Hurley, J.P. and Beauchamp, B.: Isotopic signatures of mercury contamination in latest Permian oceans. *Geology*, 45(1): 55-58. 2017a.
- Grasby, S. E., McCune, G. E., Beauchamp, B., and Galloway, J. M.: Lower Cretaceous cold snaps led to widespread glendonite occurrences in the Sverdrup Basin, *Canadian High Arctic. Bulletin*, 129(7-8), 771-787, 2017b.
- 1920 Grasby, S.E., Knies, J., Beauchamp, B., Bond, D.P.G., Wignall, P. and Sun, Y.: Global warming leads to Early Triassic nutrient stress across northern Pangea. *GSA Bulletin*, 132(5-6): 943-954, 10.1130/b32036.1, 2019a.
- Grasby, S.E., Them, T.R., Chen, Z., Yin, R. and Ardakani, O.H.: Mercury as a proxy for volcanic emissions in the geologic record. *Earth-Science Reviews*, 196: 102880, <https://doi.org/10.1016/j.earscirev.2019.102880>, 2019b.
- 1925 Grasby, S.E., Liu, X., Yin, R., Ernst, R.E. and Chen, Z.: Toxic mercury pulses into late Permian terrestrial and marine environments. *Geology*, 48(8): 830-833, 10.1130/g47295.1, 2020.



- Green, P. F., and Duddy, I. R.: Synchronous exhumation events around the Arctic including examples from Barents Sea and Alaska North Slope. In *Geological Society, London, Petroleum Geology Conference Series* (Vol. 7, No. 1, pp. 633-644). London: The Geological Society of London, 2010.
- Green, T., Renne, P.R. and Brenhin Kneller, C.: Continental flood basalts drive Phanerozoic extinctions. *Proceedings of The National Academy of Sciences*, 119 (38), e2120441119, 2022.
- Greenwood, D.R., Basinger, J.F. and Smith, R.Y.: How wet was the Arctic Eocene rain forest? Estimates of precipitation from Paleogene Arctic macrofloras. *Geology*, 38(1): 15-18, 10.1130/g30218.1, 2010.
- Grossman, E. L., Yancey, T. E., Jones, T. E., Bruckschen, P., Chuvashov, B., Mazzullo, S. J., and Mii, H. S.: Glaciation, aridification, and carbon sequestration in the Permo-Carboniferous: the isotopic record from low latitudes. *Palaeogeography, Palaeoclimatology, Palaeoecology*, 268(3-4), 222-233, 2008.
- Grossman, E.L.: Applying Oxygen Isotope Paleothermometry in Deep Time. *The Paleontological Society Papers*, 18: 39-68, 10.1017/S1089332600002540, 2012.
- Grotheer, H., Le Métayer, P., Piggott, M., Lindeboom, E., Holman, A., Twitchett, R. and Grice, K.: Occurrence and significance of phytanyl arenes across the Permian-Triassic boundary interval. *Organic Geochemistry*, 104: 42-52, 2017.
- Grundvåg, S.-A., Jelby, M.E., Śliwińska, K.K., Nøhr-Hansen, H., Aadland, T., Sandvik, S.E., Tennvassås, I., Engen, T.M. and Olausson, S.: Sedimentology and palynology of the Lower Cretaceous succession of central Spitsbergen: integration of subsurface and outcrop data. *Norwegian Journal of Geology* <https://dx.doi.org/10.17850/njg99-2-02>, 2019.
- Grundvåg, S.-A. and Olausson, S.: Sedimentology of the Lower Cretaceous at Kikutodden and Keilhaufjellet, southern Spitsbergen: implications for an onshore-offshore link. *Polar Research*, 36(1): 1302124, 10.1080/17518369.2017.1302124, 2017.
- Grundvåg, S.A., Johannessen, E.P.: Helland-Hansen, W. and Plink-Björklund, P., Depositional architecture and evolution of progradationally stacked lobe complexes in the Eocene Central Basin of Spitsbergen. *Sedimentology*, 61(2): 535-569, <https://doi.org/10.1111/sed.12067>, 2014.
- Grundvåg, S.A., Marin, D., Kairanov, B., Śliwińska, K.K., Nøhr-Hansen, H., Jelby, M.E., Escalona, A. and Olausson, S.: The Lower Cretaceous succession of the northwestern Barents Shelf: Onshore and offshore correlations. *Marine and Petroleum Geology*, 86: 834-857. <https://doi.org/10.1016/j.marpetgeo.2017.06.036>, 2017.
- Grundvåg, S.A., Helland-Hansen, W., Johannessen, E.P., Eggenhuisen, J., Pohl, F., and Sychala, Y.: Deep-water sand transfer by hyperpycnal flows, the Eocene of Spitsbergen, Arctic Norway. *Sedimentology*, 70(7): 2057-2107, 2023.
- Gruszczynski, M., Hałas, S., Hoffman, A. and Małkowski, K.: A brachiopod calcite record of the oceanic carbon and oxygen isotope shifts at the Permian/Triassic transition. *Nature*, 337(6202): 64-68, 1989.



- Gröcke, D.R., Price, G.D., Robinson, S.A., Baraboshkin, E.Y., Mutterlose, J. and Ruffell, A.H.: The Upper Valanginian (Early Cretaceous) positive carbon–isotope event recorded in terrestrial plants. *Earth and Planetary Science Letters*, 240(2): 495-509, 2005.
- 1965 Guarnieri, P.: Pre-break-up palaeostress state along the East Greenland margin. *Journal of the Geological Society*, 172(6): 727-739, 10.1144/jgs2015-053, 2015.
- Gudlaugsson, S., Faleide, J., Johansen, S. and Breivik, A.: Late Palaeozoic structural development of the southwestern Barents Sea. *Marine and Petroleum Geology*, 15(1): 73-102, [https://doi.org/10.1016/S0264-8172\(97\)00048-2](https://doi.org/10.1016/S0264-8172(97)00048-2), 1998.
- 1970 Gussone, N., Ahm, A.-S.C., Lau, K.V. and Bradbury, H.J.: Calcium isotopes in deep time: Potential and limitations. *Chemical Geology*, 544: 119601, <https://doi.org/10.1016/j.chemgeo.2020.119601>, 2020.
- Gutjahr, M., Ridgwell, A., Sexton, P.F., Anagnostou, E., Pearson, P.N., Pälike, H., Norris, R.D., Thomas, E. and Foster, G.L.: Very large release of mostly volcanic carbon during the Palaeocene–Eocene Thermal Maximum. *Nature*, 548(7669): 573-577, 10.1038/nature23646, 2017.
- 1975
- H**
- Haaland, L.C., Slagstad, T., Osmundsen, P.T., Redfield, T.: U-Pb calcite ages date oblique rifting of the Arctic-North Atlantic gateway. *Geology*, 52(8), 615-619, 2024.
- Hansen, B. B., Bucher, H. F., Schneebeli-Hermann, E., and Hammer, Ø.: Smithian and Spathian palaeontological records of the Vikinghøgda Formation in Central Spitsbergen. *Lethaia*, 57(1), 1-15, 2024.
- 1980 Hallam, A.: A review of Mesozoic climates. *Journal of the Geological Society*, 142(3): 433-445, 1985.
- Halverson, G.P., Maloof, A.C. and Hoffman, P.F.: The Marinoan glaciation (Neoproterozoic) in northeast Svalbard. *Basin Research*, 16(3): 297-324, 2004.
- Hambrey, M.J.: Late Precambrian diamictites of northeastern Svalbard. *Geological Magazine*, 119(6): 527-551, 10.1017/S0016756800027035, 1982.
- 1985 Hammer, Ø., Nakrem, H.A., Little, C.T., Hryniewicz, K., Sandy, M.R., Hurum, J.H., Druckenmiller, P., Knutsen, E.M. and Høyberget, M.: Hydrocarbon seeps from close to the Jurassic–Cretaceous boundary, Svalbard. *Palaeogeography, Palaeoclimatology, Palaeoecology*, 306(1-2): 15-26, 2011.
- Hammer, Ø., Collignon, M. and Nakrem, H.A.: Organic carbon isotope chemostratigraphy and cyclostratigraphy in the Volgian of Svalbard. *Norwegian Journal of Geology*, 92, 2012.
- 1990 Hammer, Ø., Jones, M.T., Schneebeli-Hermann, E., Hansen, B.B. and Bucher, H.: Are Early Triassic extinction events associated with mercury anomalies? A reassessment of the Smithian/Spathian boundary extinction. *Earth-Science Reviews*, 195: 179-190, <https://doi.org/10.1016/j.earscirev.2019.04.016>, 2019.



- 1995 Hanken, N.-M. and Nielsen, J.K.: Upper Carboniferous–Lower Permian Palaeoaplysina build-ups on Svalbard: the influence of climate, salinity and sea-level. Geological Society, London, *Special Publications*, 376(1): 269-305, <https://doi.org/10.1144/SP376.17>, 2013.
- Hansen, J. and Holmer, L.E.: Diversity fluctuations and biogeography of Ordovician brachiopod faunas in northeastern Spitsbergen. *Bulletin of Geosciences*, 85(3): 497-504, 2010.
- 2000 Hansen, B. B., Bucher, H. F., Schneebeil-Hermann, E., and Hammer, Ø.: Smithian and Spathian palaeontological records of the Vikinghøgda Formation in Central Spitsbergen. *Lethaia*, 57(1), 1-15, 2024
- Haq, B.U.: Cretaceous eustasy revisited. I 113: 44-58, 10.1016/j.gloplacha.2013.12.007, 2014.
- Harding, I.C., Charles, A.J., Marshall, J.E.A., Pälike, H., Roberts, A.P., Wilson, P.A., Jarvis, E., Thorne, R., Morris, E., Moremon, R., Pearce, R.B. and Akbari, S.: Sea-level and salinity fluctuations during the Paleocene–Eocene thermal maximum in Arctic Spitsbergen. *Earth and Planetary Science Letters*, 303(1): 97-107, 2005 <https://doi.org/10.1016/j.epsl.2010.12.043>, 2011.
- Harland, W.B. and Wilson, C.: The Hecla Hoek succession in Ny Friesland, Spitsbergen. *Geological Magazine*, 93(4): 265-286, 1956.
- Harland, W.B., Cutbill, J., Friend, P.F., Gobbett, D.J., Holliday, D., Maton, P., Parker, J. and Wallis, R.H.: The Billefjorden Fault Zone, Spitsbergen: the long history of a major tectonic lineament, Nor. Polarinst. Skr., 2010 161, 1974.
- Harland, W., Herod, K., Wright, A. and Moseley, F.: Ice Ages: Ancient and Modern. *Seel House Press Liverpool*, 189-126, 1975a.
- Harland, W.B., Pickton, C.A. and Reynolds, A.B.: Cambridge Svalbard Expedition, 1974. *Polar Record*, 17(109): 383-384, 10.1017/S0032247400032204, 1975b.
- 2015 Harland, W. and Wright, N.: Alternative hypothesis for the pre-Carboniferous evolution of Svalbard. *Norsk Polarinstitutt Skrifter*, 167: 89-117, 1979.
- Harland, W.B.: Svalbard. W.B. Harland (Ed.): *Geology of Svalbard*, Geological Society, London, *Memoirs* 1997.
- Harper, D.T., Suarez, M.B., Uglesich, J., You, H., Li, D. and Dodson, P.: Aptian–Albian clumped isotopes from northwest China: cool temperatures, variable atmospheric pCO₂ and regional shifts in the hydrologic cycle. 2020 *Climate of the Past*, 17(4), pp.1607-1625, 2021.
- Hatleberg, E.: Lower Triassic conodonts and biofacies interpretations: Nepal and Svalbard. *Geologica et Palaeontologica*, 18: 101-125, 1984.
- Hauser, N., Reimold, W.U., Cavosie, A.J., Crósta, A.P., Schwarz, W.H., Trieloff, M., Da Silva Maia de Souza, C., Pereira, L.A., Rodrigues, E.N. and Brown, M.: Linking shock textures revealed by BSE, CL, and EBSD with U-Pb data (LA-ICP-MS and SIMS) from zircon from the Araguinha impact structure, Brazil. *Meteoritics and Planetary Science*, 54(10): 2286-2311, <https://doi.org/10.1111/maps.13371>, 2019.



- Head, M.: A palynological investigation of Tertiary strata at Renardodden, West Spitsbergen, *6th International Palynological Conference*, Abstract, pp. 61, 1984.
- 2030 Henderson, C.M., Baud, A.: Correlation of the Permian-Triassic boundary in Arctic Canada and comparison with Meishan, China. *Proceedings, 30th International Geological Congress*. 11,143–152, 1997.
- Helland-Hansen, W.: Sedimentation in Paleogene Foreland Basin, Spitsbergen1. *AAPG Bulletin*, 74(3): 260-272, 10.1306/0c9b22bd-1710-11d7-8645000102c1865d, 1990.
- Helland-Hansen, W. and Grundvåg, S.A.: The Svalbard Eocene-Oligocene (?) Central Basin succession: Sedimentation patterns and controls. *Basin Research*, 33(1): 729-753, 10.1111/bre.12492, 2021.
- 2035 Henderson, C.M., Baud, A.: Correlation of the Permian-Triassic boundary in Arctic Canada and comparison with Meishan, China. *Proceedings, 30th International Geological Congress*. 11, 143–152, 1997.
- Henriksen, E., Bjørnseth, H., Hals, T., Heide, T., Kiryukhina, T., Kløvjan, O., Larssen, G.B., Ryseth, A., Rønning, K. and Sollid, K.: Chapter 17 Uplift and erosion of the greater Barents Sea: impact on prospectivity and petroleum systems. *Geological Society, London, Memoirs*, 35(1): 271-281, 2011a.
- 2040 Henriksen, E., Ryseth, A.E., Larssen, G.B., Heide, T., Rønning, K., Sollid, K. and Stoupakova, A.V.: Chapter 10 Tectonostratigraphy of the greater Barents Sea: implications for petroleum systems. *Geological Society, London, Memoirs*, 35(1): 163-195, 10.1144/M35.10, 2011b.
- Herrle, J.O., Schröder-Adams, C.J., Davis, W., Pugh, A.T., Galloway, J.M. and Fath, J.: Mid-Cretaceous High Arctic stratigraphy, climate, and oceanic anoxic events. *Geology*, 43(5): 403-406, 2015.
- 2045 Hesselbo, S.P., Gröcke, D.R., Jenkyns, H.C., Bjerrum, C.J., Farrimond, P., Morgans Bell, H.S. and Green, O.R.: Massive dissociation of gas hydrate during a Jurassic oceanic anoxic event. *Nature*, 406(6794): 392-395, 2000.
- Hesselbo, S.P., Jenkyns, H.C., Duarte, L.V. and Oliveira, L.C.: Carbon-isotope record of the Early Jurassic (Toarcian) Oceanic Anoxic Event from fossil wood and marine carbonate (Lusitanian Basin, Portugal). *Earth and Planetary Science Letters*, 253(3-4): 455-470, <https://doi.org/10.1016/j.epsl.2006.11.009>, 2007.
- Heyn, B. H., Shephard, G. E., and Conrad, C. P.: Prolonged multi-phase magmatism due to plume-lithosphere interaction as applied to the High Arctic Large Igneous Province. *Geochemistry, Geophysics, Geosystems*, 25, e2023GC011380. <https://doi.org/10.1029/2023GC011380>, 2024.
- 2055 Hjalmsarsdóttir, H.R., Hammer, Ø., Nagy, J. and Grundvåg, S.-A.: Foraminiferal stratigraphy and palaeoenvironment of a storm-influenced marine shelf: Upper Aptian–lower Albian, Svalbard, Arctic Norway. *Cretaceous Research*, 130: 105033, 2022.
- Hjelstuen, B. O., Elverhøi, A., and Faleide, J. I.: Cenozoic erosion and sediment yield in the drainage area of the Storfjorden Fan. *Global and Planetary Change*, 12(1-4), 95-117, 1996.



- 2060 Hochuli, P.A., Hermann, E., Vigran, J.O., Bucher, H. and Weissert, H.: Rapid demise and recovery of plant ecosystems across the end-Permian extinction event. *Global and Planetary Change*, 74(3): 144-155, <https://doi.org/10.1016/j.gloplacha.2010.10.004>, 2010.
- Hoel, A. and Orvin, A.K.: 1937. Das Festungsprofil auf Spitzbergen. I, Karbon-Kreide: Vermessungsergebnisse.
- Hoffman, P.F. and Schrag, D.P.: The snowball Earth hypothesis: testing the limits of global change. *Terra nova*, 2065 14(3): 129-155, 2002.
- Hofmann, R., Goudemand, N., Wasmer, M., Bucher, H., and Hautmann, M.: New trace fossil evidence for an early recovery signal in the aftermath of the end-Permian mass extinction. *Palaeogeography, Palaeoclimatology, Palaeoecology*, 310(3-4), 216-226, 2011.
- Hofmann, R., Hautmann, M., and Bucher, H.: A new paleoecological look at the Dinwoody Formation (Lower 2070 Triassic, Western USA): intrinsic versus extrinsic controls on ecosystem recovery after the end-Permian mass extinction. *Journal of Paleontology*, 87(5), 854-880, 2013.
- Hofmann, R., Hautmann, M., Brayard, A., Nützel, A., Bylund, K. G., Jenks, J. F., Vennin, E., Oliver, N., and Bucher, H., Recovery of benthic marine communities from the end-Permian mass extinction at the low latitudes of eastern Panthalassa. *Palaeontology*, 57(3), 547-589, 2014.
- 2075 Hofmann, R., Hautmann, M., and Bucher, H., Recovery dynamics of benthic marine communities from the Lower Triassic Werfen Formation, northern Italy. *Lethaia*, 48(4), 474-496, 2015.
- Holland, M.M. and Bitz, C.M.: Polar amplification of climate change in coupled models. *Climate dynamics*, 21(3-4): 221-232, 10.1007/s00382-003-0332-6, 2003.
- Holliday, D. and Cutbill, J.: The Ebbadalen Formation (Carboniferous), Spitsbergen. *Proceedings of the Yorkshire 2080 Geological Society*, 39(1): 1-32, 1972.
- Holmden, C., Creaser, R.A., Muehlenbachs, K., Leslie, S.A. and Bergström, S.M.: Isotopic evidence for geochemical decoupling between ancient epeiric seas and bordering oceans: Implications for secular curves. *Geology*, 26(6): 567-570, 10.1130/0091-7613(1998)026, 2.3.Co;2, 1998.
- Hönisch, B., Ridgwell, A., Schmidt, D., Thomas, E., Gibbs, S., Sluijs, A., Zeebe, R., Kump, L., Martindale, R.C., 2085 Greene, S.E., Kiessling, W., Ries, J., Zachos, J.C., Royer, D., Barker, S., Marchitto, T.M.Jr., Moyer, R., Pelejero, C., Ziveri, P., Foster, G., Williams, B.: The Geological Record of Ocean Acidification. *Science*, 335(6072): 1058-1063, 2012.
- Horota, R.K., Rossa, P., Marques, A., Gonzaga, L., Senger, K., Cazarin, C.L., Spigolon, A. and Veronez, M.R.: An Immersive Virtual Field Experience Structuring Method for Geoscience Education. *IEEE Transactions on 2090 Learning Technologies*, 16(1): 121-132, 2022.
- Hochuli, P.A., Schneebeli-Hermann, E., Mangerud, G. and Bucher, H.: Evidence for atmospheric pollution across the Permian-Triassic transition. *Geology*, 45(12): 1123-1126, 2017.



- 2095 Hovikoski, J., Fyhn, M.B.W., Nøhr-Hansen, H., Hopper, J.R., Andrews, S., Barham, M., Nielsen, L.H., Bjerager, M.,
Bojesen-Koefoed, J., Lode, S., Sheldon, E., Uchman, A., Skorstengaard, P.R., and Alsen, P.: Paleocene-
Eocene volcanic segmentation of the Norwegian-Greenland seaway reorganized high-latitude ocean
circulation. *Communications Earth and Environment*, 2: 172, 2021.
- Hryniewicz, K., Nakrem, H.A., Hammer, Ø., Little, C.T., Kaim, A., Sandy, M.R. and Hurum, J.H.: The palaeoecology
of the latest Jurassic–earliest Cretaceous hydrocarbon seep carbonates from Spitsbergen, Svalbard.
Lethaia, 48(3): 353-374, 2015.
- 2100 Hurum, J.H., Milàn, J., Hammer, Ø., Midtkandal, I., Amundsen, H. and Sæther, B.: Tracking polar dinosaurs-new
finds from the Lower Cretaceous of Svalbard. *Norwegian Journal of Geology*. 86(4), 2006.
- Hurum, J.H., Nakrem, H.A., Hammer, Ø., Knutsen, E.M., Druckenmiller, P.S., Hryniewicz, K. and Novis, L.K.: An
Arctic Lagerstätte—the Slotsmøya Member of the Agardhfjellet Formation (Upper Jurassic–Lower
Cretaceous) of Spitsbergen. *Norwegian Journal of Geology*, 92, 2012.
- 2105 Hurum, J.H., Roberts, A.J., Nakrem, H.A., Stenløkk, J.A. and Mørk, A.: The first recovered ichthyosaur from the
Middle Triassic of Edgeøya, Svalbard. *Norwegian Petroleum Directorate Bulletin*, 11: 97-110, 2014.
- Hurum, J.H., Druckenmiller, P.S., Hammer, Ø., Nakrem, H.A. and Olausen, S.: The theropod that wasn't: an
ornithomimid tracksite from the Helvetiafjellet Formation (Lower Cretaceous) of Boltodden, Svalbard.
Geological Society, London, Special Publications, 434(1): 189-206, <https://doi.org/10.1144/SP434.10>,
2110 2016a.
- Hurum, J.H., Roberts, A.J., Dyke, G.J., Grundvåg, S.-A., Nakrem, H.A., Midtkandal, I., Sliwiska, K. and Olausen,
S.: Bird or maniraptoran dinosaur? A femur from the Albian strata of Spitsbergen. *Palaeontologia Polonica*,
67: 137-47, 2016b.
- Hurum, J.H., Engelschiøn, V.S., Økland, I.H., Bratvold, J., Ekeheien, C., Roberts, A.J., Delsett, L.L., Hansen, B.B.,
2115 Mørk, A. and Nakrem, H.A.: The history of exploration and stratigraphy of the Early to Middle Triassic
vertebrate-bearing strata of Svalbard (Sassendalen Group, Spitsbergen). *Norwegian Journal of Geology*,
98(2): 165-174, 2018.
- Hutchinson, D.K., Coxall, H.K., Lunt, D.J., Steinthorsdottir, M., De Boer, A.M., Baatsen, M., von der Heydt, A.,
Huber, M., Kennedy-Asser, A.T. and Kunzmann, L.: The Eocene–Oligocene transition: a review of marine
and terrestrial proxy data, models and model–data comparisons. *Climate of the Past*, 17(1): 269-315, 2021.
- 2120 Hutchinson, D.K., Coxall, H.K., O'Regan, M., Nilsson, J., Caballero, R. and de Boer, A.M.: Arctic closure as a trigger
for Atlantic overturning at the Eocene-Oligocene Transition. *Nature Communications*, 10(1): 3797,
10.1038/s41467-019-11828-z, 2019.
- Hüneke, H., Joachimski, M., Buggisch, W. and Lützner, H.: Marine carbonate facies in response to climate and
nutrient level: The upper carboniferous and permian of central spitsbergen (Svalbard). *Facies*, 45(1): 93-
2125 135, 10.1007/BF02668107, 2001.



Høy, T. and Lundschieen, B.: Triassic deltaic sequences in the northern Barents Sea. Geological society, London, memoirs, 35(1): 249-260, <https://doi.org/10.1144/M35.15>, 2011.

I

2130 Inglis, G.N., Bragg, F., Burls, N.J., Cramwinckel, M.J., Evans, D., Foster, G.L., Huber, M., Lunt, D.J., Siler, N. and Steinig, S.: Global mean surface temperature and climate sensitivity of the early Eocene Climatic Optimum (EECO), Paleocene–Eocene Thermal Maximum (PETM), and latest Paleocene. *Climate of the Past*, 16(5): 1953-1968, 10.5194/cp-16-1953-2020, 2020.

Ingólfsson, Ó., and Landvik, J. Y.: The Svalbard–Barents Sea ice-sheet–Historical, current and future perspectives. *Quaternary Science Reviews*, 64, 33-60, 2013.

2135 Isbell, J.L., Fraiser, M.L. and Henry, L.C.: Examining the Complexity of Environmental Change during the Late Paleozoic and Early Mesozoic. *PALAIOS*, 23(5): 267-269, 10.2110/palo.2008.S03, 2008.

Ivanov, A.V., He, H., Yan, L., Ryabov, V.V., Shevko, A.Y., Palesskii, S.V. and Nikolaeva, I.V.: Siberian Traps large igneous province: Evidence for two flood basalt pulses around the Permo-Triassic boundary and in the Middle Triassic, and contemporaneous granitic magmatism. *Earth-Science Reviews*, 122: 58-76, 2140 <https://doi.org/10.1016/j.earscirev.2013.04.001>, 2013.

J

Jakobsson, M., Backman, J., Rudels, B., Nycander, J., Frank, M., Mayer, L., Jokat, W., Sangiorgi, F., O'Regan, M., and Brinkhuis, H.: The early Miocene onset of a ventilated circulation regime in the Arctic Ocean, *Nature*, 2145 447, 986–990, 2007.

Janocha, J., Wesenlund, F., Thießen, O., Grundvåg, S.-A., Koehl, J.-B., and Johannessen, E. P.: Petroleum geochemistry of Upper Paleozoic strata on Bjørnøya, western Barents Shelf, *Mar. Petrol. Geol.*, 163, 106768, <https://doi.org/10.1016/j.marpetgeo.2024.106768>, 2024.

2150 Jansen, E., Overpeck, J., Briffa, K. R., Duplessy, J.-C., Joos, F., Masson-Delmotte, V., Olago, D., Otto-Bliesner, B., Peltier, W. R., Rahmstorf, S., Ramesh, R., Raynaud, D., Rind, D., Solomina, O., Villalba, R., and Zhang, D.: *Palaeoclimate*, in: *Climate Change 2007: The Physical Science Basis. Contribution of Working Group I to the Fourth Assessment Report of the Intergovernmental Panel on Climate Change*, edited by: Solomon, S., Qin, D., Manning, M., Chen, Z., Marquis, M., Averyt, K. B., Tignor, M., and Miller, H. L., Cambridge University Press, Cambridge, United Kingdom and New York, NY, USA, 2007.

2155 Jelby, M. E., Grundvåg, S. A., Helland-Hansen, W., Olaussen, S., and Stemmerik, L.: Tempestite facies variability and storm-depositional processes across a wide ramp: Towards a polygenetic model for hummocky cross-stratification, *Sedimentology*, 67, 742–781, 2020a.



- Jelby, M. E., Śliwińska, K. K., Koevoets, M. J., Alsen, P., Vickers, M. L., Olausson, S., and Stemmerik, L.: Arctic reappraisal of global carbon-cycle dynamics across the Jurassic–Cretaceous boundary and Valanginian Weissert Event, *Palaeogeogr. Palaeoclimatol. Palaeoecol.*, 555, <https://doi.org/10.1016/j.palaeo.2020.109847>, 2020b.
- Jelby, M. E., Grundvåg, S. A., Śliwińska, K. K., Alsen, P., Vickers, M. L., Olausson, S., and Stemmerik, L.: Lower Cretaceous holostratigraphy in Svalbard: the Arctic key piece of the Boreal basin puzzle, *Geol. Soc. Lond. Spec. Publ.*, 545, SP545-2023, 2025.
- Jenkyns, H.: Cretaceous anoxic events: from continents to oceans, *J. Geol. Soc. Lond.*, 137, 171–188, 1980.
- Jenkyns, H. C.: Carbon-isotope stratigraphy and paleoceanographic significance of the Lower Cretaceous shallow-water carbonates of Resolution Guyot, Mid-Pacific Mountains, *Proc. Ocean Drill. Program Sci. Results*, 99–104, 1995.
- Jenkyns, H. C.: Geochemistry of oceanic anoxic events. *Geochemistry, Geophysics, Geosystems*, 11(3), 2010.
- Jenkyns, H. C., Schouten-Huibers, L., Schouten, S., and Sinninghe Damsté, J. S.: Warm Middle Jurassic–Early Cretaceous high-latitude sea-surface temperatures from the Southern Ocean, *Clim. Past*, 8, 215–226, 2012.
- Jin, Y., Wang, Y., Wang, W., Shang, Q., Cao, C., and Erwin, D. H.: Pattern of marine mass extinction near the Permian–Triassic boundary in South China, *Science*, 289, 432–436, 2000.
- Jin, X., Tomimatsu, Y., Yin, R., Onoue, T., Franceschi, M., Grasby, S. E., and Rigo, M.: Climax in Wrangellia LIP activity coincident with major Middle Carnian (Late Triassic) climate and biotic changes: Mercury isotope evidence from the Panthalassa pelagic domain, *Earth Planet. Sci. Lett.*, 607, 118075, 2023.
- Joachimski, M. M., Alekseev, A. S., Grigoryan, A., and Gatovsky, Y. A.: Siberian Trap volcanism, global warming and the Permian–Triassic mass extinction: New insights from Armenian Permian–Triassic sections, *GSA Bull.*, 132, 427–443, <https://doi.org/10.1130/b35108.1>, 2019.
- Joachimski, M. M., Lai, X., Shen, S., Jiang, H., Luo, G., Chen, B., Chen, J., and Sun, Y.: Climate warming in the latest Permian and the Permian–Triassic mass extinction, *Geology*, 40, 195–198, <https://doi.org/10.1130/g32707.1>, 2012.
- Joachimski, M. M., Alekseev, A. S., Grigoryan, A., and Gatovsky, Y. A.: Siberian Trap volcanism, global warming and the Permian–Triassic mass extinction: New insights from Armenian Permian–Triassic sections, *GSA Bull.*, 132, 427–443, 2020.
- Jochmann, M. M., Augland, L. E., Lenz, O., Bieg, G., Haugen, T., Grundvåg, S. A., Jelby, M. E., Midtkandal, I., Dolezych, M., and Hjálmarsdóttir, H. R.: Sylfjellet: a new outcrop of the Paleogene Van Mijenfjorden Group in Svalbard, *Arktos*, 6, 17–38, <https://doi.org/10.1007/s41063-019-00072-w>, 2020.



- 2190 Johannessen, E. P., Henningsen, T., Bakke, N. E., Johansen, T. A., Ruud, B. E., Riste, P., Elvebakk, H., Jochmann, M., Elvebakk, G., and Woldengen, M. S.: Palaeogene clinoform succession on Svalbard expressed in outcrops, seismic data, logs and cores, *First Break*, 29, <https://doi.org/10.3997/1365-2397.2011004>, 2011.
- Johannessen, E. P., and Steel, R. J.: Shelf-margin clinoforms and prediction of deepwater sands, *Basin Res.*, 17, 521–550, 2005.
- 2195 Johannessen, E. P., and Steel, R. J.: Mid-Carboniferous extension and rift-infill sequences in the Billefjorden Trough, Svalbard, *Nor. Geol. Tidsskr.*, 72, 35–48, 1992.
- Johansson, Å., Gee, D. G., Larionov, A. N., Ohta, Y., and Tebenkov, A. M.: Grenvillian and Caledonian evolution of eastern Svalbard—a tale of two orogenies, *Terra Nova*, 17, 317–325, 2005.
- Johansson, Å., Larionov, A. N., Gee, D. G., Ohta, Y., Tebenkov, A. M., and Sandelin, S.: Grenvillian and Caledonian tectono-magmatic activity in northeasternmost Svalbard, *Geol. Soc. Lond. Mem.*, 30, 207–232, <https://doi.org/10.1144/GSL.MEM.2004.030.01.17>, 2004.
- 2200 Jokat, W., and Herter, U.: Jurassic failed rift system below the Filchner-Ronne-Shelf, Antarctica: New evidence from geophysical data, *Tectonophysics*, 688, 65–83, 2016.
- Jones, M. T., Augland, L. E., Shephard, G. E., Burgess, S. D., Eliassen, G. T., Jochmann, M. M., Friis, B., Jerram, D. A., Planke, S., and Svensen, H. H.: Constraining shifts in North Atlantic plate motions during the Palaeocene by U-Pb dating of Svalbard tephra layers, *Sci. Rep.*, 7, 6822, <https://doi.org/10.1038/s41598-017-06170-7>, 2017.
- 2205 Jones, M. T., Jerram, D. A., Svensen, H. H., and Grove, C.: The effects of large igneous provinces on the global carbon and sulphur cycles, *Palaeogeogr. Palaeoclimatol. Palaeoecol.*, 441, 4–21, <https://doi.org/10.1016/j.palaeo.2015.06.042>, 2016.
- 2210 Jones, M. T., Percival, L. M. E., Stokke, E. W., Frieling, J., Mather, T. A., Riber, L., Schubert, B. A., Schultz, B., Tegner, C., Planke, S., and Svensen, H. H.: Mercury anomalies across the Palaeocene–Eocene Thermal Maximum, *Clim. Past*, 15, 217–236, <https://doi.org/10.5194/cp-15-217-2019>, 2019.
- 2215 Jones, M. T., Stokke, E. W., Rooney, A. D., Frieling, J., Pogge von Strandmann, P. A. E., Wilson, D. J., Svensen, H. H., Planke, S., Adatte, T., Thibault, N., Vickers, M. L., Mather, T. A., Tegner, C., Zuchuat, Z., and Schultz, B. P.: Tracing North Atlantic volcanism and seaway connectivity across the Paleocene-Eocene Thermal Maximum (PETM), *Clim. Past*, 19, 1623–1652, <https://doi.org/10.5194/cp-19-1623-2023>, 2023.

K

- 2220 Kanat, L., and Morris, A.: A working hypothesis for central western Oscar II Land, Spitsbergen, *Nor. Polarinst. Skr.*, 190, 1988.
- Kasbohm, J., Schoene, B., and Burgess, S.: Radiometric constraints on the timing, tempo, and effects of large igneous province emplacement, in: Large Igneous Provinces: A Driver of Global Environmental and Biotic



- Changes, edited by: Ernst, R. E., Dickson, A. J., and Bekker, A., *Am. Geophys. Union, John Wiley Sons, Inc.*, 27–82, 2021.
- 2225
- Kear, B. P., Engelschiøn, V. S., Hammer, Ø., Roberts, A. J., and Hurum, J. H.: Earliest Triassic ichthyosaur fossils push back oceanic reptile origins, *Curr. Biol.*, 33, R178–R179, 2023.
- Kele, S., Breitenbach, S. F., Capezzuoli, E., Meckler, A. N., Ziegler, M., Millan, I. M., Kluge, T., Deák, J., Hanselmann, K., John, C. M., and Yan, H.: Temperature dependence of oxygen-and clumped isotope
- 2230 fractionation in carbonates: a study of travertines and tufas in the 6–95°C temperature range, *Geochim. Cosmochim. Acta*, 168, 172–192, 2015.
- Kellogg, H. E.: Tertiary stratigraphy and tectonism in Svalbard and continental drift, *AAPG Bull.*, 59, 465–485, 1975.
- Kenrick, P., Wellman, C. H., Schneider, H., and Edgecombe, G. D.: A timeline for terrestrialization: consequences for the carbon cycle in the Palaeozoic, *Philos. Trans. R. Soc. B-Biol. Sci.*, 367, 519–536, 2012.
- 2235 Kidder, D. L., and Worsley, T. R.: Causes and consequences of extreme Permo-Triassic warming to globally equable climate and relation to the Permo-Triassic extinction and recovery, *Palaeogeogr. Palaeoclimatol. Palaeoecol.*, 203, 207–237, [https://doi.org/10.1016/S0031-0182\(03\)00667-9](https://doi.org/10.1016/S0031-0182(03)00667-9), 2004.
- Kierulf, H. P., Kohler, J., Boy, J. P., Geyman, E. C., Mémin, A., Omang, O. C., and Steffen, R.: Time-varying uplift in Svalbard—an effect of glacial changes, *Geophys. J. Int.*, 231, 1518–1534, 2022.
- 2240 Kim, S.-T., and O’Neil, J. R.: Equilibrium and nonequilibrium oxygen isotope effects in synthetic carbonates, *Geochim. Cosmochim. Acta*, 61, 3461–3475, 1997.
- Kingsbury, C. G., Kamo, S. L., Ernst, R. E., Söderlund, U., and Cousens, B. L.: U-Pb geochronology of the plumbing system associated with the Late Cretaceous Strand Fiord Formation, Axel Heiberg Island, Canada: part of the 130-90 Ma High Arctic large igneous province, *J. Geodyn.*, 118, 106–117, 2018.
- 2245 Klausen, T. G., Müller, R., Slama, J., and Helland-Hansen, W.: Evidence for Late Triassic provenance areas and Early Jurassic sediment supply turnover in the Barents Sea Basin of northern Pangea, *Lithosphere*, 9, 14–28, 2017.
- Klausen, T. G., Nyberg, B., and Helland-Hansen, W.: The largest delta plain in Earth’s history, *Geology*, 47, 470–474, <https://doi.org/10.1130/G45507.1>, 2019.
- 2250 Klausen, T. G., Paterson, N. W., and Benton, M. J.: Geological control on dinosaurs’ rise to dominance: Late Triassic ecosystem stress by relative sea level change, *Terra Nova*, 32, 434–441, <https://doi.org/10.1111/ter.12480>, 2020.
- Kleinspehn, K. L., and Teyssier, C.: Oblique rifting and the Late Eocene–Oligocene demise of Laurasia with inception of Molloy Ridge: Deformation of Forlandsundet Basin, Svalbard, *Tectonophysics*, 693, 363–377,
- 2255 2016.
- Knag, G.: Gipshuken-og Kapp Starostin formasjonen, mellom til øvre Perm, langs vestkysten av Svalbard, *Cand. real., Univ. i Bergen*, 1980.



- Knoll, A. H., and Swett, K.: Micropaleontology across the Precambrian—Cambrian boundary in Spitsbergen, *J. Paleontol.*, 61, 898–926, <https://doi.org/10.1017/S0022336000029292>, 1987.
- 2260 Koevoets, M. J., Abay, T. B., Hammer, Ø., and Olaussen, S.: High-resolution organic carbon–isotope stratigraphy of the Middle Jurassic–Lower Cretaceous Agardhfjellet Formation of central Spitsbergen, Svalbard, *Palaeogeogr. Palaeoclimatol. Palaeoecol.*, 449, 266–274, <https://doi.org/10.1016/j.palaeo.2016.02.029>, 2016.
- Koevoets, M. J., Hammer, Ø., Olaussen, S., Senger, K., and Smelror, M.: Integrating subsurface and outcrop data of the Middle Jurassic to Lower Cretaceous Agardhfjellet Formation in central Spitsbergen, *Nor. Geol. Tidsskr.*, 98, <https://doi.org/10.17850/njg98-4-01>, 2018.
- 2265 Koevoets, M., Hammer, Ø., and Little, C. T.: Palaeoecology and palaeoenvironments of the Middle Jurassic to lowermost Cretaceous Agardhfjellet Formation (Bathonian–Ryazanian), Spitsbergen, Svalbard, *Nor. J. Geol.*, 99, <https://doi.org/10.17850/njg99-1-02>, 2019.
- 2270 Korte, C., Jasper, T., Kozur, H. W., and Veizer, J.: $\delta^{18}\text{O}$ and $\delta^{13}\text{C}$ of Permian brachiopods: a record of seawater evolution and continental glaciation, *Palaeogeogr. Palaeoclimatol. Palaeoecol.*, 224, 333–351, 2005.
- Korte, C., Jasper, T., Kozur, H. W., and Veizer, J.: $^{87}\text{Sr}/^{86}\text{Sr}$ record of Permian seawater, *Palaeogeogr. Palaeoclimatol. Palaeoecol.*, 240, 89–107, <https://doi.org/10.1016/j.palaeo.2006.03.047>, 2006.
- Korte, C., and Kozur, H. W.: Carbon-isotope stratigraphy across the Permian–Triassic boundary: A review, *J. Asian Earth Sci.*, 39, 215–235, <https://doi.org/10.1016/j.jseaes.2010.01.005>, 2010.
- 2275 Krajewski, K. P.: The Botneheia Formation (Middle Triassic) in Edgeøya and Barentsøya, Svalbard: lithostratigraphy, facies, phosphogenesis, paleoenvironment, *Pol. Polar Res.*, 29, 319–364, 2008.
- Krajewski, K. P.: Organic matter–apatite–pyrite relationships in the Botneheia Formation (Middle Triassic) of eastern Svalbard: Relevance to the formation of petroleum source rocks in the NW Barents Sea shelf, *Mar. Petrol. Geol.*, 45, 69–105, 2013.
- 2280 Kristoffersen, Y.: On the tectonic evolution and paleoceanographic significance of the Fram Strait gateway, in: *Geological history of the polar oceans: Arctic versus Antarctic*, edited by: Bleil, U., and Thiede, J., Springer, Dordrecht, 63–76, 1990.
- Kristoffersen, Y., and Husebye, E. S.: Multi-channel seismic reflection measurements in the Eurasian Basin, Arctic Ocean, from US ice station FRAM-IV, *Tectonophysics*, 114, 103–115, 1985.
- 2285 Kristoffersen, Y., Ohta, Y., and Hall, J. K.: On the origin of the Yermak Plateau north Svalbard, Arctic Ocean, *Nor. J. Geol.*, 100, 1–33, 2020.
- Kröger, B., Finnegan, S., Franek, F., and Hopkins, M. J.: The Ordovician Succession Adjacent to Hinlopenstretet, Ny Friesland, Spitsbergen, *Am. Mus. Novit.*, 3882, 1–28, 2017.
- 2290 Kump, L. R., Bralower, T. J., and Ridgwell, A.: Ocean acidification in deep time, *Oceanography*, 22, 94–107, 2009.
- Kvaček, Z., and Manum, S. B.: Ferns of the Spitsbergen Palaeogene, *Palaeontogr. Abt. B*, 230, 169–181, 1993.



Kvaček, Z., Manum, S. B., and Boulter, M. C.: Angiosperms from the Palaeogene of Spitsbergen, including an unfinished work by A. G. Nathorst, *Palaeontogr. Abt. B*, 232, 103–128, 1994.

L

2295

Labandeira, C. C.: The four phases of plant-arthropod associations in deep time, *Geol. Acta*, 4, 409–438, 2006.

Large, D. J. and Marshall, C.: Use of carbon accumulation rates to estimate the duration of coal seams and the influence of atmospheric dust deposition on coal composition, *Geol. Soc. Lond. Spec. Publ.*, 404, 303–315, 2015.

2300 Large, D. J., Marshall, C., Jochmann, M., Jensen, M., Spiro, B. F., and Olausen, S.: Time, Hydrologic Landscape, and the Long-Term Storage of Peatland Carbon in Sedimentary Basins, *J. Geophys. Res.-Earth Surf.*, 126, e2020JF005762, 2021.

2305 Lasabuda, A., Laberg, J. S., Knutsen, S. M., and Safronova, P.: Cenozoic tectonostratigraphy and pre-glacial erosion: A mass-balance study of the northwestern Barents Sea margin, Norwegian Arctic, *J. Geodyn.*, 119, 149–166, 2018.

Lasabuda, A. P. E., Johansen, N. S., Laberg, J. S., Faleide, J. I., Senger, K., Rydningen, T. A., Patton, H., Knutsen, S.-M., and Hanssen, A.: Cenozoic uplift and erosion of the Norwegian Barents Shelf – A review, *Earth-Sci. Rev.*, 217, 103609, <https://doi.org/10.1016/j.earscirev.2021.103609>, 2021.

2310 Lauritzen, O. and Worsley, D.: Observations of the Upper Palaeozoic stratigraphy of the Ny Friesland area, *Norsk Polarinstitut A51*, 41 pp., 1975.

Lawver, L., Müller, R., Srivastava, S., and Roest, W.: The opening of the Arctic Ocean, in: *Geological history of the polar oceans: Arctic versus Antarctic*, edited by: Bleil, U. and Thiede, J., Springer, Dordrecht, 29–62, 1990a.

2315 Lawver, L., Scotese, C., Grantz, A., Johnson, L., and Sweeney, J.: A review of tectonic models for the evolution of the Canada Basin, in: *The Geology of North America*, edited by: Grantz, A., Johnson, G. L., and Sweeney, J. F., *Geological Society of America, Boulder, CO*, 593–618, 1990b.

Lee, C., Love, G. D., Hopkins, M. J., Kröger, B., Franeck, F., and Finnegan, S.: Lipid biomarker and stable isotopic profiles through Early-Middle Ordovician carbonates from Spitsbergen, Norway, *Org. Geochem.*, 131, 5–18, <https://doi.org/10.1016/j.orggeochem.2019.02.008>, 2019.

2320 Lee, S., Shi, G. R., Nakrem, H. A., Woo, J., and Tazawa, J.-I.: Mass extinction or extirpation: Permian biotic turnovers in the northwestern margin of Pangea, *GSA Bull.*, 134, 2399–2414, <https://doi.org/10.1130/b36227.1>, 2022.



- Leever, K. A., Gabrielsen, R. H., Faleide, J. I., and Braathen, A.: A transpressional origin for the West Spitsbergen fold-and-thrust belt: Insight from analog modelling, *Tectonics*, 30, TC2014, 2325 <https://doi.org/10.1029/2010TC002753>, 2011.
- Lehnert, O., Stouge, S., and Brandl, P. A.: Conodont biostratigraphy in the Early to Middle Ordovician strata of the Oslobreen Group in Ny Friesland, Svalbard, *Z. Dtsch. Ges. Geowiss.*, 164, 149–172, 2013.
- 2330 Leu, M., Schneebeli-Hermann, E., Hammer, Ø., Lindemann, F. J., and Bucher, H.: Spatiotemporal dynamics of nektonic biodiversity and vegetation shifts during the Smithian–Spathian transition: conodont and palynomorph insights from Svalbard, *Lethaia*, 57, 1–19, 2024.
- Lewis, S. L., and Maslin, M. A.: Defining the anthropocene, *Nature*, 519, 171–180, <https://doi.org/10.1038/nature14258>, 2015.
- 2335 Lini, A., Weissert, H., and Erba, E.: The Valanginian carbon isotope event: a first episode of greenhouse climate conditions during the Cretaceous, *Terra Nova*, 4, 374–384, <https://doi.org/10.1111/j.1365-3121.1992.tb00826.x>, 1992.
- Lipinski, M., Warning, B., & Brumsack, H. J.: Trace metal signatures of Jurassic/Cretaceous black shales from the Norwegian Shelf and the Barents Sea. *Palaeogeography, Palaeoclimatology, Palaeoecology*, 190, 459–2340 475, [https://doi.org/10.1016/S0031-0182\(02\)00619-3](https://doi.org/10.1016/S0031-0182(02)00619-3), 2003.
- Liu, Z., Pagani, M., Zinniker, D., DeConto, R., Huber, M., Brinkhuis, H., Shah, S. R., Leckie, R. M., and Pearson, A.: Global Cooling During the Eocene-Oligocene Climate Transition, *Science*, 323, 1187–1190, <https://doi.org/10.1126/science.1166368>, 2009.
- Lopes, G., Mangerud, G., and Clayton, G.: The palynostratigraphy of the Mississippian Birger Johnsonfjellet 2345 section, Spitsbergen, Svalbard, *Palynology*, 43, 631–649, 2019.
- Lord, G. S., Johansen, S. K., Støen, S. J., and Mørk, A.: Facies development of the Upper Triassic succession on Barentsøya, Wilhelmøya and NE Spitsbergen, Svalbard, *Nor. J. Geol.*, 97, <https://doi.org/10.17850/njg97-1-03>, 2017.
- Lord, G. S., Mørk, A., Haugen, T., Boxaspen, M. A., Husteli, B., Forsberg, C. S., and Olausen, S.: Stratigraphy 2350 and palaeosol profiles of the Upper Triassic Isfjorden Member, Svalbard, *Nor. J. Geol.*, 2022.
- Lourens, L. J., Sluijs, A., Kroon, D., Zachos, J. C., Thomas, E., Röhl, U., Bowles, J., and Raffi, I.: Astronomical pacing of late Palaeocene to early Eocene global warming events, *Nature*, 435, 1083–1087, <https://doi.org/10.1038/nature03814>, 2005.
- Ludwig, P.: The marine transgression in the Middle Carboniferous of Brøggerhalvøya (Svalbard), *Polar Res.*, 9, 2355 65–76, <https://doi.org/10.3402/polar.v9i1.6779>, 1991.



- Lundschieen, B. A., Høy, T., and Mørk, A.: Triassic hydrocarbon potential in the Northern Barents Sea; integrating Svalbard and stratigraphic core data, *Nor. Pet. Dir. Bull.*, 11, 3–20, 2014.
- Luo, G., Yang, H., Algeo, T. J., Hallmann, C., and Xie, S.: Lipid biomarkers for the reconstruction of deep-time environmental conditions, *Earth-Sci. Rev.*, 189, 99–124, <https://doi.org/10.1016/j.earscirev.2018.03.005>, 2019.
- Lüthje, C. J., Milàn, J., and Hurum, J. H.: Paleocene tracks of the mammal pantodont genus Titanoides in coal-bearing strata, Svalbard, Arctic Norway, *J. Vertebr. Paleontol.*, 30, 521–527, 2010.
- Lüthje, C. J., Nichols, G., and Jerrett, R.: Sedimentary facies and reconstruction of a transgressive coastal plain with coal formation, Paleocene, Spitsbergen, Arctic Norway, *Nor. J. Geol.*, 100, 2010.
- ## M
- Macdonald, F.A.: Deep-Time paleoclimate proxies. *AGU Advances*, 1(3), <https://doi.org/10.1029/2020av000244>, 2020.
- Mackey, T.J., Jost, A.B., Creveling, J.R. and Bergmann, K.D.: A Decrease to Low Carbonate Clumped Isotope Temperatures in Cryogenian Strata. *AGU Advances*, 1(3), e2019AV000159, <https://doi.org/10.1029/2019AV000159>, 2020.
- Maher Jr, H. D., Braathen, A., Bergh, S., Dallmann, W., and Harland, W. B.: Tertiary or Cretaceous age for Spitsbergen's fold-thrust belt on the Barents Shelf. *Tectonics*, 14(6), 1321-1326, <https://doi.org/10.1029/95TC01257>, 1995.
- Maher, Jr., Hays, T., Shuster, R. and Mutrux, J.: Petrography of Lower Cretaceous sandstones on Spitsbergen. *Polar Research*, 23(2): 147-165, <https://doi.org/10.3402/polar.v23i2.6276>, 2004.
- Maher, J.H.D.: Manifestations of the Cretaceous High Arctic Large Igneous Province in Svalbard. *The Journal of Geology*, 109(1): 91-104, <https://doi.org/10.1086/317960>, 2001.
- Mahoney, J., Storey, M., Duncan, R., Spencer, K. and Pringle, M.: Geochemistry and age of the Ontong Java Plateau, in: *The Mesozoic Pacific: Geology, tectonics, and volcanism*, edited by Pringle, M.S., Sager, W.W., Sliter W.V. and Stein, S., Wiley, Washington, D. C: *American Geophysical Union*, 233-261, <https://doi.org/10.1029/GM077p0233> 1993.
- Majka, J. and Kościńska, K.: Magmatic and metamorphic events recorded within the Southwestern Basement Province of Svalbard. *Arktos* 3, 5, <https://doi.org/10.1007/s41063-017-0034-7>, 2017.
- Major, H., Nagy, J., Haremo, P., Dallmann, W.K., Andersen, A., Salvigsen, O.: Adventdalen. In: *Geological Map Svalbard 1:100 000, Sheet C9G. Norsk Polarinstitut*, 1992.



- Mangerud, G. and Konieczny, R.: Palynology of the Permian succession of Spitsbergen, Svalbard. *Polar Research*, 12(1): 65-93, <https://doi.org/10.3402/polar.v12i1.6704>, 1993.
- 2390 Mangerud, G. and Konieczny, R.M.: Palynological investigations of Permian rocks from Nordaustlandet, Svalbard. *Polar Research*, 9(2), 155-167, <https://doi.org/10.3402/polar.v9i2.6788>, 1991.
- Manum, S.: Some dinoflagellates and hystrichosphaerids from the Lower Tertiary of Spitsbergen. *Nytt Magasin for Botanik* 8: 17-25, 1960.
- Manum, S.: Studies in the Tertiary Flora of Spitsbergen: With Notes on Tertiary Floras of Ellesmere Island, Greenland, and Iceland, a Palynological Investigation. *Norsk Polarinstitutt Skrifter*, 125. Pp. 128 + 21 plates, Norsk Polarinstitutt, Oslo University Press, 127 pages, 1962.
- 2395
- Manum, S.B. and Thronsen, T.: Rank of coal and dispersed organic matter and its geological bearing in the Spitsbergen Tertiary. *Norsk Polarinstitutt Årbok*, 1977: 159-177, 1978.
- Manum, S.B. and Thronsen, T.: Age of Tertiary formations on Spitsbergen. *Polar Research*, 4(2): 103-131, <https://doi.org/10.3402/polar.v4i2.6927>, 1986.
- 2400
- Marin, D., Escalona, A., Śliwińska, K.K., Nøhr-Hansen, H. and Mordasova, A.: Sequence stratigraphy and lateral variability of Lower Cretaceous clinofms in the southwestern Barents Sea. *AAPG Bulletin*, 101(9): 1487-1517, <https://doi.org/10.1306/10241616010>, 2017.
- Marshall, C.J.: Palaeogeographic development and economic potential of the coal-bearing Palaeocene Todalen Member, Spitsbergen, *PhD University of Nottingham*, 360 pp., <https://eprints.nottingham.ac.uk/13794/>, 2013.
- 2405
- Marshall, C., Large, D. J., Meredith, W., Snape, C. E., Uguna, C., Spiro, B. F., Orheim, A., Jochmann, M., Mokogwu, I., Wang, Y., and Friis, B.: Geochemistry and petrology of Palaeocene coals from Spitsbergen— Part 1: Oil potential and depositional environment. *International Journal of Coal Geology*, 143, 22-33, <https://doi.org/10.1016/j.coal.2015.03.006>, 2015.
- 2410
- Martinez, M., Aguirre-Urreta, B., Dera, G., Lescano, M., Omarini, J., Tunik, M., O'Dogherty, L., Aguado, R., Company, M. and Bodin, S.: Synchrony of carbon cycle fluctuations, volcanism and orbital forcing during the Early Cretaceous. *Earth-Science Reviews*, 239, 104356, <https://doi.org/10.1016/j.earscirev.2023.104356>, 2023.
- 2415
- Matysik, M., Stemmerik, L., Olaussen, S. and Brunstad, H.: Diagenesis of spiculites and carbonates in a Permian temperate ramp succession—Tempelfjorden Group, Spitsbergen, Arctic Norway. *Sedimentology*, 65(3): 745-774, <https://doi.org/10.1111/sed.12404>, 2018.
- Matthiessen, J.: Biostratigraphie tertiärer Ablagerungen (Paläozän) Am Van Keulenfjord (Spitzbergen) nach Dinoflagellaten-Zysten. (*Diploma thesis*), Christian-Albrechts-Universität zu Kiel, Kiel, 94 pp., 1986.



- 2420 Maxwell, E.E. and Kear, B.P.: Triassic ichthyopterygian assemblages of the Svalbard archipelago: a reassessment of taxonomy and distribution. *Journal of the Geological Society of Sweden* 135, 85-94, <https://doi.org/10.1080/11035897.2012.759145>, 2013.
- McArthur, J.M., Mutterlose, J., Price, G.D., Rawson, P.F., Ruffell, A. and Thirlwall, M.F.: Belemnites of Valanginian, Hauterivian and Barremian age: Sr-isotope stratigraphy, composition ($^{87}\text{Sr}/^{86}\text{Sr}$, $\delta^{13}\text{C}$, $\delta^{18}\text{O}$, Na, Sr, Mg), and palaeo-oceanography. *Palaeogeography, Palaeoclimatology, Palaeoecology*, 202(3-4), 253-272, [https://doi.org/10.1016/S0031-0182\(03\)00638-2](https://doi.org/10.1016/S0031-0182(03)00638-2) 2004.
- 2425 McArthur, J. M., Janssen, N. M. M., Reboulet, S., Leng, M. J., Thirlwall, M. F., and Van de Schootbrugge, B.: Palaeotemperatures, polar ice-volume, and isotope stratigraphy (Mg/Ca, $\delta^{18}\text{O}$, $\delta^{13}\text{C}$, $^{87}\text{Sr}/^{86}\text{Sr}$): the early cretaceous (Berriasian, Valanginian, Hauterivian). *Palaeogeography, Palaeoclimatology, Palaeoecology*, 248(3-4), 391-430, <https://doi.org/10.1016/j.palaeo.2006.12.0152007>, 2007.
- 2430 McCann Andrew, J.: Deformation of the Old Red Sandstone of NW Spitsbergen; links to the Ellesmerian and Caledonian orogenies. *Geological Society, London, Special Publications*, 180(1): 567-584, <https://doi.org/10.1144/GSL.SP.2000.180.01.30>, 2000.
- McClelland*, W.C., von Gosen*, W., Piepjohn*, K.: Tonian and Silurian magmatism in Nordaustlandet: Svalbard's place in the Caledonian orogen, in: *Circum-Arctic Structural Events: Tectonic Evolution of the Arctic Margins and Trans-Arctic Links with Adjacent Orogens*, edited by: Piepjohn, K., Strauss, J.V., Reinhardt, L. and McClelland, W.C.: Boulder, Colorado, Geological Society of America, Special Paper 541, 63 – 80, [https://doi.org/10.1130/2018.2541\(04\)](https://doi.org/10.1130/2018.2541(04)). 2019.
- 2435
- McDannell, K.T. and Flowers, R.M.: Vestiges of the Ancient: Deep-Time Noble Gas Thermochronology. *Elements*, 16(5): 325-330, <https://doi.org/10.2138/gselements.16.5.325>, 2020.
- 2440
- McInerney, F. A., and Wing, S. L.: The Paleocene-Eocene Thermal Maximum: a perturbation of carbon cycle, climate, and biosphere with implications for the future. *Annual Review of Earth and Planetary Sciences*, 39: 489-516, <https://doi.org/10.1146/annurev-earth-040610-133431>, 2011.
- McKerrow, W.S., Scotese, C.R. and Brasier, M.D.: Early Cambrian continental reconstructions. *Journal of the Geological Society, London*, 149, 599-606, <https://doi.org/10.1144/gsjgs.149.4.0599>, 1992.
- 2445
- Meissner, P., Mutterlose, J., and Bodin, S.: Latitudinal temperature trends in the northern hemisphere during the Early Cretaceous (Valanginian–Hauterivian). *Palaeogeography, Palaeoclimatology, Palaeoecology*, 424, 17-39, <https://doi.org/10.1016/j.palaeo.2015.02.003>, 2015.
- Menegatti, A.P., Weissert, H., Brown, R.S., Tyson, R.V., Farrimond, P., Strasser, A. and Caron, M.: High-resolution $\delta^{13}\text{C}$ stratigraphy through the early Aptian “Livello Selli” of the Alpine Tethys. *Paleoceanography*, 13(5): 530-545, 1998.
- 2450
- Michelsen, J.K. and Khorasani, G.K.: A regional study on coals from Svalbard: organic facies, maturity and thermal history. *Bulletin de la Société Géologique de France*, 162 (2): 385–397, 1991.



- 2455 Midtkandal, I. and Nystuen, J.: Depositional architecture of a low-gradient ramp shelf in an epicontinental sea: The lower Cretaceous of Svalbard. *Basin Research*, 21(5): 655-675, <https://doi.org/10.1111/j.1365-2117.2009.00399.x>, 2009.
- Midtkandal, I., Nystuen, J.P., Nagy, J., Mørk, A.: Lower Cretaceous lithostratigraphy across a regional subaerial unconformity in Spitsbergen: the Rurikfjellet and Helvetiafjellet formations. *Nor. J. Geol.* 88 (4), 287–304, 2008.
- 2460 Midtkandal, I., Svensen, H.H., Planke, S., Corfu, F., Polteau, S., Torsvik, T.H., Faleide, J.I., Grundvåg, S.-A., Selnes, H., Kürschner, W. and Olaussen, S.: The Aptian (Early Cretaceous) oceanic anoxic event (OAE1a) in Svalbard, Barents Sea, and the absolute age of the Barremian-Aptian boundary. *Palaeogeography, Palaeoclimatology, Palaeoecology*, 463: 126-135, <https://doi.org/10.1016/j.palaeo.2016.09.023>, 2016.
- 2465 Mii, H.-s., Grossman, E.L. and Yancey, T.E.: Stable carbon and oxygen isotope shifts in Permian seas of West Spitsbergen-Global change or diagenetic artifact? *Geology*, 25(3): 227-230, [https://doi.org/10.1130/0091-7613\(1997\)025<0227:SCAOIS>2.3.CO;2](https://doi.org/10.1130/0091-7613(1997)025<0227:SCAOIS>2.3.CO;2), 1997.
- Miller, K.G., Kominz, M.A., Browning, J.V., Wright, J.D., Mountain, G.S., Katz, M.E., Sugarman, P.J., Cramer, B.S., Christie-Blick, N. and Pekar, S.F.: The Phanerozoic record of global sea-level change. *Science* 310,1293-1298(2005). <https://doi.org/10.1126/science.1116412>, 2005.
- 2470 Mueller, S., Hounslow, M. W., and Kürschner, W. M.: Integrated stratigraphy and palaeoclimate history of the Carnian Pluvial Event in the Boreal realm; new data from the Upper Triassic Kapp Toscana Group in central Spitsbergen (Norway). *Journal of the Geological Society*, 173(1), 186-202, 2016
- Müller, R. D., Cannon, J., Qin, X., Watson, R. J., Gurnis, M., Williams, S., Pfaffelmoser, T., Seton, M., Russell, S. H. J., Zahirovic S.: GPlates: Building a virtual Earth through deep time. *Geochemistry, Geophysics, Geosystems*, 19, 2243-2261. <https://doi.org/10.1029/2018GC007584>, 2018.
- 2475 Minakov, A., Mjelde, R., Faleide, J.I., Flueh, E.R., Dannowski, A. and Keers, H.: Mafic intrusions east of Svalbard imaged by active-source seismic tomography. *Tectonophysics*, 518: 106-118, 2012.
- Montañez, I.P. and Poulsen, C.J.: The Late Paleozoic ice age: an evolving paradigm. *Annual Review of Earth and Planetary Sciences*, 41: 629-656, 2013.
- 2480 Montañez, I.P., Tabor, N.J., Niemeier, D., DiMichele, W.A., Frank, T.D., Fielding, C.R., Isbell, J.L., Birgenheier, L.P. and Rygel, M.C.: CO₂-forced climate and vegetation instability during Late Paleozoic deglaciation. *Science*, 315(5808): 87-91, <https://doi.org/10.1126/science.1134207>, 2007.
- Moody-Stuart, M.: High- and low-sinuosity stream deposits, with examples from the Devonian of Spitsbergen. *Journal of Sedimentary Research*, 36(4): 1102-1117, <https://doi.org/10.1306/74D71609-2B21-11D7-8648000102C1865D>, 1966.
- 2485



- Morgans-Bell, H.S., Coe, A.L., Hesselbo, S.P., Jenkyns, H.C., Weedon, G.P., Marshall, J.E.A., Tyson, R.V. and Williams, C.J.: Integrated stratigraphy of the Kimmeridge Clay Formation (Upper Jurassic) based on exposures and boreholes in south Dorset, UK. *Geological Magazine*, 138(5), 511-539, 2001
- Mulrooney, M., Larsen, L., Rismyhr, B., Van Stappen, J., Senger, K., Braathen, A., Mørk, M., Olaussen, S., Cnudde, V. and Ogata, K.: Fluid flow properties of a potential unconventional CO₂ storage unit in central Spitsbergen: the Upper Triassic to Middle Jurassic Wilhelmøya Subgroup. *Norwegian Journal of Geology*, 99: 85-116, 2019.
- Mulrooney, M.J., Larsen, L., Van Stappen, J., Rismyhr, B., Senger, K., Braathen, A., Olaussen, S., Mørk, M.B.E., Ogata, K. and Cnudde, V.: Fluid flow properties of the Wilhelmøya Subgroup, a potential unconventional CO₂ storage unit in central Spitsbergen. *Norwegian Journal of Geology*, 99: 85-116, 2018.
- Myhre, P.I., Corfu, F. and Andresen, A.: Caledonian anatexis of Grenvillian crust: a U/Pb study of Albert I Land, NW Svalbard. *Norwegian Journal of Geology*, 89(173): e191, 2008.
- Müller, R., Klausen, T.G., Faleide, J.I., Olaussen, S., Eide, C.H. and Suslova, A.: Linking regional unconformities in the Barents Sea to compression-induced forebulge uplift at the Triassic-Jurassic transition. *Tectonophysics*, 765: 35-51, 2019
- Müller, R.D. and Spielhagen, R.F.: Evolution of the Central Tertiary Basin of Spitsbergen: towards a synthesis of sediment and plate tectonic history. *Palaeogeography, Palaeoclimatology, Palaeoecology*, 80(2): 153-172, 1990.
- Mørk, A., Knarud, R. and Worsley, D.: Depositional and diagenetic environments of the Triassic and Lower Jurassic succession of Svalbard. *Arctic Geology and Geophysics: Proceedings of the Third International Symposium on Arctic Geology — Memoir 8*, 371-398, 1982.
- Mørk, A. and Bjørøy, M.: Mesozoic source rocks on Svalbard, *Petroleum Geology of the North European Margin: Proceedings of the North European Margin Symposium (NEMS'83), organized by the Norwegian Petroleum Society* and held at the Norwegian Institute of Technology (NTH) in Trondheim 9–11 May, 1983. Springer, pp. 371-382, 1984
- Mørk, A., Embry, A.F. and Weitschat, W.: Triassic transgressive-regressive cycles in the Sverdrup Basin, Svalbard and the Barents Shelf, *Correlation in Hydrocarbon Exploration: Proceedings of the conference Correlation in Hydrocarbon Exploration organized by the Norwegian Petroleum Society* and held in Bergen, Norway, 3–5 October 1988. Springer, pp. 113-130, 1989.
- Mørk, A., Vigran, J.O., Korchinskaya, M.V., Pchelina, T.M., Fefilova, L.A., Vavilov, M.N. and Weitschat, W.: a Triassic rocks in Svalbard, the Arctic Soviet islands and the Barents Shelf: bearing on their correlations. *In: Norwegian Petroleum Society Special Publications, edited by: T.O. Vorren, E. Bergsager, Ø.A. Dahl-Stamnes, E. Holter, B. Johansen, E. Lie and T.B. Lund*, Elsevier, 457-479, <https://doi.org/10.1016/B978-0-444-88943-0.50033-2>, 1993



- 2520 Mørk, A., Dallmann, W., Dypvik, H., Johannessen, E., Larssen, G., Nagy, J., Nøttvedt, A., Olausson, S., Pchelina, T. and Worsley, D.: Mesozoic lithostratigraphy. *Lithostratigraphic lexicon of Svalbard. Upper Palaeozoic to Quaternary bedrock. Review and recommendations for nomenclature use*: 127-214, 1999a.
- Mørk, A., Elvebakk, G., Forsberg, A.W., Hounslow, M.W., Nakrem, H.A., Vigran, J.O. and Weitschat, W.: The type section of the Vikinghogda Formation: a new Lower Triassic unit in central and eastern Svalbard. *Polar Research*, 18(1): 51-82, 1999b.
- 2525 Mørk, A., and Worsley, D.: Triassic of Svalbard and the Barents shelf. In *NGF Abstracts and proceedings* (Vol. 3, pp. 23-29), 2006.
- Mørk, A. and Grundvåg, S.: Festningen-A 300-million-year journey through shoreline exposures of the Carboniferous and Mesozoic in 7 kilometers. *Geological Society of Norway— geological guides 2020-7*, https://www.geologi.no/images/GeologiskeGuider/Festningen_red.pdf, 2020.
- 2530

N

- Nabbefeld, B., Grice, K., Twitchett, R. J., Summons, R. E., Hays, L., Böttcher, M. E., and Asif, M.: An integrated biomarker, isotopic and palaeoenvironmental study through the Late Permian event at Lusitaniadalen, Spitsbergen, *Earth Planet. Sci. Lett.*, 291, 84–96, 2010.
- 2535
- Naber, T. V., Grasby, S. E., Cuthbertson, J. P., Rayner, N., and Tegner, C.: New constraints on the age, geochemistry, and environmental impact of High Arctic Large Igneous Province magmatism: Tracing the extension of the Alpha Ridge onto Ellesmere Island, Canada, *GSA Bull.*, 133, 1695–1711, 2021.
- 2540
- Nagy, J.: Delta-influenced foraminiferal facies and sequence stratigraphy of Paleocene deposits in Spitsbergen, *Palaeogeogr. Palaeoclimatol. Palaeoecol.*, 222, 161–179, <https://doi.org/10.1016/j.palaeo.2005.03.014>, 2005.
- 2545
- Nagy, J., and Berge, S. H.: Micropalaeontological evidence of brackish water conditions during deposition of the Knorringfjellet Formation, Late Triassic–Early Jurassic, Spitsbergen, *Polar Res.*, 27, 413–427, <https://doi.org/10.1111/j.1751-8369.2007.00038.x>, 2008.
- Nagy, J., Jargvoll, D., Dypvik, H., Jochmann, M., and Riber, L.: Environmental changes during the Paleocene–Eocene Thermal Maximum in Spitsbergen as reflected by benthic foraminifera, *Polar Res.*, 32, 19737, <https://doi.org/10.3402/polar.v32i0.19737>, 2013.
- 2550



- Nagy, J., and Naoroz, M.: Changing depositional environments reflected by foraminifera in a transgressive-regressive sequence of the Lower Cretaceous on Spitsbergen, *Palaeogeogr. Palaeoclimatol. Palaeoecol.*, 511, 144–167, 2018.
- 2555 Nakrem, H. A., and Mørk, A.: New Early Triassic Bryozoa (Trepotomata) from Spitsbergen, with some remarks on the stratigraphy of the investigated horizons, *Geol. Mag.*, 128, 129–140, 1991.
- Nakrem, H. A., Orchard, M. J., Weitschat, W., Hounslow, M. W., Beatty, T. W., and Mørk, A.: Triassic conodonts from Svalbard and their Boreal correlations, *Polar Res.*, 27, 523–539, <https://doi.org/10.1111/j.1751-8369.2007.00038.x>, 2008.
- 2560 Nance, R. D., Worsley, T. R., and Moody, J. B.: The supercontinent cycle, *Sci. Am.*, 259, 72–79, 1988.
- Nicolaisen, J., Elvebakk, G., Ahokas, J., Bojesen-Koefoed, J., Olausson, S., Rinna, J., Skeie, J., and Stemmerik, L.: Characterization of upper Palaeozoic organic-rich units in Svalbard: Implications for the petroleum systems of the Norwegian Barents shelf, *J. Petrol. Geol.*, 42, 59–78, 2019.
- Nielsen, J. K., Błażejowski, B., Gieszczyk, P., and Nielsen, J. K.: Carbon and oxygen isotope records of Permian brachiopods from relatively low and high palaeolatitudes: climatic seasonality and evaporation, *Geol. Soc. Lond. Spec. Publ.*, 376, 387–406, 2013.
- 2565 Nøttvedt, A.: Askeladden delta sequence (Paleocene) on Spitsbergen sedimentation and controls on delta formation, *Polar Res.*, 3, 21–48, 1985.
- Nøttvedt, A., Cecchi, M., Gjelberg, J., Kristensen, S., Lønøy, A., Rasmussen, A., Rasmussen, E., Skott, P., and Van Veen, P.: Svalbard-Barents Sea correlation: a short review, *Nor. Pet. Soc. Spec. Publ.*, 2, 363–375, 1993.
- O**
- Oakey, G. N., and Chalmers, J. A.: A new model for the Paleogene motion of Greenland relative to North America: Plate reconstructions of the Davis Strait and Nares Strait regions between Canada and Greenland, *J. Geophys. Res.-Sol. Ea.*, 117, <https://doi.org/10.1029/2011jb008942>, 2012.
- 2575 Ogata, K., Senger, K., Braathen, A., Tveranger, J., and Olausson, S.: The importance of natural fractures in a tight reservoir for potential CO₂ storage: a case study of the upper Triassic-middle Jurassic Kapp Toscana Group (Spitsbergen, Arctic Norway), *Geol. Soc. Lond. Spec. Publ.*, 374, 395–415, 2014.
- Ogata, K., Senger, K., Braathen, A., Tveranger, J., and Olausson, S.: Fracture systems and mesoscale structural patterns in the siliciclastic Mesozoic reservoir-caprock succession of the Longyearbyen CO₂ Lab project: Implications for geological CO₂ sequestration in Central Spitsbergen, Svalbard, *Nor. J. Geol.*, 94, 121–154, 2014b.
- 2580 Ogata, K., Weert, A., Betlem, P., Birchall, T., and Senger, K.: Shallow and deep subsurface sediment remobilization and intrusion in the Middle Jurassic to Lower Cretaceous Agardhfjellet Formation (Svalbard), *Geosphere*, 19, 801–822, 2023.
- 2585



- Ogden, D. E., and Sleep, N. H.: Explosive eruption of coal and basalt and the end-Permian mass extinction, *Proc. Natl. Acad. Sci. USA*, 109, 59–62, <https://doi.org/10.1073/pnas.1118675109>, 2012.
- Olaussen, S., Larssen, G. B., Helland-Hansen, W., Johannessen, E. P., Nøttvedt, A., Riis, F., Rismyhr, B., Smelror, M., and Worsley, D.: Mesozoic strata of Kong Karls Land, Svalbard, Norway; a link to the northern Barents Sea basins and platforms, *Nor. J. Geol.*, 98, 2018.
- 2590 Olaussen, S., Senger, K., Braathen, A., Grundvåg, S.-A., and Mørk, A.: You learn as long as you drill; research synthesis from the Longyearbyen CO₂ Laboratory, Svalbard, Norway, *Nor. J. Geol.*, 99, 157–187, 2019.
- Olaussen, S., Grundvåg, S.-A., Senger, K., Anell, I., Betlem, P., Braathen, A., Dallmann, W., Jochmann, M., Johannessen, E. P., Lord, G., Mørk, A., Osmundsen, P. T., Smyrak-Sikora, A., and Stemmerik, L.: Svalbard Composite Tectono-Stratigraphic Element, Barents Sea, *Geol. Soc. Lond. Mem.*, 57, <https://doi.org/10.1144/M57-2021-36>, 2023.
- 2595 Olempska, E., and Błaszyk, J.: Ostracods from Permian of Spitsbergen, *Pol. Polar Res.*, 3–20, 1996.
- Oordt, A. J., Soreghan, G. S., Stemmerik, L., and Hinnov, L. A.: A record of dust deposition in northern, mid-latitude Pangaea during peak icehouse conditions of the late Paleozoic ice age, *J. Sediment. Res.*, 90, 337–363, <https://doi.org/10.2110/jsr.2020.15>, 2020.
- 2600 O'Regan, M., Williams, C. J., Frey, K. E., and Jakobsson, M.: A synthesis of the long-term paleoclimatic evolution of the Arctic, *Oceanography*, 24, 66–80, 2011.

P

- 2605 Pankhurst, M. J., Stevenson, C. J., and Coldwell, B. C.: Meteorites that produce K-feldspar-rich ejecta blankets correspond to mass extinctions, *J. Geol. Soc. Lond.*, 179, jgs2021-055, <https://doi.org/10.1144/jgs2021-055>, 2022.
- Park, J., Stein, H. J., Hannah, J. L., Georgiev, S. V., Hammer, Ø., and Olaussen, S.: Paleoenvironment in the circum-Arctic region from the Middle Jurassic to Lower Cretaceous: Trace element and stable isotope geochemistry of the Agardhfjellet Formation, Svalbard, *Palaeogeogr. Palaeoclimatol. Palaeoecol.*, 112333, 2024.
- 2610 Parkinson, I. J., Schaefer, B. F., and Arculus, R. J.: A lower mantle origin for the world's biggest LIP? A high precision Os isotope isochron from Ontong Java Plateau basalts drilled on ODP Leg 192, *Geochim. Cosmochim. Acta*, 66, A580, 2002.
- 2615 Patterson, W. P., and Walter, L. M.: Depletion of ¹³C in seawater ΣCO₂ on modern carbonate platforms: Significance for the carbon isotopic record of carbonates, *Geology*, 22, 885–888, [https://doi.org/10.1130/0091-7613\(1994\)022<0885:Docisc>2.3.Co;2](https://doi.org/10.1130/0091-7613(1994)022<0885:Docisc>2.3.Co;2), 1994.



- Paterson, N. W., Mangerud, G., Cetean, C. G., Mørk, A., Lord, G. S., Klausen, T. G., and Mørkved, P. T.: A multidisciplinary biofacies characterisation of the Late Triassic (late Carnian–Rhaetian) Kapp Toscana Group on Hopen, Arctic Norway, *Palaeogeogr. Palaeoclimatol. Palaeoecol.*, 464, 16–42, 2016.
- 2620 Paterson, N. W., and Mangerud, G.: A revised palynozonation for the Middle–Upper Triassic (Anisian–Rhaetian) *Series of the Norwegian Arctic*, *Geol. Mag.*, 157, 1568–1592, <https://doi.org/10.1017/s0016756819000906>, 2019.
- Payne, J. L., Lehrmann, D. J., Wei, J., Orchard, M. J., Schrag, D. P., and Knoll, A. H.: Large perturbations of the carbon cycle during recovery from the end-Permian extinction, *Science*, 305, 506–509, 2004.
- 2625 Payne, J. L., and Kump, L. R.: Evidence for recurrent Early Triassic massive volcanism from quantitative interpretation of carbon isotope fluctuations, *Earth Planet. Sci. Lett.*, 256, 264–277, 2007.
- Pearson, P. N., and Palmer, M. R.: Atmospheric carbon dioxide concentrations over the past 60 million years, *Nature*, 406, 695–699, 2000.
- 2630 Penn, J. L., Deutsch, C., Payne, J. L., and Sperling, E. A.: Temperature-dependent hypoxia explains biogeography and severity of end-Permian marine mass extinction, *Science*, 362, eaat1327, 2018.
- Peppe, D. J., Royer, D. L., Cariglino, B., Oliver, S. Y., Newman, S., Leight, E., Enikolopov, G., Fernandez-Burgos, M., Herrera, F., and Adams, J. M.: Sensitivity of leaf size and shape to climate: global patterns and paleoclimatic applications, *New Phytol.*, 190, 724–739, 2011.
- 2635 Percival, L., Tedeschi, L. R., Creaser, R., Bottini, C., Erba, E., Giraud, F., Svensen, H., Savian, J., Trindade, R., and Coccioni, R.: Determining the style and provenance of magmatic activity during the Early Aptian Oceanic Anoxic Event (OAE 1a), *Global Planet. Change*, 200, 103461, 2021.
- Petersen, T. G., Thomsen, T. B., Olausen, S., and Stemmerik, L.: Provenance shifts in an evolving Eureka foreland basin: the Tertiary Central Basin, Spitsbergen, *J. Geol. Soc. Lond.*, 173, 634–648, 2016.
- 2640 Petrov, O., Morozov, A., Shokalsky, S., Kashubin, S., Artemieva, I. M., Sobolev, N., Petrov, E., Ernst, R. E., Sergeev, S., and Smelror, M.: Crustal structure and tectonic model of the Arctic region, *Earth-Sci. Rev.*, 154, 29–71, <https://doi.org/10.1016/j.earscirev.2015.11.013>, 2016.
- Petterson, C. H., Pease, V., and Frei, D.: U–Pb zircon provenance of metasedimentary basement of the Northwestern Terrane, Svalbard: Implications for the Grenvillian–Sveconorwegian orogeny and development of Rodinia, *Precambrian Res.*, 175, 206–220, 2009.
- 2645 Peucker-Ehrenbrink, B., and Ravizza, G.: The marine osmium isotope record, *Terra Nova*, 12, 205–219, <https://doi.org/10.1046/j.1365-3121.2000.00295.x>, 2000.
- Piepjohn, K.: The Svalbardian–Ellesmerian deformation of the Old Red Sandstone and the pre-Devonian basement in NW Spitsbergen (Svalbard), *Geol. Soc. Lond. Spec. Publ.*, 180, 585–601, <https://doi.org/10.1144/GSL.SP.2000.180.01.31>, 2000.
- 2650



- Piepjohn, K., Brinkmann, L., Grewing, A., and Kerp, H.: New data on the age of the uppermost ORS and the lowermost post-ORS strata in Dickson Land (Spitsbergen) and implications for the age of the Svalbardian deformation, *Geol. Soc. Lond. Spec. Publ.*, 180, 603–609, <https://doi.org/10.1144/GSL.SP.2000.180.01.32>, 2000.
- 2655 Piepjohn, K., and Dallmann, W. K.: Stratigraphy of the uppermost Old Red Sandstone of Svalbard (Mimerdalen Subgroup), *Polar Res.*, 33, 19998, <https://doi.org/10.3402/polar.v33.19998>, 2014.
- Piepjohn, K., and von Gosen, W.: Structural transect through Ellesmere Island (Canadian Arctic): superimposed Palaeozoic Ellesmerian and Cenozoic Eureka deformation, *Geol. Soc. Lond. Spec. Publ.*, 460, 33–56, 2018.
- 2660 Piepjohn, K., von Gosen, W., Tessensohn, F., Reinhardt, L., McClelland, W. C., Dallmann, W., Gaedicke, C., and Harrison, J. C.: Tectonic map of the Ellesmerian and Eureka deformation belts on Svalbard, North Greenland, and the Queen Elizabeth Islands (Canadian Arctic), *Arktos*, 1, 12, <https://doi.org/10.1007/s41063-015-0015-7>, 2015.
- Piepjohn, K., von Gosen, W., and Tessensohn, F.: The Eureka deformation in the Arctic: an outline, *J. Geol. Soc. Lond.*, 173, 1007–1024, 2016.
- 2665 Pietsch, C., and Bottjer, D. J.: The importance of oxygen for the disparate recovery patterns of the benthic macrofauna in the Early Triassic, *Earth-Sci. Rev.*, 137, 65–84, 2014.
- Podlaha, O. G., Mutterlose, J., and Veizer, J.: Preservation of delta 18O and delta 13C in belemnite rostra from the Jurassic/Early Cretaceous successions, *Am. J. Sci.*, 298, 324–347, 1998.
- 2670 Pogge von Strandmann, P. A. E., Jones, M. T., West, A. J., Murphy, M. J., Stokke, E. W., Tarbuck, G., Wilson, D. J., Pearce, C. R., and Schmidt, D. N.: Lithium isotope evidence for enhanced weathering and erosion during the Paleocene-Eocene Thermal Maximum, *Sci. Adv.*, 7, eabh4224, <https://doi.org/10.1126/sciadv.abh4224>, 2021.
- 2675 Polteau, S., Hendriks, B. W., Planke, S., Ganerød, M., Corfu, F., Faleide, J. I., Midtkandal, I., Svensen, H. S., and Myklebust, R.: The Early Cretaceous Barents Sea Sill Complex: distribution, 40Ar/39Ar geochronology, and implications for carbon gas formation, *Palaeogeogr. Palaeoclimatol. Palaeoecol.*, 441, 83–95, 2016.
- Polteau, S., Planke, S., Faleide, J. I., Svensen, H., and Myklebust, R.: The Cretaceous high Arctic large igneous province, *EGU Gen. Assem. Conf. Abstr.*, 13216, 2010.
- Pott, C.: The Upper Triassic Flora of Svalbard, *Acta Palaeontol. Pol.*, 59, 709–740, 2012.
- 2680 Price, G. D.: The evidence and implications of polar ice during the Mesozoic, *Earth-Sci. Rev.*, 48, 183–210, 1999.
- Price, G. D., Bajnai, D., and Fiebig, J.: Carbonate clumped isotope evidence for latitudinal seawater temperature gradients and the oxygen isotope composition of Early Cretaceous seas, *Palaeogeogr. Palaeoclimatol. Palaeoecol.*, 552, 109777, 2020.



- Price, G. D., Főzy, I., and Pálffy, J.: Carbon cycle history through the Jurassic–Cretaceous boundary: A new global $\delta^{13}\text{C}$ stack, *Palaeogeogr. Palaeoclimatol. Palaeoecol.*, 451, 46–61, <https://doi.org/10.1016/j.palaeo.2016.03.016>, 2016.
- Price, G. D., Hart, M. B., Wilby, P. R., and Page, K. N.: Isotopic analysis of Jurassic (Callovian) mollusks from the Christian Malford Lagerstätte (UK): Implications for ocean water temperature estimates based on belemnoids, *Palaios*, 30, 645–654, 2015.
- 2690 Price, G. D., and Passey, B. H.: Dynamic polar climates in a greenhouse world: Evidence from clumped isotope thermometry of Early Cretaceous belemnites, *Geology*, 41, 923–926, 2013.
- Price, G. D., and Nunn, E. V.: Valanginian isotope variation in glendonites and belemnites from Arctic Svalbard: Transient glacial temperatures during the Cretaceous greenhouse, *Geology*, 38, 251–254, <https://doi.org/10.1130/g30593.1>, 2010.
- 2695 Price, G. D., and Rogov, M. A.: An isotopic appraisal of the Late Jurassic greenhouse phase in the Russian Platform, *Palaeogeogr. Palaeoclimatol. Palaeoecol.*, 273, 41–49, <https://doi.org/10.1016/j.palaeo.2008.11.011>, 2009a.
- Price, G. D., and Rogov, M. A.: An isotopic appraisal of the Late Jurassic greenhouse phase in the Russian Platform, *Palaeogeogr. Palaeoclimatol. Palaeoecol.*, 273, 41–49, 2009b.
- 2700 Price, G. D., and Mutterlose, J.: Isotopic signals from late Jurassic–early Cretaceous (Volgian–Valanginian) sub-Arctic belemnites, Yatria River, Western Siberia, *J. Geol. Soc. Lond.*, 161, 959–968, <https://doi.org/10.1144/0016-764903-169>, 2004.
- Price, G. D.: New constraints upon isotope variation during the early Cretaceous (Barremian–Cenomanian) from the Pacific Ocean, *Geol. Mag.*, 140, 513–522, 2003.
- 2705 Pucéat, E., Lécuyer, C., Sheppard, S. M., Dromart, G., Reboulet, S., and Grandjean, P.: Thermal evolution of Cretaceous Tethyan marine waters inferred from oxygen isotope composition of fish tooth enamels, *Paleoceanography*, 18, 2003.
- Pörtlner, H.-O., Roberts, D. C., Adams, H., Adler, C., Aldunce, P., Ali, E., Begum, R. A., Betts, R., Kerr, R. B., Biesbroek, R., Birkmann, J., Bowen, K., Castellanos, E. C., Constable, A., Cramer, W., Dodman, D., Eriksen, S. H., Fischlin, A., Garschagen, M., Glavovic, B., Gilmore, E., Haasnoot, M., Harper, S., Hasegawa, T., Hayward, B., Hirabayashi, Y., Howden, M., Kalaba, K., Kiessling, W., Lasco, R., Lawrence, J., Lemos, M. F., Lempert, R., Ley, D., Lissner, T., Lluch-Cota, S., Loeschke, S., Lucatello, S., Luo, Y., Mackey, B., Maharaj, S., Mendez, C., Mintenbeck, K., Moncassim Vale, M., Morecroft, M. D., Mukherji, A., Mycoo, M., Mustonen, T., Nalau, J., Okem, A., Ometto, J. P., Parmesan, C., Pelling, M., Pinho, P., Poloczanska, E., Racault, M.-F., Reckien, D., Pereira, J., Revi, A., Rose, S., Sanchez-Rodriguez, R., Schipper, E. L. F., Schmidt, D., Schoeman, D., Shaw, R., Singh, C., Solecki, W., Stringer, L., Thomas, A., Totin, E., Trisos, C., Viner, D., van Aalst, M., Wairiu, M., Warren, R., Yanda, P., and Zaiton Ibrahim, Z.:



Climate change 2022: Impacts, adaptation and vulnerability, IPCC Sixth Assessment Report, <https://edepot.wur.nl/565644>, 2022.

2720

Q

Quattrini, A. M., Rodríguez, E., Faircloth, B. C., Cowman, P. F., Brugler, M. R., Farfan, G. A., Hellberg, M. E., Kitahara, M. V., Morrison, C. L., Paz-García, D. A., Reimer, J. D., and McFadden, C. S.: Palaeoclimate ocean conditions shaped the evolution of corals and their skeletons through deep time, *Nat. Ecol. Evol.*, 4, 1531–1538, <https://doi.org/10.1038/s41559-020-01291-1>, 2020.

2725

R

Rantanen, M., Karpechko, A. Y., Lipponen, A., Nordling, K., Hyvärinen, O., Ruosteenoja, K., Vihma, T., and Laaksonen, A.: The Arctic has warmed nearly four times faster than the globe since 1979, *Commun. Earth Environ.*, 3, 1–10, <https://doi.org/10.1038/s43247-022-00498-3>, 2022.

2730

Rauzi, S., Foster, W. J., Takahashi, S., Hori, R. S., Beaty, B. J., Tarhan, L. G., and Isson, T.: Lithium isotopic evidence for enhanced reverse weathering during the Early Triassic warm period, *Proc. Natl. Acad. Sci. USA*, 121, e2318860121, 2024.

2735

Reichow, M. K., Pringle, M. S., Al'Mukhamedov, A. I., Allen, M., Andreichev, V. L., Buslov, M. M., Davies, C., Fedoseev, G. S., Fitton, J. G., and Inger, S.: The timing and extent of the eruption of the Siberian Traps large igneous province: Implications for the end-Permian environmental crisis, *Earth Planet. Sci. Lett.*, 277, 9–20, 2009.

Retallack, G. J., and Conde, G. D.: Deep time perspective on rising atmospheric CO₂, *Global Planet. Change*, 189, 103177, <https://doi.org/10.1016/j.gloplacha.2020.103177>, 2020.

2740

Rigo, M., Preto, N., Roghi, G., Tateo, F., and Mietto, P.: A rise in the carbonate compensation depth of western Tethys in the Carnian (Late Triassic): deep-water evidence for the Carnian Pluvial Event, *Palaeogeogr. Palaeoclimatol. Palaeoecol.*, 246, 188–205, 2007.

Rigo, M., and Joachimski, M. M.: Palaeoecology of Late Triassic conodonts: Constraints from oxygen isotopes in biogenic apatite, *Acta Palaeontol. Pol.*, 55, 471–478, 2010.

2745

Rigo, M., Jin, X., Godfrey, L., Katz, M. E., Sato, H., Tomimatsu, Y., and Onoue, T.: Unveiling a new oceanic anoxic event at the Norian/Rhaetian boundary (Late Triassic), *Sci. Rep.*, 14, 15574, 2024.

Riis, F., Lundschieen, B. A., Høy, T., Mørk, A., and Mørk, M. B. E.: Evolution of the Triassic shelf in the northern Barents Sea region, *Polar Res.*, 27, 318–338, <https://doi.org/10.1111/j.1751-8369.2008.00086.x>, 2008.



- 2750 Riis, F., and Fjeldskaar, W.: On the magnitude of the Late Tertiary and Quaternary erosion and its significance for the uplift of Scandinavia and the Barents Sea, in: *Structural and tectonic modelling and its application to petroleum geology*, edited by: Larsen, R. M., Brekke, H., Larsen, B. T., and Talleraas, E., Elsevier, Amsterdam, 163–185, 1992.
- 2755 Rismyhr, B., Bjærke, T., Olaussen, S., Mulrooney, M. J., and Senger, K.: Facies, palynostratigraphy and sequence stratigraphy of the Wilhelmøya Subgroup (Upper Triassic–Middle Jurassic) in western central Spitsbergen, Svalbard, *Nor. Geol. Tidsskr.*, 99, 35–64, 2018.
- Rizzo, R. E., Inskip, N. F., Fazeli, H., Betlem, P., Bisdorn, K., Kampman, N., and Busch, A.: Modelling geological CO₂ leakage: Integrating fracture permeability and fault zone outcrop analysis, *Int. J. Greenh. Gas Control*, 133, 104105, 2024.
- 2760 Roberts, A. J., Engelschion, V. S., and Hurum, J. H.: First three-dimensional skull of the Middle Triassic mixosaurid ichthyosaur *Phalarodon fraasi* from Svalbard, Norway, *Acta Palaeontol. Pol.*, 67, 51–62, 2022.
- Rocha, B. C., Davies, J. H., Janasi, V. A., Schaltegger, U., Nardy, A. J., Greber, N. D., and Lucchetti, A. C. F.: Rapid eruption of silicic magmas from the Parana magmatic province (Brazil) did not trigger the Valanginian event, *Geology*, 48, 1174–1178, 2020.
- 2765 Rodriguez Blanco, L., Swart, P. K., Eberli, G. P., & Weger, R. J.: Negative $\delta^{13}\text{C}$ carb values at the Jurassic–Cretaceous boundary – Vaca Muerta Formation, Neuquén Basin, Argentina. *Palaeogeography, Palaeoclimatology, Palaeoecology*, **603**, 111208. <https://doi.org/10.1016/j.palaeo.2022.111208>, 2022.
- Rodríguez-Tovar, F. J., Dorador, J., Zuchuat, V., Planke, S., and Hammer, Ø.: Response of macrobenthic trace maker community to the end-Permian mass extinction in Central Spitsbergen, Svalbard, *Palaeogeogr. Palaeoclimatol. Palaeoecol.*, 581, 2021.
- 2770 Roest, W. R., and Srivastava, S. P.: Sea-floor spreading in the Labrador Sea: A new reconstruction, *Geology*, 17, 1000–1003, [https://doi.org/10.1130/0091-7613\(1989\)017<1000:Sfsitl>2.3.Co;2](https://doi.org/10.1130/0091-7613(1989)017<1000:Sfsitl>2.3.Co;2), 1989.
- Roghi, G.: Palynological investigations in the Carnian of the Cave del Predil area (Julian Alps, NE Italy), *Rev. Palaeobot. Palynol.*, 132, 1–35, 2004.
- 2775 Rogov, M., and Zakharov, V.: Jurassic and Lower Cretaceous glendonite occurrences and their implication for Arctic paleoclimate reconstructions and stratigraphy, *Earth Sci. Front.*, 17, 345–347, 2010.
- Rogov, M. A., Ershova, V. B., Shchepetova, E. V., Zakharov, V. A., Pokrovsky, B. G., and Khudoley, A. K.: Earliest Cretaceous (late Berriasian) glendonites from Northeast Siberia revise the timing of initiation of transient Early Cretaceous cooling in the high latitudes, *Cretac. Res.*, 71, 102–
- 2780 112, <https://doi.org/10.1016/j.cretres.2016.11.011>, 2017.



- Rogov, M. A.: Ammonites and infrazonal stratigraphy of the Kimmeridgian and Volgian stages of Panboreal Superrealm. *Transactions of the Geological Institute*, 627, 1–732, https://doi.org/10.54896/00023272_2021_627_1, 2021.
- 2785 Rogov, M. A., Zakharov, V., & Kiselev, D.: Refined ammonite and bivalve biostratigraphy of the Agardhfjellet and lowermost Rurikfjellet formations (Bathonian–Ryazanian) of the Longyearbyen area, Spitsbergen. *Neues Jahrbuch für Geologie und Paläontologie, Abhandlungen*, **309**(2), 169–198. <https://doi.org/10.1127/njgpa/2023/1158>, 2023.
- Rooney, A. D., Strauss, J. V., Brandon, A. D., and Macdonald, F. A.: A Cryogenian chronology: Two long-lasting synchronous Neoproterozoic glaciations, *Geology*, 43, 459–462, 2015.
- 2790 Royer, D. L., Berner, R. A., Montañez, I. P., Tabor, N. J., and Beerling, D. J.: CO₂ as a primary driver of Phanerozoic climate, *GSA Today*, 14, 4–10, 2004.
- Royer, D. L.: Linkages between CO₂, climate, and evolution in deep time, *Proc. Natl. Acad. Sci. USA*, 105, 407–408, <https://doi.org/10.1073/pnas.0710915105>, 2008.

2795

S

- Salamon, M.A., Hanken, N., Gorzelak, P., Riise, H.E. and Ferré, B., 2015. Crinoids from Svalbard in the aftermath of the end- Permian mass extinction. *Polish Polar Research: 225-238-225-238*,
- 2800 Salamon, M. A., Hanken, N., Gorzelak, P., Riise, H. E., and Ferré, B.: Crinoids from Svalbard in the aftermath of the end-Permian mass extinction, *Pol. Polar Res.*, 36, 225–238, 2015.
- Sangiorgi, F., Brumsack, H. J., Willard, D. A., Schouten, S., Stickley, C. E., O'Regan, M., Reichart, G. J., Sinninghe Damsté, J. S., and Brinkhuis, H.: A 26 million year gap in the central Arctic record at the greenhouse-icehouse transition: Looking for clues, *Paleoceanography*, 23, 2008.
- Sanei, H., Grasby, S. E., & Beauchamp, B.: Latest Permian mercury anomalies. *Geology*, 40(1), 63-66, (2012).
- 2805 Scheibner, C., Hartkopf-Fröder, C., Blomeier, D., and Forke, H.: The Mississippian (Lower Carboniferous) in northeast Spitsbergen (Svalbard) and a re-evaluation of the Billefjorden Group, *Z. Dtsch. Ges. Geowiss.*, 163, 293, 2012.
- Schlanger, S. O., and Jenkyns, H.: Cretaceous oceanic anoxic events: causes and consequences, *Geol. Mijnb.*, 55, 1976.
- 2810 Schlegel, A., Lisker, F., Dörr, N., Jochmann, M., Schubert, K., and Spiegel, C.: Petrography and geochemistry of siliciclastic rocks from the Central Tertiary Basin of Svalbard—implications for provenance, tectonic setting and climate, *Z. Dtsch. Ges. Geowiss.*, 164, 173–186, 2013.



- 2815 Schobben, M., Joachimski, M. M., Korn, D., Leda, L., and Korte, C.: Palaeotethys seawater temperature rise and an intensified hydrological cycle following the end-Permian mass extinction, *Gondwana Res.*, 26, 675–683, 2014.
- Schobben, M., Foster, W. J., Sleveland, A. R., Zuchuat, V., Svensen, H. H., Planke, S., Bond, D. P., Marcelis, F., Newton, R. J., and Wignall, P. B.: A nutrient control on marine anoxia during the end-Permian mass extinction, *Nat. Geosci.*, 13, 640–646, 2020.
- 2820 Schröder-Adams, C. J., Herrle, J. O., Embry, A. F., Haggart, J. W., Galloway, J. M., Pugh, A. T., and Harwood, D. M.: Aptian to Santonian foraminiferal biostratigraphy and paleoenvironmental change in the Sverdrup Basin as revealed at Glacier Fiord, Axel Heiberg Island, Canadian Arctic Archipelago, *Palaeogeogr. Palaeoclimatol. Palaeoecol.*, 413, 81–100, 2014.
- Schweitzer, J., Paulsen, B., Antonovskaya, G. N., Fedorov, A. V., Konechnaya, Y. V., Asming, V. E., and Pirli, M.: A 24-Yr-Long Seismic Bulletin for the European Arctic, *Seismol. Res. Lett.*, 92, 2758–2767, <https://doi.org/10.1785/0220210018>, 2021.
- 2825 Schaaf, N. W., Osmundsen, P. T., Van der Lelij, R., Schönenberger, J. L., OK, R. T., and Senger, K.: Tectono-sedimentary evolution of the eastern Forlandsundet Graben, Svalbard, *Nor. J. Geol.*, 100, <https://doi.org/10.1785/njg100-4-4>, 2021.
- Schobben, Martin, William J. Foster, Arve RN Sleveland, Valentin Zuchuat, Henrik H. Svensen, Sverre Planke, 2830 David PG Bond et al. "A nutrient control on marine anoxia during the end-Permian mass extinction." *Nature Geoscience* 13, no. 9: 640-646. 2020.
- Scotese, C. R., Bambach, R. K., Barton, C., Van der Voo, R., and Ziegler, A. M.: Paleozoic base maps, *J. Geol.*, 87, 217–277, <https://doi.org/10.1086/628416>, 1979.
- Scotese, C. R., and Wright, N.: PALEOMAP Paleodigital Elevation Models (PaleoDEMs) for the Phanerozoic, 2835 PALEOMAP Project, <https://www.earthbyte.org/paleodem-resource-scotese-and-wright-2018>, 2018.
- Scotese, C. R., Boucot, A. J., and McKerrow, W. S.: Gondwanan palaeogeography and palaeoclimatology, *J. Afr. Earth Sci.*, 28, 99–114, 1999.
- Scotese, C. R., Song, H., Mills, B. J. W., and van der Meer, D. G.: Phanerozoic paleotemperatures: The earth's 2840 changing climate during the last 540 million years, *Earth-Sci. Rev.*, 215, <https://doi.org/10.1016/j.earscirev.2021.103503>, 2021.
- Screen, J. A., and Simmonds, I.: The central role of diminishing sea ice in recent Arctic temperature amplification, *Nature*, 464, 1334–1337, <https://doi.org/10.1038/nature09051>, 2010.
- Scrutton, C., Horsfield, W., and Harland, W.: Silurian fossils from western Spitsbergen, *Geol. Mag.*, 113, 519–523, 1976.
- 2845 Sellwood, B., and Price, G.: Sedimentary facies as indicators of Mesozoic palaeoclimate, *Philos. Trans. R. Soc. Lond. B Biol. Sci.*, 341, 225–233, 1993.



- Senger, K., Brugmans, P., Grundvåg, S.-A., Jochmann, M. M., Nøttvedt, A., Olaussen, S., Skotte, A., and Smyrak-Sikora, A.: Petroleum, coal and research drilling onshore Svalbard: a historical perspective, *Norwegian Journal of Geology*, Vol 99 Nr.3, 1-30, <https://dx.doi.org/10.17850/njg99-3-1>, 2019.
- 2850 Senger, K., Planke, S., Polteau, S., Ogata, K., and Svensen, H.: Sill emplacement and contact metamorphism in a siliciclastic reservoir on Svalbard, Arctic Norway, *Nor. J. Geol.*, 94, 2014a.
- Senger, K., Tveranger, J., Ogata, K., Braathen, A., and Planke, S.: Late Mesozoic magmatism in Svalbard: A review, *Earth-Sci. Rev.*, 139, 123–144, 2014b.
- Senger, K., Tveranger, J., Braathen, A., Olaussen, S., Ogata, K., and Larsen, L.: CO₂ storage resource estimates
2855 in unconventional reservoirs: insights from a pilot-sized storage site in Svalbard, Arctic Norway, *Environ. Earth Sci.*, 73, 3987–4009, <https://doi.org/10.1007/s12665-014-3684-9>, 2015.
- Senger, K., Betlem, P., Birchall, T., Gonzaga Jr, L., Grundvåg, S.-A., Horota, R. K., Laake, A., Kuckero, L., Mørk, A., and Planke, S.: Digitising Svalbard's geology: the Festningen digital outcrop model, *First Break*, 40, 47–55, 2022.
- 2860 Senger, K., Betlem, P., Braathen, A., Olaussen, S., and Sand, G.: Longyearbyen CO₂ Lab project - from a vision of a CO₂-neutral Svalbard to a geoscience data eldorado, *Arct. Sci.*, <https://doi.org/10.1139/as-2024-0019>, 2024.
- Sepkoski, J. J.: Patterns of Phanerozoic extinction: a perspective from global data bases, in: *Global events and event stratigraphy in the Phanerozoic*, edited by: Walliser, O. H., Springer, Berlin, Heidelberg, 35–
2865 51, https://doi.org/10.1007/978-3-642-79634-0_4, 1996.
- Servais, T., and Harper, D. A.: The great Ordovician biodiversification event (GOBE): definition, concept and duration, *Lethaia*, 51, 151–164, 2018.
- Sharma, M., Papanastassiou, D. A., and Wasserburg, G. J.: The concentration and isotopic composition of osmium in the oceans, *Geochim. Cosmochim. Acta*, 61, 3287–3299, [https://doi.org/10.1016/S0016-7037\(97\)00210-X](https://doi.org/10.1016/S0016-7037(97)00210-X), 1997.
- 2870 Silva, D., Lana, C., and de Souza Filho, C. R.: Petrographic and geochemical characterization of the granitic rocks of the Araguinha impact crater, Brazil, *Meteorit. Planet. Sci.*, 51, 443–467, <https://doi.org/10.1111/maps.12601>, 2016.
- Simms, M. J., and Ruffell, A. H.: Synchronicity of climatic change and extinctions in the Late Triassic, *Geology*, 17,
2875 265–268, 1989.
- Śliwińska, K. K., Coxall, H. K., Hutchinson, D. K., Liebrand, D., Schouten, S., and de Boer, A. M.: Sea surface temperature evolution of the North Atlantic Ocean across the Eocene–Oligocene transition, *Clim. Past*, 19, 123–140, 2023.



- 2880 Śliwińska, K. K., and Head, M. J.: New species of the dinoflagellate cyst genus *Svalbardella* Manum, 1960, emend. from the Paleogene and Neogene of the northern high to middle latitudes, *J. Micropalaeontol.*, 39, 139–154, 2020.
- Śliwińska, K. K., and Heilmann-Clausen, C.: Early Oligocene cooling reflected by the dinoflagellate cyst *Svalbardella cooksoniae*, *Palaeogeogr. Palaeoclimatol. Palaeoecol.*, 305, 138–149, 2011.
- 2885 Śliwińska, K. K., Jelby, M. E., Grundvåg, S.-A., Nøhr-Hansen, H., Alsen, P., and Olausen, S.: Dinocyst stratigraphy of the Valanginian–Aptian Rurikfjellet and Helvetiafjellet formations on Spitsbergen, Arctic Norway, *Geol. Mag.*, 157, 1693–1714, <https://doi.org/10.1017/S0016756819001249>, 2020.
- Śliwińska, K. K., Thomsen, E., Schouten, S., Schoon, P. L., and Heilmann-Clausen, C.: Climate-and gateway-driven cooling of Late Eocene to earliest Oligocene sea surface temperatures in the North Sea Basin, *Sci. Rep.*, 9, 4458, 2019.
- 2890 Sluijs, A., Frieling, J., Inglis, G. N., Nierop, K. G., Peterse, F., Sangiorgi, F., and Schouten, S.: Late Paleocene–early Eocene Arctic Ocean sea surface temperatures: reassessing biomarker paleothermometry at Lomonosov Ridge, *Clim. Past*, 16, 2381–2400, 2020.
- Smelror, M., Olausen, S., Dumais, M. A., Grundvåg, S. A., and Abay, T. B.: Northern Svalbard Composite Tectono-Sedimentary Element, *Geol. Soc. Lond. Mem.*, 57, M57-2023, 2024.
- 2895 Smelror, M., Grenne, T., Gasser, D., and Bøe, R.: Deep-water trace fossils in the Ilfjellet rift basin (Middle Ordovician), central Norwegian Caledonides, *Palaeoworld*, 32, 63–78, 2023.
- Smelror, M., Olausen, S., Dumais, M. A., Grundvåg, S. A., and Abay, T. B.: Northern Svalbard Composite Tectono-Sedimentary Element, *Geol. Soc. Lond. Mem.*, 57, M57-2023, 2024.
- 2900 Smyrak-Sikora, A., Johannessen, E. P., Olausen, S., Sandal, G., and Braathen, A.: Sedimentary architecture during Carboniferous rift initiation – the arid Billefjorden Trough, Svalbard, *J. Geol. Soc. Lond.*, 176, 225–252, <https://doi.org/10.1144/jgs2018-100>, 2018.
- Smyrak-Sikora, A., Nicolaisen, J. B., Braathen, A., Johannessen, E. P., Olausen, S., and Stemmerik, L.: Impact of growth faults on mixed siliciclastic-carbonate-evaporite deposits during rift climax and reorganisation—Billefjorden Trough, Svalbard, Norway, *Basin Res.*, 33, 2643–2674, <https://doi.org/10.1111/bre.12578>, 2905 2021.
- Smyrak-Sikora, A., Engelschiøn, V., Foster, W., Jelby, M. E., Jones, M., Mosociova, T., Śliwińska, K., Vickers, M. L., & Zuchuat, V.: Table: Review of Phanerozoic Paleoenvironmental and Paleoclimatic Evolution in Svalbard [Data set]. Zenodo. <https://doi.org/10.5281/zenodo.14334261>, 2024.
- 2910 Solomon, S., Qin, D., Manning, M., Averyt, K., and Marquis, M.: Climate change 2007-the physical science basis: Working group I contribution to the fourth assessment report of the IPCC, Cambridge University Press, 2007.



- Song, H., Wignall, P. B., Tong, J., Bond, D. P., Song, H., Lai, X., and Chen, Y.: Geochemical evidence from biapatite for multiple oceanic anoxic events during Permian–Triassic transition and the link with end-Permian extinction and recovery, *Earth Planet. Sci. Lett.*, 353, 12–21, 2012.
- 2915 Song, H., Wignall, P. B., Song, H., Dai, X., and Chu, D.: Seawater temperature and dissolved oxygen over the past 500 million years, *J. Earth Sci.*, 30, 236–243, 2019.
- Soreghan, G. S.: Déjà-Vu All Over Again: Deep Time (Climate) Is Here To Stay, *PALAIOS*, 19, 1–2, [https://doi.org/10.1669/0883-1351\(2004\)019<0001:Daoadt>2.0.Co;2](https://doi.org/10.1669/0883-1351(2004)019<0001:Daoadt>2.0.Co;2), 2004.
- Sorento, T., Olausson, S., and Stemmerik, L.: Controls on deposition of shallow marine carbonates and evaporites – lower Permian Gipsbukken Formation, central Spitsbergen, Arctic Norway, *Sedimentology*, 67, 207–238, <https://doi.org/10.1111/sed.12640>, 2020.
- 2920 Soua, M.: Early Carnian anoxic event as recorded in the southern Tethyan margin, Tunisia: an overview, *Int. Geol. Rev.*, 56, 1884–1905, 2014.
- Speelman, E. N., van Kempen, M. M. L., Barke, J., Brinkhuis, H., Reichert, G. J., Smolders, A. J. P., Roelofs, J. G. M., Sangiorgi, F., de Leeuw, J. W., Lotter, A. F., and Sinninghe Damsté, J. S.: The Eocene Arctic Azolla bloom: environmental conditions, productivity and carbon drawdown, *Geobiology*, 7, 155–170, <https://doi.org/10.1111/j.1472-4669.2009.00195.x>, 2009.
- 2925 Spielhagen, R. F., and Tripathi, A.: Evidence from Svalbard for near-freezing temperatures and climate oscillations in the Arctic during the Paleocene and Eocene, *Palaeogeogr. Palaeoclimatol. Palaeoecol.*, 278, 48–56, <https://doi.org/10.1016/j.palaeo.2009.04.012>, 2009.
- 2930 Stanley Jr, G. D.: The evolution of modern corals and their early history, *Earth-Sci. Rev.*, 60, 195–225, 2003.
- Stanley, S. M.: Estimates of the magnitudes of major marine mass extinctions in earth history, *Proc. Natl. Acad. Sci. USA*, 113, E6325–E6334, <https://doi.org/10.1073/pnas.161309411>, 2016.
- Steel, R. J., Gjelberg, J., and Haarr, G.: Helvetiafjellet Formation (Barremian) at Festningen, Spitsbergen— a field guide, *Nor. Polarinst. Årbok*, 111–128, 1978.
- 2935 Steel, R. J., Dalland, A., Kalgraff, K., and Larsen, V.: The Central Tertiary Basin of Spitsbergen: sedimentary development of a sheared-margin basin, *Geology of the North Atlantic Borderlands — Memoir 7, CSPG Special Publications*, 647-664, 1981.
- Steel, R., Gjelberg, J., Helland-Hansen, W., Kleinspehn, K., Nøttvedt, A., and Rye-Larsen, M.: The Tertiary strike-slip basins and orogenic belt of Spitsbergen, *Special Publications of SEPM*, 1985.
- 2940 Steel, R. J., and Worsley, D.: Svalbard's post-Caledonian strata—an atlas of sedimentational patterns and palaeogeographic evolution, in: *Petroleum geology of the North European margin*, edited by: Spencer, A. M., Springer, Dordrecht, 109–135, https://doi.org/10.1007/978-94-009-5626-1_9, 1984.
- Stemmerik, L.: Late Palaeozoic evolution of the North Atlantic margin of Pangea, *Palaeogeogr. Palaeoclimatol. Palaeoecol.*, 161, 95–126, 2000.
- 2945



- Stemmerik, L.: Influence of late Paleozoic Gondwana glaciations on the depositional evolution of the northern Pangean shelf, North Greenland, Svalbard, and the Barents Sea, *Geol. Soc. Am. Spec. Pap.*, 441, 2008.
- Stemmerik, L., Bendix-Almgreen, S. E., and Piasecki, S.: The Permian–Triassic boundary in central East Greenland: past and present views, *Bull. Geol. Soc. Den.*, 48, 159–167, 2001.
- 2950 Stemmerik, L., and Worsley, D.: 30 years on-Arctic Upper Palaeozoic stratigraphy, depositional evolution and hydrocarbon prospectivity, *Nor. J. Geol.*, 85, 2005.
- Stewart, I.: Sustainable geoscience, *Nat. Geosci.*, 9, 262, 2016.
- Stickley, C. E., Brinkhuis, H., Schellenberg, S. A., Sluijs, A., Röhl, U., Fuller, M., Grauert, M., Huber, M., Warnaar, J., and Williams, G. L.: Timing and nature of the deepening of the Tasmanian Gateway, *Paleoceanography*, 19, <https://doi.org/10.1029/2004PA001022>, 2004.
- 2955 Stickley, C. E., St John, K., Koç, N., Jordan, R. W., Passchier, S., Pearce, R. B., and Kearns, L. E.: Evidence for middle Eocene Arctic sea ice from diatoms and ice-rafted debris, *Nature*, 460, 376–379, <http://www.nature.com/doi/10.1038/nature08163>, 2009.
- Stordal, F., Svensen, H. H., Aarnes, I., and Roscher, M.: Global temperature response to century-scale degassing from the Siberian Traps Large igneous province, *Palaeogeogr. Palaeoclimatol. Palaeoecol.*, 471, 96–107, <https://doi.org/10.1016/j.palaeo.2017.01.045>, 2017.
- 2960 Storey, M., Duncan, R. A., and Tegner, C.: Timing and duration of volcanism in the North Atlantic Igneous Province: Implications for the geodynamics and links to the Iceland hotspot, *Chem. Geol.*, 241, 264–281, 2007a.
- Storey, M., Duncan, R. A., and Swisher III, C. C.: Paleocene-Eocene Thermal Maximum and the opening of the Northeast Atlantic, *Science*, 316, 587–589, 2007b.
- 2965 Stouge, S., Christiansen, J. L., and Holmer, L. E.: Lower palaeozoic stratigraphy of Murchisonfjorden and Sparreneset, Nordaustlandet, Svalbard, *Geogr. Ann. Ser. A-Phys. Geogr.*, 93, 209–226, 2011.
- Stouge, S., Harper, D. A., Boyce, W. D., and Christiansen, I. K. L.: Development of the lower Cambrian–Middle Ordovician carbonate platform: North Atlantic Region, 2012.
- 2970 Straume, E. O., Gaina, C., Medvedev, S., and Nisancioglu, K. H.: Global Cenozoic paleobathymetry with a focus on the Northern Hemisphere oceanic gateways, *Gondwana Res.*, 86, 126–143, <https://doi.org/10.1016/j.gr.2020.05.011>, 2020.
- Straume, E. O., Nummelin, A., Gaina, C., and Nisancioglu, K. H.: Climate transition at the Eocene–Oligocene influenced by bathymetric changes to the Atlantic–Arctic oceanic gateways, *Proc. Natl. Acad. Sci. USA*, 119, e2115346119, <https://doi.org/10.1073/pnas.2115346119>, 2022.
- 2975 Suan, G., Popescu, S.-M., Suc, J.-P., Schnyder, J., Fauquette, S., Baudin, F., Yoon, D., Piepjohn, K., Sobolev, N. N., and Labrousse, L.: Subtropical climate conditions and mangrove growth in Arctic Siberia during the early Eocene, *Geology*, 45, 539–542, <https://doi.org/10.1130/G38547.1>, 2017.



- 2980 Suc, J.-P., Fauquette, S., Popescu, S.-M., and Robin, C.: Subtropical mangrove and evergreen forest reveal
Paleogene terrestrial climate and physiography at the North Pole, *Palaeogeogr. Palaeoclimatol.*
Palaeoecol., 551, 109755, 2020.
- Sudermann, M., Galloway, J. M., Greenwood, D. R., West, C. K., and Reinhardt, L.: Palynostratigraphy of the lower
Paleogene Margaret Formation at Stenkul Fiord, Ellesmere Island, Nunavut, Canada, *Palynology*, 45, 459–
476, 2021.
- 2985 Summerhayes, C. P.: Earth's climate evolution, John Wiley and Sons, 2015.
- Summons, R. E., Welander, P. V., and Gold, D. A.: Lipid biomarkers: molecular tools for illuminating the history of
microbial life, *Nat. Rev. Microbiol.*, 20, 174–185, 2022.
- Sun, Y. D., Wignall, P. B., Joachimski, M. M., Bond, D. P., Grasby, S. E., Lai, X. L., and Sun, S.: Climate warming,
euxinia and carbon isotope perturbations during the Carnian (Triassic) Crisis in South China, *Earth Planet.*
2990 *Sci. Lett.*, 444, 88–100, 2016.
- Svensen, H., Planke, S., Malthe-Sørensen, A., Jamtveit, B., Myklebust, R., Rasmussen Eidem, T., and Rey, S.
S.: Release of methane from a volcanic basin as a mechanism for initial Eocene global warming, *Nature*,
429, 542–545, 2004.
- Svensen, H., Planke, S., Polozov, A. G., Schmidbauer, N., Corfu, F., Podladchikov, Y. Y., and Jamtveit, B.: Siberian
2995 gas venting and the end-Permian environmental crisis, *Earth Planet. Sci. Lett.*, 277, 490–
500, <https://doi.org/10.1016/j.epsl.2008.11.015>, 2009.
- Svensen, H. H., Frolov, S., Akhmanov, G. G., Polozov, A. G., Jerram, D. A., Shiganova, O. V., Melnikov, N. V.,
Iyer, K., and Planke, S.: Sills and gas generation in the Siberian Traps, *Philos. Trans. R. Soc. A-Math.*
Phys. Eng. Sci., 376, 20170080, <https://doi.org/10.1098/rsta.2017.0080>, 2018.
- 3000 Svensen, H. H., Jerram, D. A., Polozov, A. G., Planke, S., Neal, C. R., Augland, L. E., and Emeleus, H. C.: Thinking
about LIPs: A brief history of ideas in Large igneous province research, *Tectonophysics*, 760, 229–251,
2019.
- Swainson, I. P., and Hammond, R. P.: Ikaite, CaCO₃·6H₂O: Cold comfort for glendonites as paleothermometers,
Am. Mineral., 86, 1530–1533, <https://doi.org/10.2138/am-2001-11-1223>, 2001.
- 3005

T

- Tarduno, J., Sliter, W., Kroenke, L., Leckie, M., Mayer, H., Mahoney, J., Musgrave, R., Storey, M., and Winterer,
E.: Rapid formation of Ontong Java Plateau by Aptian mantle plume volcanism, *Science*, 254, 399–403,
1991.



- 3010 Tejada, M., Mahoney, J., Neal, C., Duncan, R., and Petterson, M.: Basement geochemistry and geochronology of Central Malaita, Solomon Islands, with implications for the origin and evolution of the Ontong Java Plateau, *J. Petrol.*, 43, 449–484, 2002.
- Tejada, M. L. G., Suzuki, K., Kuroda, J., Coccioni, R., Mahoney, J. J., Ohkouchi, N., Sakamoto, T., and Tatsumi, Y.: Ontong Java Plateau eruption as a trigger for the early Aptian oceanic anoxic event, *Geology*, 37, 855–
3015 858, 2009.
- Thordarson, T.: Accretionary-lapilli-bearing pyroclastic rocks at ODP Leg 192 Site 1184: a record of subaerial phreatomagmatic eruptions on the Ontong Java Plateau, *Geol. Soc. Lond. Spec. Publ.*, 229, 275–306, 2004.
- Thronsdon, T.: Vitrinite reflectance studies of coals and dispersed organic matter in Tertiary deposits in the
3020 Adventdalen area, Svalbard, *Polar Res.*, 2, 77–91, 1982.
- Toggweiler, J., and Bjornsson, H.: Drake Passage and palaeoclimate, *J. Quat. Sci.*, 15, 319–328, 2000.
- Tohver, E., Lana, C., Cawood, P. A., Fletcher, I. R., Jourdan, F., Sherlock, S., Rasmussen, B., Trindade, R. I. F., Yokoyama, E., Souza Filho, C. R., and Marangoni, Y.: Geochronological constraints on the age of a Permo–Triassic impact event: U–Pb and $^{40}\text{Ar}/^{39}\text{Ar}$ results for the 40 km Araguainha structure of central
3025 Brazil, *Geochim. Cosmochim. Acta*, 86, 214–227, <https://doi.org/10.1016/j.gca.2012.03.005>, 2012.
- Tomimatsu, Y., Onoue, T., and Rigo, M.: Conodont and radiolarian biostratigraphic age constraints on Carnian (Upper Triassic) chert-hosted stratiform manganese deposits from Panthalassa: Formation of deep-sea mineral resources during the Carnian pluvial episode, *Mar. Micropaleontol.*, 171, 102084, 2022.
- Torsvik, T. H., Carlos, D., Mosar, J., Cocks, L. R. M., and Malme, T.: Global reconstructions and North Atlantic paleogeography 440 Ma to recent, in: BATLAS–Mid Norway plate reconstruction atlas with global and Atlantic perspectives, edited by: Eide, E. A., *Geol. Surv. Norw.*, Trondheim, 18–39, 2002a.
3030
- Torsvik, T. H., Carlos, D., Mosar, J., Cocks, L. R. M., and Malme, T.: Global reconstructions and North Atlantic paleogeography 440 Ma to recent, in: BATLAS–Mid Norway plate reconstruction atlas with global and Atlantic perspectives, edited by: Eide, E. A., *Geol. Surv. Norw.*, Trondheim, 18, 39, 2002b.
- 3035 Torsvik, T. H., and Cocks, L. R. M.: The integration of palaeomagnetism, the geological record and mantle tomography in the location of ancient continents, *Geol. Mag.*, 156, 242–260, 2019.
- Torsvik, T. H., Van der Voo, R., Preeden, U., Mac Niocaill, C., Steinberger, B., Doubrovine, P. V., Van Hinsbergen, D. J., Domeier, M., Gaina, C., and Tohver, E.: Phanerozoic polar wander, palaeogeography and dynamics, *Earth-Sci. Rev.*, 114, 325–368, 2012.
- 3040 Tozer, E. T., and Parker, J. R.: Notes on the Triassic biostratigraphy of Svalbard, *Geol. Mag.*, 105, 526–542, 1968.
- Tozer, E. T.: A standard for Triassic Time, *Geol. Surv. Can. Bull.*, 156, 1–103, 1967.

Tremolada, F., Bornemann, A., Bralower, T. J., Koeberl, C., and van de Schootbrugge, B.: Paleooceanographic changes across the Jurassic/Cretaceous boundary: The calcareous phytoplankton response, *Earth Planet. Sci. Lett.*, 241, 361–371, <https://doi.org/10.1016/j.epsl.2005.11.047>, 2006.

3045 Tripathi, A., and Darby, D.: Evidence for ephemeral middle Eocene to early Oligocene Greenland glacial ice and pan-Arctic sea ice, *Nat. Commun.*, 9, 1038, 2018.

Twitchett, R. J., Looy, C. V., Morante, R., Visscher, H., and Wignall, P. B.: Rapid and synchronous collapse of marine and terrestrial ecosystems during the end-Permian biotic crisis, *Geology*, 29, 351–354, 2001.

3050

U

Uchman, A., Hanken, N.-M., Nielsen, J. K., Grundvåg, S.-A., and Piasecki, S.: Depositional environment, ichnological features and oxygenation of Permian to earliest Triassic marine sediments in central Spitsbergen, Svalbard, *Polar Res.*, 35, 24782, 2016.

3055 Uhl, D., Traiser, C., Griesser, U., and Denk, T.: Fossil leaves as palaeoclimate proxies in the Palaeogene of Spitsbergen (Svalbard), *Acta Palaeobot.*, 47, 89, 2007

V

Van Der Meer, D. G., Zeebe, R. E., van Hinsbergen, D. J., Sluijs, A., Spakman, W., and Torsvik, T. H.: Plate tectonic controls on atmospheric CO₂ levels since the Triassic, *Proc. Natl. Acad. Sci. USA*, 111, 4380–4385, 2014.

3060 Van der Meer, D. G., van Saparoea, A. V. D. B., Van Hinsbergen, D. J. J., Van de Weg, R. M. B., Godderis, Y., Le Hir, G., and Donnadieu, Y.: Reconstructing first-order changes in sea level during the Phanerozoic and Neoproterozoic using strontium isotopes, *Gondwana Res.*, 44, 22–34, 2017.

3065 van de Schootbrugge, B., Föllmi, K. B., Bulot, L. G., and Burns, S. J.: Paleooceanographic changes during the early Cretaceous (Valanginian–Hauterivian): evidence from oxygen and carbon stable isotopes, *Earth Planet. Sci. Lett.*, 181, 15–31, 2000.

3070 Veizer, J., Ala, D., Azmy, K., Bruckschen, P., Buhl, D., Bruhn, F., Carden, G. A. F., Diener, A., Ebner, S., Godderis, Y., Jasper, T., Korte, C., Pawellek, F., Podlaha, O. G., and Strauss, H.: ⁸⁷Sr/⁸⁶Sr, $\delta^{13}\text{C}$ and $\delta^{18}\text{O}$ evolution of Phanerozoic seawater, *Chem. Geol.*, 161, 59–88, [https://doi.org/10.1016/s0009-2541\(99\)00081-9](https://doi.org/10.1016/s0009-2541(99)00081-9), 1999.

Veizer, J., and Prokoph, A.: Temperatures and oxygen isotopic composition of Phanerozoic oceans, *Earth-Sci. Rev.*, 146, 92–104, 2015.



- Vérard, C., and Veizer, J.: On plate tectonics and ocean temperatures, *Geology*, 47, 881–885, 2019.
- Verba, M.: Kollektornye svoystva porod osadochnogo chekhla arkhipelaga Shpitsbergen [Sedimentary cover
3075 reservoir of Svalbard archipelago], *Neftegaz. Geol. Teor. Prakt.*, 8, 1–45, 2013.
- Vickers, M. L., Price, G. D., Jerrett, R. M., and Watkinson, M.: Stratigraphic and geochemical expression of
Barremian–Aptian global climate change in Arctic Svalbard, *Geosphere*, 12, 1594–
1605, <https://doi.org/10.1130/ges01344.1>, 2016.
- Vickers, M. L., Price, G. D., Jerrett, R. M., Sutton, P., Watkinson, M. P., and FitzPatrick, M.: The duration and
3080 magnitude of Cretaceous cool events: Evidence from the northern high latitudes, *GSA Bull.*, 131, 1979–
1994, <https://doi.org/10.1130/b35074.1>, 2019a.
- Vickers, M. L., Bajnai, D., Price, G. D., Linckens, J., and Fiebig, J.: Southern high-latitude warmth during the
Jurassic–Cretaceous: New evidence from clumped isotope thermometry, *Geology*, 47, 724–728, 2019b.
- Vickers, M. L., Fernandez, A., Hesselbo, S. P., Price, G. D., Bernasconi, S. M., Lode, S., Ullmann, C. V., Thibault,
3085 N., Hougaard, I. W., and Korte, C.: Unravelling Middle to Late Jurassic palaeoceanographic and
palaeoclimatic signals in the Hebrides Basin using belemnite clumped isotope thermometry, *Earth Planet.
Sci. Lett.*, 546, 116401, 2020.
- Vickers, M. L., Bernasconi, S. M., Ullmann, C. V., Lode, S., Looser, N., Morales, L. G., Price, G. D., Wilby, P. R.,
Hougaard, I. W., Hesselbo, S. P., and Korte, C.: Marine temperatures underestimated for past greenhouse
3090 climate, *Sci. Rep.*, 11, 19109, 2021.
- Vickers, M. L., Jelby, M. E., Śliwińska, K. K., Percival, L. M., Wang, F., Sanei, H., Price, G. D., Ullmann, C. V.,
Grasby, S. E., and Reinhardt, L.: Volcanism and carbon cycle perturbations in the High Arctic during the
Late Jurassic–Early Cretaceous, *Palaeogeogr. Palaeoclimatol. Palaeoecol.*, 613, 111412, 2023.
- Vigran, J. O.: Spores from Devonian deposits, Mimerdalen, Spitsbergen, *Norsk Polarinstitutt Skrifter*, v.132, p.1–33,
3095 1964.
- Vigran, J. O., Mangerud, G., Mørk, A., Worsley, D., and Hochuli, P. A.: Palynology and geology of the Triassic
succession of Svalbard and the Barents Sea, *Nor. Geol. Unders.*, 14, 2014.
- Vogt, T.: Geology of a Middle Devonian cannel coal from Spitsbergen, *Nor. Geol. Tidsskr.*, 21, 1–12, 1941.
- von Appen, W.-J., Schauer, U., Somavilla, R., Bauerfeind, E., and Beszczynska-Möller, A.: Exchange of warming
3100 deep waters across Fram Strait, *Deep-Sea Res. Pt. I*, 103, 86–
100, <https://doi.org/10.1016/j.dsr.2015.06.003>, 2015.



W

- 3105 Wagner, M., Hendy, I. L., & Lai, B.: Characterizing Ag uptake and storage in the marine diatom *Thalassiosira pseudonana*: Implications for Ag biogeochemical cycling. *Marine Chemistry*, **247**, 104175. <https://doi.org/10.1016/j.marchem.2022.1041>, 2022.
- Wappler, T. and Denk, T.: Herbivory in early Tertiary Arctic forests. *Palaeogeography, Palaeoclimatology, Palaeoecology*, 310(3-4): 283-295, 2011.
- 3110 Ware, D., Jenks, J. F., Hautmann, M., and Bucher, H.: Dienerian (Early Triassic) ammonoids from the Candelaria Hills (Nevada, USA) and their significance for palaeobiogeography and palaeoceanography. *Swiss Journal of Geosciences*, 104, 161-181, 2011.
- Watson, R., Baste, I., Larigauderie, A., Leadley, P., Pascual, U., Baptiste, B., ... and Mooney, H.: Summary for policymakers of the global assessment report on biodiversity and ecosystem services of the Intergovernmental Science-Policy Platform on Biodiversity and Ecosystem Services. *IPBES Secretariat: Bonn, Germany*, 22-47, 2019.
- 3115 Webby, B.D., Paris, F., Droser, M.L. and Percival, I.G.: The great Ordovician biodiversification event. Columbia University Press, 2004.
- Weber, M.: Paleoenvironments during the Paleogene in the High Arctic of Spitsbergen – Evidence from Sedimentology and Palynology, Master thesis, Institute of Applied Geoscience, Technical University of Darmstadt University Centre in Svalbard, 100 pp., 2019.
- 3120 Weger, R.J., Eberli, G.P., Rodriguez Blanco, L., Tenaglia, M. and Swart, P.K.: Finding a VOICE in the Southern Hemisphere: A new record of global organic carbon? *Geological Society of America bulletin*, 10.1130/B36405.1, 2022.
- Weijers, J.W., Schouten, S., Sluijs, A., Brinkhuis, H. and Damsté, J.S.S.: Warm arctic continents during the Palaeocene–Eocene thermal maximum. *Earth and Planetary Science Letters*, 261(1-2): 230-238, <https://doi.org/10.1016/j.epsl.2007.06.033>, 2007.
- 3125 Weissert, H. and Channell, J.E.T.: Tethyan carbonate carbon isotope stratigraphy across the Jurassic-Cretaceous boundary: An indicator of decelerated global carbon cycling? *Paleoceanography*, 4(4): 483-494, <https://doi.org/10.1029/PA004i004p00483>, 1989.
- 3130 Weissert, H. and Erba, E.: Volcanism, CO₂ and palaeoclimate: a Late Jurassic–Early Cretaceous carbon and oxygen isotope record. *Journal of the Geological Society*, 161(4): 695-702, 10.1144/0016-764903-087, 2004.
- 3135 Weissert, H., Lini, A., Föllmi, K.B. and Kuhn, O.: Correlation of Early Cretaceous carbon isotope stratigraphy and platform drowning events: a possible link? *Palaeogeography, Palaeoclimatology, Palaeoecology*, 137(3): 189-203, [https://doi.org/10.1016/S0031-0182\(97\)00109-0](https://doi.org/10.1016/S0031-0182(97)00109-0), 1998.



- Wesenlund, F., Grundvåg, S.-A., Engelschiøn, V.S., Thießen, O. and Pedersen, J.H.: Linking facies variations, organic carbon richness and bulk bitumen content—A case study of the organic-rich Middle Triassic shales from eastern Svalbard. *Marine and Petroleum Geology*, 132: 105168, 2021.
- 3140 Wesenlund, F., Grundvåg, S.-A., Engelschiøn, V.S., Thießen, O. and Pedersen, J.H.: Multi-elemental chemostratigraphy of Triassic mudstones in eastern Svalbard: Implications for source rock formation in front of the World's largest delta plain. *The Depositional Record*, 8(2): 718-753, <https://doi.org/10.1002/dep2.182>, 2022a.
- Wesenlund, F., Grundvåg, S.A., Engelschiøn, V.S., Thießen, O. and Pedersen, J.H.: Multi-elemental chemostratigraphy of Triassic mudstones in eastern Svalbard: Implications for source rock formation in front of the World's largest delta plain. *The Depositional Record*, 8(2): 718-753, 2022b.
- 3145 West, C.K., Greenwood, D.R. and Basinger, J.F.: Was the Arctic Eocene 'rainforest' monsoonal? Estimates of seasonal precipitation from early Eocene megafloras from Ellesmere Island, Nunavut. *Earth and Planetary Science Letters*, 427: 18-30, <https://doi.org/10.1016/j.epsl.2015.06.036>, 2015.
- Westbury, M., Baleka, S., Barlow, A., Hartmann, S., Paijmans, J.L., Kramarz, A., Forasiepi, A.M., Bond, M., Gelfo, J.N. and Reguero, M.A.: A mitogenomic timetree for Darwin's enigmatic South American mammal *Macrauchenia patachonica*. *Nature Communications*, 8(1): 15951, 2017.
- 3150 Westerhold, T., Marwan, N., Drury, A.J., Liebrand, D., Agnini, C., Anagnostou, E., Barnet, J.S., Bohaty, S.M., De Vleeschouwer, D. and Florindo, F.: An astronomically dated record of Earth's climate and its predictability over the last 66 million years. *Science*, 369(6509): 1383-1387, 10.1126/science.aba6853, 2020.
- 3155 Wieczorek, R., Fantle, M.S., Kump, L.R. and Ravizza, G.: Geochemical evidence for volcanic activity prior to and enhanced terrestrial weathering during the Paleocene Eocene Thermal Maximum. *Geochimica et Cosmochimica Acta*, 119: 391-410, <https://doi.org/10.1016/j.gca.2013.06.005>, 2013.
- Wierzbowski, H., Bajnai, D., Wacker, U., Rogov, M.A., Fiebig, J. and Tesakova, E.M.: Clumped isotope record of salinity variations in the Subboreal Province at the Middle–Late Jurassic transition. *Glob. Planet. Change*, 3160 167, 172-189, 2018.
- Wignall, P.B. and Twitchett, R.J.: Oceanic Anoxia and the End Permian Mass Extinction. *Science*, 272(5265): 1155-1158, doi:10.1126/science.272.5265.1155, 1996.
- Wignall, P., Morante, R. and Newton, R.: The Permo-Triassic transition in Spitsbergen: $\delta^{13}\text{C}_{\text{org}}$ chemostratigraphy, Fe and S geochemistry, facies, fauna and trace fossils. *Geological Magazine*, 135(1): 47-62, <https://doi.org/10.1017/S0016756897008121>, 1998.
- 3165 Wignall, P.B., Bond, D.P.G., Sun, Y., Grasby, S.E., Beauchamp, B., Joachimski, M.M. and Blomeier, D.P.G.: Ultra-shallow-marine anoxia in an Early Triassic shallow-marine clastic ramp (Spitsbergen) and the suppression of benthic radiation. *Geological Magazine*, 153(2): 316-331, 10.1017/s0016756815000588, 2016.



- 3170 Wilkinson, C.M., Ganerød, M., Hendriks, B.W. and Eide, E.A.: Compilation and appraisal of geochronological data
from the North Atlantic Igneous Province (NAIP). Geological Society, London, Special Publications, 447(1):
69-103 <https://doi.org/10.1144/SP447.10>, 2017.
- Willard, D.A., Donders, T.H., Reichgelt, T., Greenwood, D.R., Sangiorgi, F., Peterse, F., Nierop, K.G., Frieling, J.,
Schouten, S. and Sluijs, A.: Arctic vegetation, temperature, and hydrology during Early Eocene transient
global warming events. *Global and Planetary Change*, 178: 139-152,
3175 <https://doi.org/10.1016/j.gloplacha.2019.04.012>, 2019.
- Wiman, C.: Ichthyosaurier aus der Trias Spitzbergens. *Bulletin of the Geological Institution of the University of
Upsala*, 10, 124-148, 1910.
- Wiman, C.: Eine neue marine Reptilien-Ordnung aus der Trias Spitzbergens. *Bulletin of the Geological Institute of
the University of Uppsala*, 22, 183-196, 1928.
- 3180 Wisshak, M., Volohonsky, E., and Blomeier, D.: Acanthodian fish trace fossils from the Early Devonian of
Spitsbergen, *Acta Palaeontol. Pol.*, 49, 2004a.
- Wisshak, M., Volohonsky, E., Seilacher, A., and Freiwald, A.: A trace fossil assemblage from fluvial Old Red
deposits (Wood Bay Formation; Lower to Middle Devonian) of NW-Spitsbergen, Svalbard, *Lethaia*, 37,
149–163, 2004b.
- 3185 Woods, A. D.: Paleoceanographic and paleoclimatic context of Early Triassic time, *C. R. Palevol*, 4, 463–
472, <https://doi.org/10.1016/j.crpv.2005.07.003>, 2005.
- Worsley, D.: Sedimentological observations on the Grey Hoek Formation of northern Andrée Land, Spitsbergen,
Nor. *Polarinst. Årbok*, 1970, 102–111, 1972.
- Worsley, D., Agdestein, T., Gjelberg, J., Kirkemo, K., Mørk, A., Nilsson, I., Olausson, S., Steel, R. J., and
3190 Stemmerik, L.: The geological evolution of Bjørnøya, Arctic Norway: implications for the Barents shelf, *Nor.
J. Geol.*, 81, 195–234, 2001.
- Worsley, D.: The post-Caledonian development of Svalbard and the western Barents Sea, *Polar Res.*, 27, 298–
317, <https://doi.org/10.1111/j.1751-8369.2008.00085.x>, 2008.
- Wu, Y., Chu, D., Tong, J., Song, H., Dal Corso, J., Wignall, P. B., Song, H., Du, Y., and Cui, Y.: Six-fold increase
3195 of atmospheric pCO₂ during the Permian–Triassic mass extinction, *Nat. Commun.*, 12,
2137, <https://doi.org/10.1038/s41467-021-22298-7>, 2021.

Z

- 3200 Zachos, J., Pagani, M., Sloan, L., Thomas, E. and Billups, K., 2001. Trends, Rhythms, and Aberrations in Global
Climate 65 Ma to Present. *Science*, 292(5517): 686-693, doi:10.1126/science.1059412.

Zachos, J., Pagani, M., Sloan, L., Thomas, E., and Billups, K.: Trends, Rhythms, and Aberrations in Global Climate 65 Ma to Present, *Science*, 292, 686–693, <https://doi.org/10.1126/science.1059412>, 2001.

3205 Zachos, J. C., Bohaty, S. M., John, C. M., McCarren, H., Kelly, D. C., and Nielsen, T.: The Palaeocene–Eocene carbon isotope excursion: constraints from individual shell planktonic foraminifer records, *Philos. Trans. R. Soc. A-Math. Phys. Eng. Sci.*, 365, 1829–1842, 2007.

Zachos, J. C., Dickens, G. R., and Zeebe, R. E.: An early Cenozoic perspective on greenhouse warming and carbon-cycle dynamics, *Nature*, 451, 279–283, <https://doi.org/10.1038/nature06588>, 2008.

3210 Žák, K., Košťák, M., Man, O., Zakharov, V. A., Rogov, M. A., Pruner, P., Rohovec, J., Dzyuba, O. S., and Mazuch, M.: Comparison of carbonate C and O stable isotope records across the Jurassic/Cretaceous boundary in the Tethyan and Boreal Realms, *Palaeogeogr. Palaeoclimatol. Palaeoecol.*, 299, 83–96, <https://doi.org/10.1016/j.palaeo.2010.10.038>, 2011.

3215 Zakharov, V. A., Rogov, M. A., Dzyuba, O. S., Žák, K., Košťák, M., Pruner, P., Skupien, P., Chadima, M., Mazuch, M., and Nikitenko, B. L.: Palaeoenvironments and palaeoceanography changes across the Jurassic/Cretaceous boundary in the Arctic realm: case study of the Nordvik section (north Siberia, Russia), *Polar Res.*, 33, 19714, <https://doi.org/10.3402/polar.v33.19714>, 2014.

Zanin, Y. N., Zamirailova, A. G., & Eder, V. G.: Chalcophile elements in black shales of the Bazhenov Formation, West Siberian sea basin. *Russian Geology and Geophysics*, 57(4), 608–616. <https://doi.org/10.1016/j.rgg.2015.03.018>, 2016.

3220 Zeebe, R. E., Ridgwell, A., and Zachos, J. C.: Anthropogenic carbon release rate unprecedented during the past 66 million years, *Nat. Geosci.*, 9, 325–329, <http://dx.doi.org/10.1038/ngeo2681>, 2016.

3225 Zhang, H., Zhang, F., Chen, J.-B., Erwin, D. H., Syverson, D. D., Ni, P., Rampino, M., Chi, Z., Cai, Y.-F., Xiang, L., Li, W.-Q., Liu, S.-A., Wang, R.-C., Wang, X.-D., Feng, Z., Li, H.-M., Zhang, T., Cai, H.-M., Zheng, W., Cui, Y., Zhu, X.-K., Hou, Z.-Q., Wu, F.-Y., Xu, Y.-G., Planavsky, N., and Shen, S.-Z.: Felsic volcanism as a factor driving the end-Permian mass extinction, *Sci. Adv.*, 7, eabh1390, <https://doi.org/10.1126/sciadv.abh1390>, 2021a.

Zhang, L., Wang, C., Li, X., Cao, K., Song, Y., Hu, B., Lu, D., Wang, Q., Du, X., and Cao, S.: A new paleoclimate classification for deep time, *Palaeogeogr. Palaeoclimatol. Palaeoecol.*, 443, 98–106, <https://doi.org/10.1016/j.palaeo.2015.11.041>, 2016.

3230 Zhang, Y., Ogg, J. G., Minguez, D., Hounslow, M. W., Olausson, S., Gradstein, F. M., and Esmeray-Senlet, S.: Magnetostratigraphy of U-Pb–dated boreholes in Svalbard, Norway, implies that magnetochron M0r (a proposed Barremian-Aptian boundary marker) begins at 121.2 ± 0.4 Ma, *Geology*, 49, 733–737, <https://doi.org/10.1130/g48591.1>, 2021b.

Zhao, Y., Wei, W., Li, S., Yang, T., Zhang, R., Somerville, I., Santosh, M., Wei, H., Wu, J., Yang, J., Chen, W., and Tang, Z.: Rare earth element geochemistry of carbonates as a proxy for deep-time environmental



3235 reconstruction, *Palaeogeogr. Palaeoclimatol. Palaeoecol.*, 574, 110443, <https://doi.org/10.1016/j.palaeo.2021.110443>, 2021.

Zuchuat, V., A Sedimentary Investigation of the Lower Triassic Formations and Their Underlying Permo-Carboniferous Units Across Spitsbergen, Svalbard. Institutt for geologi og bergteknikk, Norwegian University of Science and Technology. 165 pages, 2014.

3240 Zuchuat, V., Sleveland, A. R. N., Twitchett, R. J., Svensen, H. H., Turner, H., Augland, L. E., Jones, M. T., Hammer, Ø., Hauksson, B. T., Hafliðason, H., Midtkandal, I., and Planke, S.: A new high-resolution stratigraphic and palaeoenvironmental record spanning the End-Permian Mass Extinction and its aftermath in central Spitsbergen, Svalbard, *Palaeogeogr. Palaeoclimatol. Palaeoecol.*, 554, 109732, <https://doi.org/10.1016/j.palaeo.2020.109732>, 2020.

3245

Økland, I. H., Delsett, L. L., Roberts, A. J., and Hurum, J. H.: A *Phalarodon fraasi* (Ichthyosauria: Mixosauridae) from the Middle Triassic of Svalbard, *Norwegian Journal of Geology*, 98, 267–288. <https://doi.org/10.17850/njg98-2-06>, 2018.

3250